

CARBON PARTICLE OXIDATION IN FLAMES

A thesis submitted for the degree of

Doctor of Philosophy

by

HÜSEYİN FİKRET ATEŞ

in

The University of Aston in Birmingham

186849 26 NOV 1975

JULY 1975

Thesis  
541.361  
ATE

## SUMMARY

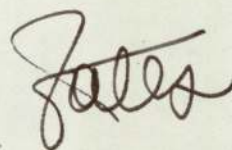
In the oxidation of carbon particles in fuel-rich flames of  $H_2/O_2/N_2$ , the principal oxidant has been investigated, where a controversy lies in the literature. Light scattering technique is used in following the rate of disappearance of carbon particles.

The theoretical background for both the light scattering technique and the nature of carbon particles in the flames is discussed. Measurements were made within the temperature limits of 1690 - 2170 K, where the limits are analysed together with the experimental procedure in the text. The apparatus used in the production and oxidation of such particles, together with the measuring system is described.

The possible oxidants are most likely to be the oxygen atoms and the hydroxyl radicals. Considering their thermodynamic equilibrium values and the possible disequilibrium excess, the experimental evidence strongly supports a predominant attack by hydroxyl radicals in the oxidation process of carbon particles in fuel rich flames.

## PREFACE

This thesis, which is being submitted for the Degree of Doctor of Philosophy in the University of Aston in Birmingham, is an account of the work done under the supervision of Professor F. M. Page, B.A., Ph.D., Sc.D., in the Department of Chemistry of the University of Aston in Birmingham from January 1972 to May 1975. Except where references have been given in the text, the work described herein is original and has not been submitted for a degree at any other University.

A handwritten signature in cursive script, appearing to read "J. A. Jones".



We know accurately only  
when we know little;  
with knowledge doubt increases.

Goethe



### ACKNOWLEDGEMENTS

I wish to express my gratitude to Professor F. M. Page for his continued guidance and encouragement throughout the course of this work.

I also wish to thank Dr D. E. Jensen and Dr G. Jones (R.P.E. Westcott) for their help, and Mrs. J. Broad for typing this thesis. Thanks are also due to two great friends Surendra Patel and M. Mehmet Konuray, with whom the most enjoyable and rewarding years are shared.

I would also like to thank my wife, for her patience and inspiration, whom this work is dedicated to.

Finally, I am grateful to H.M. Ministry of Defence for the award of the research grant.

To my dear wife and  
my mother

## CONTENTS

	Page
1. INTRODUCTION	1
2. SCATTERING OF LIGHT BY PARTICLES	4
2.1. THE RAYLEIGH THEORY OF SCATTERING BY SMALL PARTICLES	5
2.1.1. SCATTERING CROSS SECTION AND EFFICIENCY	11
2.2. GENERALISATION OF RAYLEIGH SCATTERING TO PARTICLE CLOUDS	12
2.3. GENERAL THEORY OF LIGHT SCATTERING	13
2.4. THE USE OF LIGHT SCATTERING IN FLAME STUDIES	15
2.4.1. DISTRIBUTION OF SIZE IN SCATTERING MEASUREMENTS	18
2.5. SCATTERING BY NON-SPHERICAL PARTICLES	20
3. CARBON PARTICLES IN FLAMES	22
3.1. CARBON FORMATION IN FLAMES	22
3.2. NUCLEATION AND GROWTH OF CARBON PARTICLES IN FLAMES	26
3.3. OXIDATION OF CARBON PARTICLES IN FLAMES	29
3.3.1. THE OXIDATION MECHANISM	30
3.3.2. NATURE OF THE OXIDANT	35
3.3.3. HYDROXYL RADICALS AS THE OXIDISING SPECIES	39
4. APPARATUS	42
4.1. THE BURNER SYSTEM	42
4.1.1. PRIMARY BURNER	43
4.1.2. SECONDARY BURNER	46
4.1.3. THE CONICAL NEXUS	49
4.2. GAS SUPPLY SYSTEM	54



4.3.	GAS ANALYSIS ARRANGEMENTS	57
4.3.1.	GAS SAMPLING SYSTEM	57
4.3.2.	ANALYSIS BY GAS CHROMATOGRAPHY	60
4.4.	DETERMINATION OF FLAME TEMPERATURES	68
4.4.1.	METHOD	68
4.4.2.	APPLICATIONS	71
4.4.3.	THEORETICAL FLAME TEMPERATURES	75
4.5.	FLAME MAPPING FOR SOOT	77
4.6.	THE LIGHT SCATTERING SYSTEM	79
5.	LIGHT SCATTERING STUDIES OF SOOT OXIDATION IN FLAMES	83
5.1.	EXPERIMENTAL	85
5.1.1.	THE SYSTEM SETTLING TIME	85
5.1.2.	WORKING TIME LIMITATIONS	87
5.1.3.	LIGHT SCATTERING AS A FUNCTION OF FLAME HEIGHT	88
5.2.	CHEMICAL KINETIC ANALYSIS OF THE FUEL-RICH $H_2-O_2$ FLAME	90
5.2.1.	BIMOLECULAR RADICAL REACTIONS	90
5.2.2.	THREE-BODY RADICAL RECOMBINATION REACTIONS	93
5.2.3.	PARTIAL EQUILIBRIUM	96
5.2.4.	THE STATE OF DISEQUILIBRIUM	99
6.	RESULTS AND DISCUSSIONS	105
6.1.	ANALYSIS OF THE RESULTS	108
6.2.	THEORETICAL APPROACH	117
7.	CONCLUSIONS	122
	APPENDIX	125
	REFERENCES	128

LIST OF FIGURES

	page
FIG. (II.1) RAYLEIGH SCATTERING GEOMETRY	6
FIG. (II.2) RAYLEIGH SCATTERING DIAGRAM	8
FIG. (II.3) EFFECTS OF PARTICLE SIZE ON SCATTERING PATTERN	10
FIG.(III.1) EFFECT OF PARTICLE-SIZE AND ACCELERATION ON MASS TRANSFER RATES	32
FIG. (IV.1) BURNER SYSTEM	44
FIG. (IV.2) PRIMARY BURNER	45
FIG. (IV.3) SECONDARY BURNER	47
FIG. (IV.4) INITIAL NEXUS DESIGN	51
FIG. (IV.5) THE SOOT DISTRIBUTOR	52
FIG. (IV.6) GAS SUPPLY SYSTEM	55
FIG. (IV.7) GAS SAMPLING SYSTEM	58
FIG. (IV.8) TCD	62
FIG. (IV.9) GAS ANALYSIS COLUMN SYSTEM	64
FIG. (IV.10) A TYPICAL CHROMATOGRAM	67
FIG. (IV.11) TEMPERATURE MEASURING SYSTEM	69
FIG. (IV.12) THE ATOMIZER	72
FIG. (IV.13) THE ELUTRIATOR	74
FIG. (IV.14) FLAME TEMPERATURES	76
FIG. (IV.15) FLAME MAP	78
FIG. (IV.16) LIGHT SCATTERING SYSTEM	80
FIG. (IV.17) PM CIRCUIT	82
FIG. ( V.1 ) EXPERIMENTAL LIMITS	84

FIG. (V.2)	SYSTEM SETTLING TIME	86
FIG. (V.3)	ATOMIC HYDROGEN CONCENTRATIONS IN HYDROGEN + OXYGEN + NITROGEN FLAMES	101
FIG. (V.4)	DISEQUILIBRIUM PARAMETER	103
FIG. (VI.1)	SCATTERED INTENSITY vs. FLAME HEIGHT	106
FIG. (VI.2)	COMPOSITION RELATIONS	109
FIG. (VI.3)	TEMPERATURE RELATIONS	110
FIG. (VI.4)	ELECTRON MICROGRAPHS	118



LIST OF TABLES

	page
TABLE (IV-1) TYPICAL COMPOSITION OF PRIMARY BURNER PRODUCTS AND FLAME CONDITIONS	66
TABLE (VI-1) FLAME CONDITIONS	107
TABLE (VI-2) AVERAGE INTENSITIES & $d \log I/dh$	111
TABLE (VI-3) CALCULATED RADICAL & ATOM CONCENTRATIONS AT THERMODYNAMIC EQUILIBRIUM	114
TABLE (VI-4) RATE FUNCTIONS & CORRELATIONS	116
TABLE (VI-5) CORRELATIONS REGARDING DISEQUILIBRIUM	120

## CHAPTER 1

### 1. INTRODUCTION

Although we have a clear idea what is meant by a flame, no precise definition has been put forward. Flames can be cool, such as in cool ether flames, which is only a few hundred degrees K. They can be very hot, as in acetylene flames. They vary in luminosity. Although they are generally associated with oxidation, there are reactions such as between some halogens and hydrocarbons where no oxygen is involved. Additives to flames also have varying effects. For example some additives are known to increase the sooting of flames while others decrease the same property.

The formation and oxidation of solid carbon particles in flames has been an area of great interest from both the industrial and academic point of view. Davy in the last century was one of the first to realise that carbon particles were the cause of luminous flames and made the following comment. "Whenever a flame is remarkably brilliant and dense, it may be always concluded that some solid matter is produced in it; on the contrary, when a flame is extremely feeble and transparent, it may be inferred that no solid is formed." Being the cause of flame luminosity, these carbon particles increase the flame emissivity. Their presence might therefore be desirable in some applications.



But if they stay in the media longer than might be desired, they tend to become a pollution problem and decrease the thermal efficiency of the combustion.

Fenimore & Jones (1969) argued that if particles can be prevented growing beyond roughly 10 nm in diameter and from coagulating, they should ultimately be oxidised in the system and not escape as smoke.

The purpose of this work is to make measurements on the oxidation of soot particles in flames and investigate the species involved in the oxidation process. Lee et al (1962) argued that  $O_2$  molecules were the responsible species for the oxidation of carbon particles in laminar flames. Later Fenimore & Jones (1967) pointed out that an additional mechanism besides oxidation by  $O_2$  is important and favoured an oxidation by hydroxyl radicals. The experimental techniques of the both workers involved sampling from the flame and making the measurements outside the media. Methods for the analysis of carbon particles in flames as a tool in determining the oxidation process includes treatments such as optical and electron microscopy, filtration, sedimentation, light scattering, etc. All the other methods but light scattering, are based on measurements made outside the flame by sampling, thus disturbing the system. Light scattering methods have the advantage of providing in situ measurements without significant perturbation.



This dissertation gives an account of the work done in the field of carbon particle oxidation in flames using laser scattering as a diagnostic tool. Chapter two deals with the theory of light scattering by particles, starting with Rayleigh theory and generalising it to particle clouds. A survey of previous work about the use of the technique in flame studies is also included. Having established the theoretical background for light scattering, the nature of carbon particles in flames is analysed in chapter three. Their formation and the possible routes including the proposed oxidation mechanisms is discussed in the same chapter together with the possible oxidants. Chapter four gives a detailed description of the apparatus designed for the purpose and presents the basic experimental procedures that are carried out for the groundwork in the final analysis. The experimental technique adopted throughout the work is dealt with in chapter five together with the limitations involved. A kinetic analysis of the flame reactions is also given in the same chapter. Finally the results are analysed and discussed in chapter six with relevant theoretical approaches.

## CHAPTER 2

### 2. SCATTERING OF LIGHT BY PARTICLES

The attempts to account for the colour and the polarisation of skylight initiated the development of a light scattering theory during the second half of the last century. In fact al-Hasan ibn al-Haytham, known to the Latin medieval writers by the name Alhazen, related the brightness of the sky to the reflection of the sunlight by the particles in the air, in early eleventh century, Sabra (1967).

Rayleigh (1881) assumed that the variables which effect the scattering are the volume  $V$  of the spherical particle, the distance  $R$  to the observation point, the wavelength  $\lambda$ , and the indices of refraction of the particle and of the medium  $n_1$  and  $n_2$ . If the particles are non absorbing i.e. the refractive indices are not complex, and bearing in mind the fact that the scattered intensity  $I$  is proportional to the incident radiation  $I_0$ , then,

$$I = f(V, R, \lambda, n_1, n_2) I_0 \quad (2-1)$$

It is clear that  $f(V, R, \lambda, n_1, n_2)$  is dimensionless. The energy is radiated in all directions hence the intensity must fall as  $1/R^2$ . The intensity is proportional to the square of the field. As the field of the dipole is proportional to the dipole moment, which is in turn proportional to the volume of the particle, The intensity should vary as  $V^2$ . The refractive indices are themselves dimensionless, so whatever their functional dependence is, they will have no effect on the dimensional analysis. Hence the wavelength dependence can be given as,



$$I = f'(n_1, n_2) (v^2/R^2 \lambda^4) I_0 \quad (2-2)$$

This dependence was applied by Rayleigh to explain the blue of the sky. The light which reaches the observer unless one is looking directly at the sun, has been scattered by dust particles or the molecules of the atmosphere. Since the wavelength of the visible light is much longer than the radius of these particles, the fourth power dependence on the wavelength is valid. And the short wavelengths in the sunlight is strongly scattered, relative to those near the red end of the spectrum.

## 2.1 THE RAYLEIGH THEORY OF SCATTERING BY SMALL SPHERES

The arguments of Rayleigh were based on a single spherical particle isolated from the medium and illuminated by a parallel beam of light which is linearly polarised. For an incident wave of unit intensity, the intensity of the scattered wave is given by Stratton (1941)

$$I = \frac{16\pi^4 a^6}{R^2 \lambda^4} \left[ \frac{n^2 - 1}{n^2 + 2} \right]^2 \sin^2 \psi \quad (2-3)$$

Where  $a$  is the radius of the sphere,  $R$  is the distance to the observation point,  $\lambda$  is the wavelength in the medium,  $n$  is the relative refractive index ( $n_1/n_2$ ), and  $\psi$  is the angle measured from the scatterings direction to the dipole. Fig. (II-1)

Scattering is often accompanied by absorption. Both scattering and absorption remove energy from a beam of light passing through the



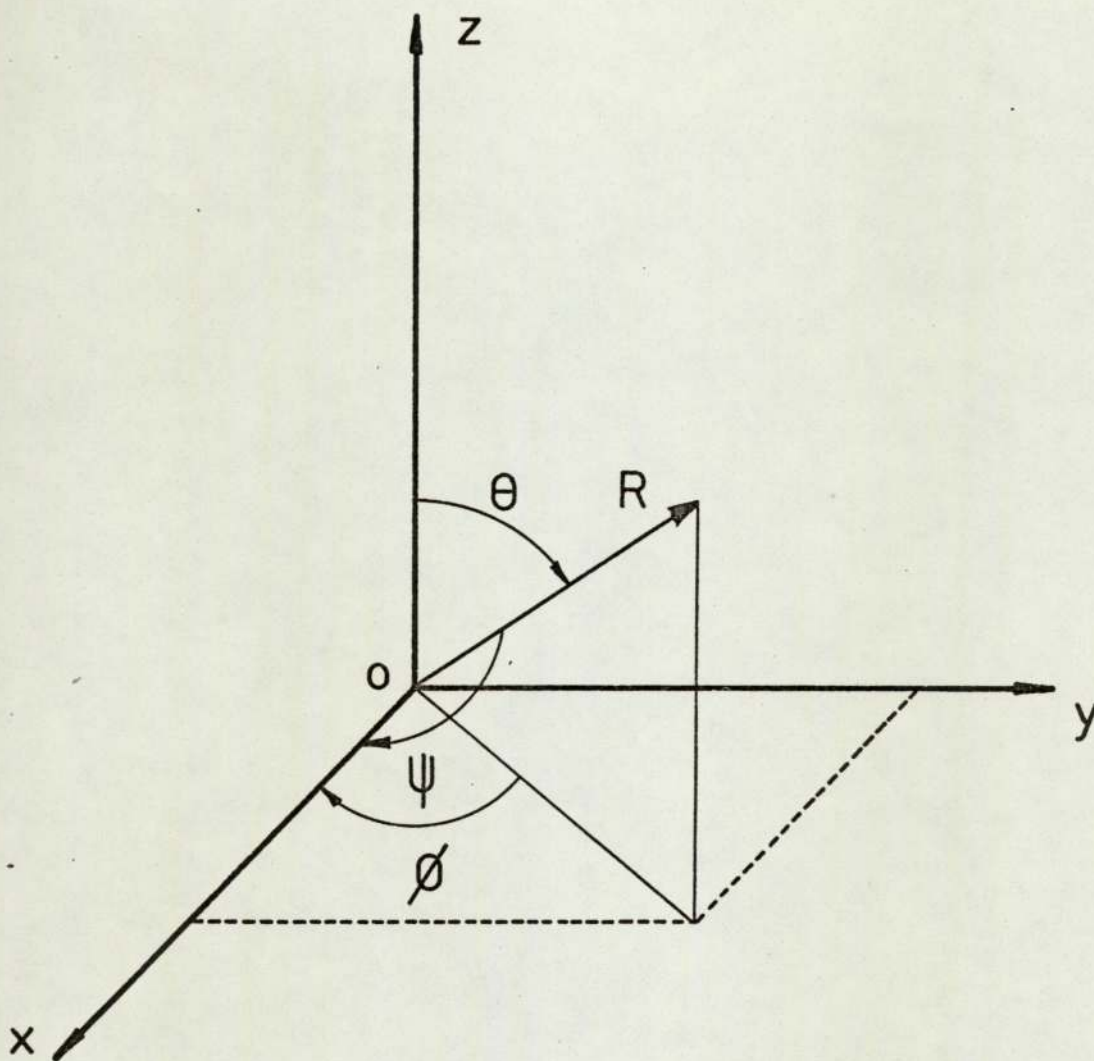


FIGURE II-1 RAYLEIGH SCATTERING  
GEOMETRY

$\theta$ , angle of observation;  
Incident wave travelling  
along positive z-axis;  
 $R, \phi, \theta$ , spherical coordinates

medium. Hence the beam is attenuated. This attenuation is called extinction.

If the scattering particle is absorptive, it is characterised by a complex relative refractive index,  $m$ . When the absorption is small compared to the real part of the relative refractive index eq. (2-3) can be expressed as,

$$I = \frac{16 \pi^4 a^6}{R^2 \lambda^4} \left| \frac{m^2 - 1}{m^2 + 2} \right|^2 \sin^2 \psi \quad (2-4)$$

When the incident radiation is perpendicularly polarized with respect to the scattering field and  $\psi = 90^\circ$ , the scattered radiation will have an intensity

$$I_{\perp} = \frac{16 \pi^4 a^6}{R^2 \lambda^4} \left[ \frac{n^2 - 1}{n^2 + 2} \right]^2 \quad (2-5)$$

in the case when the polarisation is parallel to the scattering field, where  $\psi = (\pi/2) - \theta$ , the scattered intensity will be

$$I_{\parallel} = \frac{16 \pi^4 a^6}{R^2 \lambda^4} \left[ \frac{n^2 - 1}{n^2 + 2} \right]^2 \cos^2 \theta \quad (2-6)$$

The Rayleigh scattering pattern is illustrated in Fig. (II-2). As the particle size increases compared with  $\lambda$  the scattering pattern becomes irregular and forward scattering dominates, and  $I_{\parallel} (90)$  is no longer

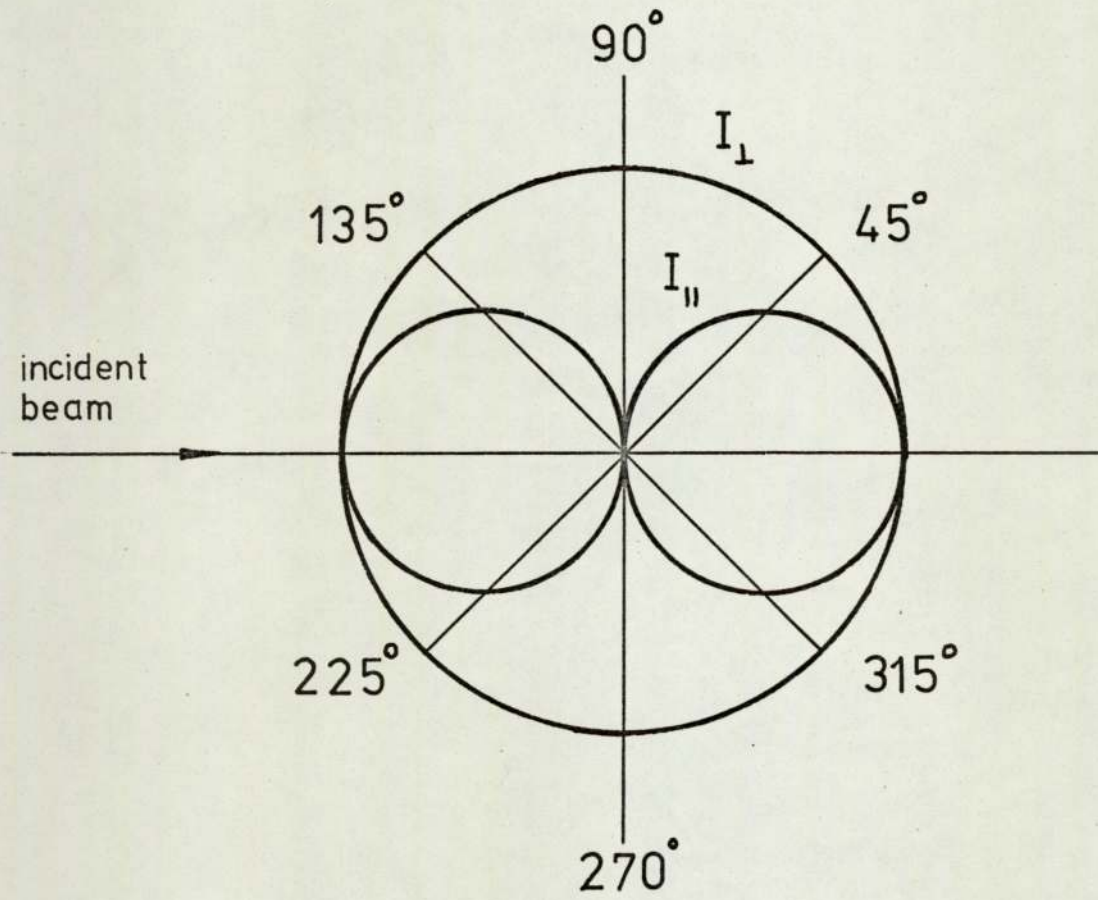


FIGURE II- 2 RAYLEIGH SCATTERING  
DIAGRAM



zero, this was shown by Olaf & Robock (1961), Fig. II-3)

With the aid of eq.(2-5&6) an unpolarized incident wave can be resolved into two components, which are the parallel and perpendicular to the scattering field. Sinclair (1947),

$$I_{\text{unpol}} = \frac{I_{\perp} + I_{\parallel}}{2} = \frac{8\pi^4 a^6}{R^2 \lambda^4} \left[ \frac{n^2 - 1}{n^2 + 2} \right]^2 (1 + \cos^2 \theta) \quad (2-7)$$

When the particle volume dependence is introduced eq.(2-7) becomes,

$$I = \frac{9 \pi^2 V^2}{2R^2 \lambda^4} \left[ \frac{n^2 - 1}{n^2 + 2} \right]^2 (1 + \cos^2 \theta) \quad (2-8)$$

and in defining the particle size dependence of the scattered intensity a dimensionless size parameter  $x$  will be introduced, such that,

$$x = 2 \pi a / \lambda \quad (2-9)$$

where  $a$  is the particle radius.

The limit of  $x$  for which the Rayleigh equation is accepted to be valid in the literature is  $x \leq 0.3$ . Van de Hulst (1957) lists the validity of various methods with respect to the size parameters. These limits depend strongly on the precision of the instruments and are somewhat arbitrary.

Scattering diagram for spheres with  $m = 2.0 - 0.5i$

(Olaf & Robock 1961)

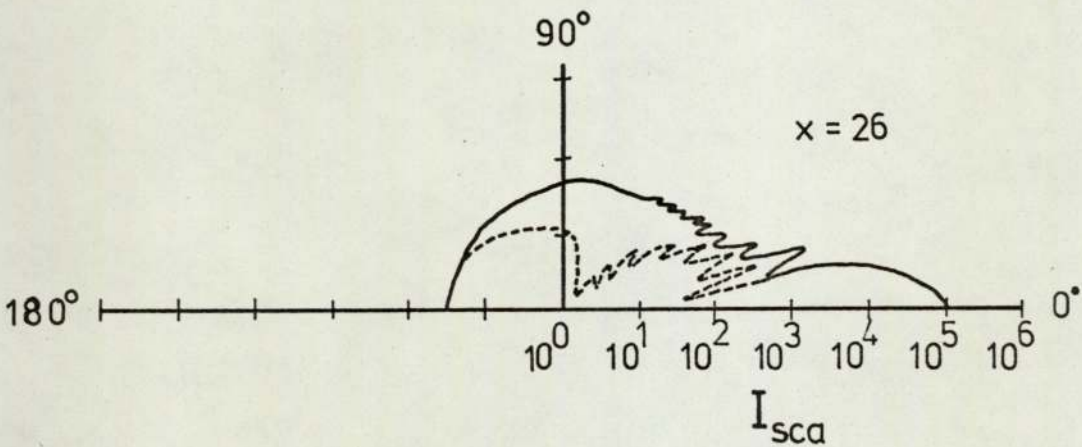
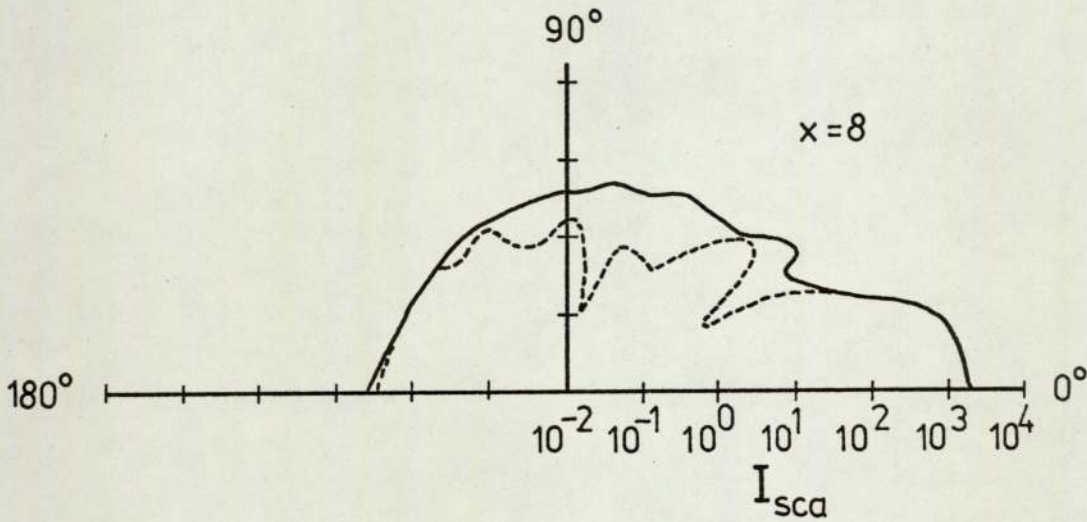
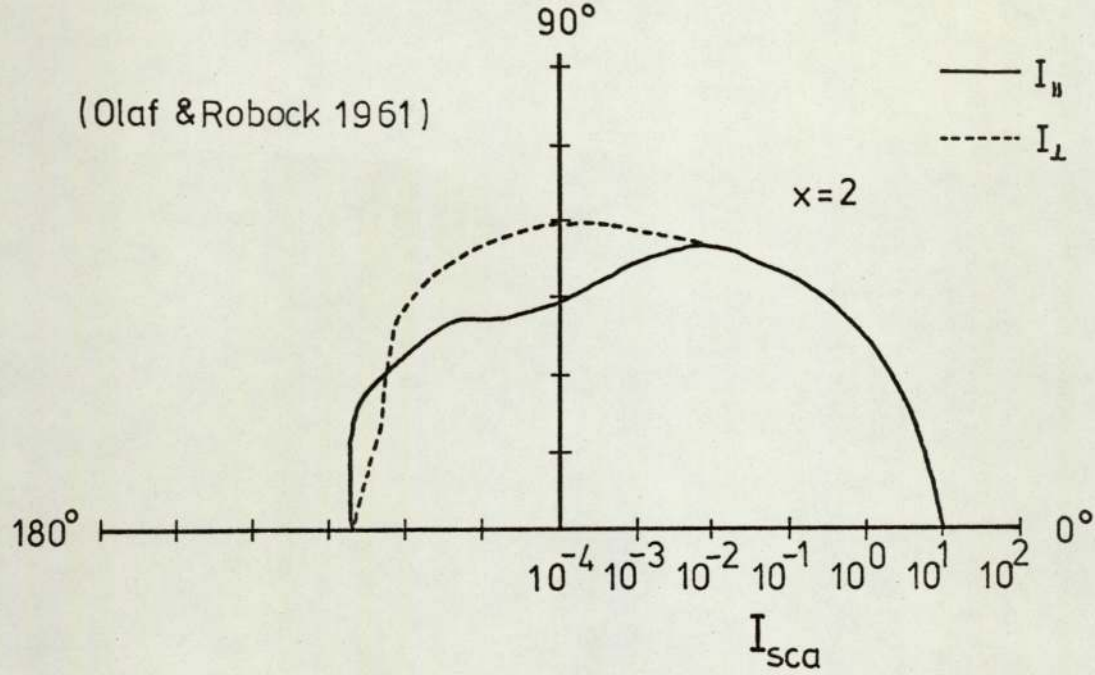


FIGURE II - 3 EFFECT OF PARTICLE SIZE ON SCATTERING PATTERN



### 2.1.1. SCATTERING CROSS SECTION AND EFFICIENCY

The scattering cross section can be obtained by integrating eq.(2-3) over the surface of the sphere, and is the total energy scattered by a particle in all directions,

$$C_{\text{sca}} = \frac{128 \pi^5 a^6}{3 \lambda^4} \left[ \frac{n^2 - 1}{n^2 + 2} \right]^2 \quad (2-10)$$

and has the dimensions of an area. A cross section for absorption may be defined similarly, both the scattering and absorption attenuate the beam and the total loss of power is extinction, as previously described. The extinction cross section is given by,

$$C_{\text{ext}} = C_{\text{sca}} + C_{\text{abs}} \quad (2-11)$$

The scattering efficiency is a function of the incident and scattered intensities and power. The scattering power is expressed by,

$$P_{\text{sca}} = C_{\text{sca}} I_0 \quad (2-12)$$

A power for absorption can also be defined in a similar way. Following this argument an extinction power is defined in the same way as the extinction cross section,

$$P_{\text{ext}} = P_{\text{sca}} + P_{\text{abs}} \quad (2-13)$$

The incident power depends on the incident intensity and the cross section of the particle, hence the efficiency of the scattering pro-



ness can be expressed by,

$$\frac{P_{sca}}{P_o} = \frac{C_{sca} I_o}{a^2 \pi I_o} = \frac{C_{sca}}{\pi a^2} = Q_{sca} \quad (2-14)$$

$$Q_{sca} = \frac{128 \pi^4 a^4}{3 \lambda^4} \left[ \frac{n^2 - 1}{n^2 + 2} \right]^2 \quad (2-15)$$

Introducing the dimensionless size parameter  $x$

$$Q_{sca} = \frac{8}{3} x^4 \left[ \frac{n^2 - 1}{n^2 + 2} \right]^2 \quad (2-16)$$

The same relation as in the extinction cross section and the extinction power can be introduced for the extinction efficiency

$$Q_{ext} = Q_{sca} + Q_{abs} \quad (2-17)$$

## 2.2. GENERALISATION OF RAYLEIGH SCATTERING TO PARTICLE CLOUDS

The previous expressions were based on the argument that the scattering is from a single particle. Those results can be generalised to clouds of particles, with the following assumptions:

1. Each individual particle behaves as a single particle and unaware of the others. For this a distance of three part-

icle radius between the particles is sufficient. Van de Hulst(1957)

2. There is no multiple scattering.
3. Particles are randomly positioned. And there is no interference between the light scattered by different particles. Under these conditions the scattering intensities for each particle can be added.

In a random distribution of identical particles the scattering is incoherent. Following the above assumption the total intensity scattered is the sum of the effect from each particle, Kerker(1969). From eq.(2-6) for N particles per unit volume, the intensity scattered per unit volume is

$$I_u^N = \frac{8N \pi^4 a^6}{R^2 \lambda^4} \left[ \frac{n^2 - 1}{n^2 + 2} \right]^2 (1 + \cos^2 \theta) \quad (2-18)$$

In terms of the total volume of scatterers, the scattered intensity dependence was expressed in eq. (2-8) , where V is the volume of the particle. Hence the total energy scattered by a cloud of particles is proportional to the volume of each particle.

### 2.3. GENERAL THEORY OF LIGHT SCATTERING

In the previous section Rayleigh scattering was discussed, which was valid for particles that are small compared to the



wavelength. For very large particles  $x \gg 10$  scattering is considered in terms of geometrical optics and as a combination of reflection, refraction and diffraction. For intermediate particle sizes the scattering is found from wave theory. The solutions for spherical particles was derived by Mie (1908). And in terms of perpendicular ( $S_1$ ) and parallel ( $S_2$ ) scattering functions, where

$$S_1 = \sum_{n=1}^{\infty} \frac{2n + 1}{n(n + 1)} \left\{ a_n \mu_n + b_n \nu_n \right\} \quad (2-19)$$

$$S_2 = \sum_{n=1}^{\infty} \frac{2n + 1}{n(n + 1)} \left\{ a_n \nu_n + b_n \mu_n \right\} \quad (2-20)$$

the intensities of scattering are given by

$$I_{\perp} = \frac{\lambda^2}{R^2 4\pi} \left| S_1 \right|^2 \quad I_{\parallel} = \frac{\lambda^2}{R^2 4\pi} \left| S_2 \right|^2 \quad (2-21)$$

The coefficients  $a_n$  and  $b_n$  are functions of particle size and refractive index. They are tabulated, Lowan (1948). It is also possible to calculate them from Aden's (1951) recurrence relations.  $\mu_n$  and  $\nu_n$  are the angular functions and expressed in terms of a Legendre polynomial.

Scattering and extinction cross sections and efficiencies have



been evaluated by Mie (1908) following the above arguments, and are given by,

$$C_{\text{sca}} = \left( \lambda^2 / 2\pi \right) \sum_{n=1}^{\infty} (2n+1) \left\{ |a_n|^2 + |b_n|^2 \right\} \quad (2-22)$$

$$C_{\text{ext}} = \left( \lambda^2 / 2\pi \right) \sum_{n=1}^{\infty} (2n+1) \left\{ \text{Re} (a_n + b_n) \right\} \quad (2-23)$$

$$Q_{\text{sca}} = (2/x^2) \sum_{n=1}^{\infty} (2n+1) \left\{ |a_n|^2 + |b_n|^2 \right\} \quad (2-24)$$

$$Q_{\text{ext}} = (2/x^2) \sum_{n=1}^{\infty} (2n+1) \left\{ \text{Re} (a_n + b_n) \right\} \quad (2-25)$$

Different ways of evaluating  $C_{\text{ext}}$  are given by Van de Hulst (1949) and Jones (1955).

#### 2.4. THE USE OF LIGHT SCATTERING IN FLAME STUDIES

The general use of light scattering techniques in flame studies were in the field of particle size determination, and the particle concentration measurements. Size distribution had also been a field of major interest.

Soot, being an important flame particle, received much

attention in the application of this technique. Erickson et. al (1964) developed a light scattering method for determining the soot particle size and concentration in flames. They have measured the relative scattering intensities for both the perpendicular and parallel polarisation components at a number of angular positions. These results were compared with theoretical curves which were calculated from general scattering theory for  $m = 1.71 - 0.76i$ , Stull & Plass (1960), and for different values of the size parameter  $x$ . From the best fit of the scattering pattern with the theoretical curves the particle size was determined. Their initial assumption was that the system of particles was monodisperse. A dispersion is said to be monodisperse when all of the particles are of the same size. Erickson's monodisperse assumption did not fit the theoretical curves well, especially at  $\sim 90^\circ$ . But with the bidisperse approach of about 1%, by mass, agglomerates and the rest having a particle diameter of 25 nm, they get a better agreement with the theory. The agglomerates were assumed to be in the form of equivalent spheres of 185 nm in diameter. Their result was the product of combining electron microscopy and light scattering measurements.

Kunugi & Jinno (1967) used a different approach. Their refractive index value was not calculated from the dispersion relations of Stull & Plass (1960) as done by Erickson et al (1964) but from Senfleben & Benedict (1917). The value was,  $m = 1.91 - 0.675i$ . Soot particle diameters were rather large



and lie between 120 -200 nm. They didn't take the agglomeration into account but concluded that since the scattering intensity is proportional to  $d^6$ , where  $d$  is the particle diameter, the light scattering method discriminates against small particles and gives only the longer ones, which scatter more effectively. Initial approach by Kunugi & Jinno was by measuring the scattered intensity from a suspensoid with a known size and concentration then relating the light scattering measurements from flames to the suspensoids of polystyrene particles.

Electron micrographs of soot particles in flames show agglomerates of various sizes, Place & Weinberg (1967). Although sampling from the flame disturbs the system and may be responsible for some of the agglomerate formation, it cannot account for the existence of all the agglomerates. Following this argument and the wide range of particle sizes as shown by the previous workers it can be concluded that the assumption of the agglomeration of soot particles in flames cannot be rejected. Contrary to the fact that Millikan (1962) argued that the particles are unagglomerated in the flame, Dalzell, et al (1970) developed a cluster model for the scattering particles, following the bidisperse model of Erickson, et al and the monodisperse model of Kunugi & Jinno. It is important to bear in mind the fact that Mie theory does not apply to agglomerates, but rather to homogeneous spheres. Dalzell et al developed the model by



combining the theory for clusters of point scatterers and each point scatterer was assumed to be located at the centre of a spherical soot particle 35 nm in diameter. It was also assumed that the cluster would have an end-to-end length. Their final approach was again by plotting the theoretically predicted scattered intensities vs the scattering angle  $\Theta$  for several values of cluster length to wavelength ratios, and compare these with the experimental curves. The refractive index of each point scatterer was assumed to be 1 ( $m \sim 1$ ). They found the average end-to-end length of the cluster as 370 nm, and the ratio of  $4.3 \times 10^{-2}$  of number of clusters to small particles, in a propane air flame.

#### 2.4.1 DISTRIBUTION OF SIZE IN SCATTERING MEASUREMENTS

Erickson's bimodal and Kunugi's monodisperse approach, leads to the problem of determining the particle size distribution by light scattering where the spheres in the medium are no longer of nearly the same size. The main objective of such an investigation is the determination of the distribution function, such that

$$P(a) = \int_a^{a+\Delta a} p(a) da \quad (2-26)$$

where  $p(a)$  is the distribution function, and  $P(a)$  would be

the fraction of particles with radius  $a \rightarrow (a + \Delta a)$ . The normal distribution function given by Hald (1962) is,

$$p(a) = \frac{1}{(2\pi)^{\frac{1}{2}} \sigma} \exp \left[ - \frac{(a - \bar{a})^2}{2 \sigma^2} \right] \quad (2-27)$$

where  $\bar{a}$  and  $\sigma$  are the average and standard deviation. Here the exponential factor in the function describes a Gaussian distribution. For a higher precision a log - normal distribution can also be used, Kerker (1969), which would eliminate the possibility of 'a' having negative values. Espencheid et al (1964) described a different distribution function, the ZOLD, zeroth order logarithmic function. And given by,

$$p(a) = \frac{\exp \left[ - \frac{(\log a - \log a_m)^2}{2 \sigma_0^2} \right]}{(2\pi)^{\frac{1}{2}} \sigma_0 a_m \exp\{\sigma_0^2/2\}} \quad (2-28)$$

The ZOLD is defined by  $a_m$  which is the modal value of 'a' and  $\sigma_0$  the breadth diameter. Values of  $a_m$  and  $\sigma_0$  are derived from the experiments by a method of trial - error. The scattered intensities should be calculated from the Mie theory for various values of  $x$  and assuming  $a_m$  and  $\sigma_0$  the calculated intensities are compared with the experimental values. Hence determining the modal value and the breadth diameter for the distribution function.



## 2.5. SCATTERING BY NON - SPHERICAL PARTICLES

Scattering of light by particles that are spherical or there is an equivalent sphere, was discussed in the previous sections. In practice these particles are generally non spherical or in form of agglomerates. These agglomerates are generally in chains and there is an extension in one dimension, Dalzel et al (1970). One approach in modelling these particles is the assumption of prolate spheroids. That is, the agglomerate has an elliptical cross section on one axis and a circular one on the other. Rayleigh theory can be applied to these elongated particles, van de Hulst (1957). In fact an explicit solution for the scattering coefficients has only been obtained for the special case of prolate spheroids. In principle scattering of electromagnetic waves by an ellipsoid of arbitrary size and optical properties can be solved exactly, using the method of separation of the variable. The classical method would be by formulating them in ellipsoidal coordinates and expressing the solutions of wave equation in terms of ellipsoidal harmonics. (Whittaker & Watson 1947).

The scattering and absorption cross sections for ellipsoids are given by Gans (1912)

$$C_{sca} = (8\pi^3/\lambda^4) v^2 \left[ (L')^2 + 2(L'')^2 \right] \quad (2-29)$$



$$C_{\text{abs}} = (2\pi V/\lambda) \left[ L' \sin \psi_1' + 2L'' \sin \psi_1'' \right] \quad (2-30)$$

Where  $L'$  and  $L''$  are functions of refractive index and eccentricity. The phase functions  $\psi_1'$  and  $\psi_1''$  appear whenever the refractive indices are complex.

The effect of elongation on scattering cross section was studied by Atlas et al (1953) for water and the particles at microwave wavelengths. Their results showed that elongation increases the scattering significantly. Jones (1972) carried out similar calculations on absorption cross sections for soot particles at wavelengths of 1 and  $5 \mu\text{m}$  and showed the significant increases in absorption cross sections as a result of elongation. And concluded that if absorptivity of such a system is used to estimate the particle concentration assuming that they are spherical, the concentration might be overestimated.

## CHAPTER 3.

### 3. CARBON PARTICLES IN FLAMES

In flames where the oxidant is present in excess of the amount necessary to convert all the carbon to carbon monoxide, carbon would not be expected to be formed. However in practice this is not the case. Carbon formation can be observed in mixtures that are considerably less rich than the amount necessary to liberate carbon in equilibrium conditions. Street & Thomas (1955), Fenimore Jones & Moore (1957). For fuels such as methane, ethane, propane, butane carbon formation was observed well before the rich limit, whereas they would not be expected to be formed even at the limit.

Carbon samples collected from flames generally show big agglomerates as well as single particles. These agglomerates can be 200 nm in size, whereas the single particles are around 25 nm in diameter. The fundamental problem in understanding the nature of these particles is the mechanism whereby simple fuel molecules are converted to large agglomerates so rapidly.

#### 3.1. CARBON FORMATION IN FLAMES

A precise definition on how the carbon particles are formed in flames has not yet been established. The subject has been



treated extensively by Palmer & Cullis (1965), Homann & Wagner (1968), Gaydon & Wolfhard (1970), Minkoff & Tipper (1962) and Fenimore (1964).

The various factors that affect and control the formation of these particles in flames usually have opposite effects on diffusion and on premixed flames. Unfortunately most of the early workers did not specify the type of flames used.

In a sooting flame C/H ratio in the fuel is an important factor in determining the carbon formation, the structure of the fuel molecule is another contributor. It was shown by Clarke Hunter & Garner (1946) that unsaturation and branching of the fuel molecules increases the amount of carbon liberated as soot. In general the tendency to soot seems to increase with compactness. The simplest qualitative test for carbon formation is the flame luminosity but this property is also dependent on the temperature. Carbon formation varies from fuel to fuel. Following Behren (1952), Homann & Wagner (1968) has grouped the flames into two types:

(i.) acetylene type; where carbon is formed throughout the outer cone

(ii.) benzene type; in which carbon is formed at the tip of the inner cone.

On the whole high pressure seems to favour soot formation



while low pressure suppresses it. Smith (1940) has carried the pressure effect experiments in ethylene flames. Macfarlane, Holderness & Whitcher (1964) studied various hydrocarbon fuels at pressures up to 20 atm using turbulent and laminar flames. They concluded that heat losses to the burner depended on pressure, and <sup>consequent</sup> changes in flame temperature could effect the carbon formation, since they reported that there was practically no increase in soot with rising pressure. Parker & Wolfhard (1950) also studied the pressure effects with acetylene - air mixtures, at pressures of 25 mmHg they found no carbon formation, but as the pressure was raised a luminous zone appeared near the centre of the flame and gradually increasing in size. At a pressure of 180 mmHg visible soot formation occurred. Fenimore Jones & Moore (1957) argued that the higher the pressure, the greater is the O/C ratio needed to suppress carbon formation.

The effects of temperature change on the soot formation is more complex. In very rich flames it may increase the formation while at the rich limit it suppresses the same property. Street & Thomas (1955), Millikan (1962), Homann & Wagner (1968).

Formation of carbon in flames is not only determined by equilibrium conditions. Additives also have different effects on the phenomena. Gaydon & Whittingham (1947) showed that by adding 0.1% SO<sub>3</sub> to the air supply of a fully aerated bunsen

burner, using town gas, causes the flame to show strong carbon luminosity. Later Fenimore Jones & Moore (1957) found a 40% increase in carbon by adding 0.2%  $\text{SO}_3$  to premixed isobutane/air mixture. While increasing carbon formation in premixed flames  $\text{SO}_3$  plays a different role in the diffusion case. Wolfhard & Parker (1950) showed that  $\text{SO}_3$  actually reduces the carbon formation in diffusion flames. Street & Thomas (1955) discussed the effect of  $\text{N}_2$  and found that it increases the carbon formation in kerosene or benzene premixed flames but it has the opposite effect on diffusion flames (Gaydon & Wolfhard 1970), this probably is a temperature effect. The process of sooting can be stopped in methane diffusion flames with the addition of 45%  $\text{CO}_2$  Arthur (1950).

Application of electric fields also effects the formation of carbon particles in flames. Payne & Weinberg (1959), Weinberg (1968) studied this phenomena in detail. Under fairly strong electric fields of either sign the soot production is reduced in a counter flow diffusion flame of  $\text{C}_2\text{H}_4 + \text{N}_2$  and  $\text{O}_2 + \text{N}_2$  Weinberg (1968). There was also a reduction in particle size. On applying a strong electric field they found that the particle sizes were reduced to 10 nm from 110 nm. Size measurements were made from electron micrographs.

The complex behaviour in the formation of carbon particles in flames leads to an argument where all the above mentioned



factors such as the effect of temperature, pressure, etc should be included in modelling this behaviour. A treatment of this kind is beyond the scope of this work and will not be considered here.

Behaviour of carbon particles in flames can be analysed in the following sequence:

- (1) Nucleation
- (2) Coagulation and growth
- (3) Oxidation

these factors will be discussed in the following sections.

With a greater emphasis on the oxidation process which is the main concern of this study.

### 3.2. NUCLEATION AND GROWTH OF CARBON PARTICLES IN FLAMES

A true mathematical theory on the nucleation process has not yet been developed. As in the formation process, nucleation also remains obscure kinetically. When a hydrocarbon vapour is passed through a hot tube, carbon is formed on the surface and once this initial surface is established its growth continues. But the exact route of this procedure is uncertain.

Gill (1958) gave an account of various theories on this procedure. Some of the theories mentioned are applicable to nucleation where others to growth processes. Smith (1940) suggested  $C_2$  polymerisation to solid carbon, and argued that this might account for the carbon formation. How-



ever in cyanogen/oxygen flames where  $C_2$  radiation is very high as observed by Gaydon & Wolfhard (1970) solid carbon is not formed, and in most flames  $C_2$  concentration is very low. It seems unlikely that this polymerisation process has a role in carbon formation, but it is possible that  $C_2$  acts as a nuclei, Fairbairn & Gaydon (1955). Tesner (1959) has considered the growth of carbon particles from nuclei which were not specified. He argued that the rate of temperature rise in the system is primarily responsible for the number of nuclei formed. He studied the phenomena in a hydrocarbon flowing furnace and followed the growth of individual particle with electron micrographs. He argued that growth occurs by actual decomposition on the nuclei and there is no intermediary polymerisation route. Place & Weinberg (1967) studied the effect of positive ions on nucleation and concluded that these may act as nuclei, the ions do not even have to be organic origin,  $C_3$  ion also caused nucleation. Their argument was supported by Miller (1967), Jensen (1973) made a modelling approach in soot formation in liquid propelled rocket motors using isopropyl nitrate and favoured  $C_2$ ,  $C_2H$  or  $C_3$  as initial nucleus and  $C_2H_2$  as the growth species confirming Tesner, Snegiriova & Knorre (1971).

Growth process in a premixed  $C_2H_2 - O_2$  flame is studied by Homann & Wagner (1968). They showed from electron micrographs that there is an intermediate phase in the carbon formation where particles with small diameters react with each other to form larger particles. This process was different from the later phase

where particles of  $\sim 20\text{nm}$  and larger agglomerates form chains

Soot growth is a very complex process. A correlation relating the growth to temperature, pressure and fuel concentration with fuel/oxidant ratio is needed in practice. Datschefshi (1962) studied the soot formation in very rich propane-air flames, this technique was extended to soot formation from methane by Narasimhan & Foster (1965). They derived a growth rate, which was based on the model where growth occurred by direct decomposition on particle surface, and given by

$$dC/dt = A (C)^{2/3} (N_s)^{1/3} (x/T^{0.5}) \exp(-E/RT) \quad (3-1)$$

where  $C$  is the soot mass concentration in  $\text{mg-cm}^{-3}$ ,  $N_s$  = particle concentration in  $\text{cm}^{-3}$ ,  $x$  is the mole fraction of  $\text{CH}_4$  where  $A$  is a constant. Their data fit the expression well when  $E = 240 \text{ KJ}$ .

The various attempts in solving the carbon formation problem in flames as mentioned above were in searching for a formation mechanism as if it was unique. Instead of such an approach it might be a more constructive attempt if the relations in particular carbon forming systems and the differences amongst those are considered.



### 3.3. OXIDATION OF CARBON PARTICLES IN FLAMES

In combustion systems the carbon particles draw attention for various reasons. They can be observed in the exhaust of many internal combustion engines, especially in diesels. In the wake of jet aircrafts they appear as black smoke. Together with carbon monoxide, nitric oxide and unburnt hydrocarbons it is considered to be the main contributor to air pollution created by hydrocarbon fuels and discharged from the stacks of industrial plants. Oxidation of these particles and the mechanism of the process is also an important problem in fluidized bed reactors and fluidized bed boilers as far as the heat transfer properties are concerned. Gas turbine engines also suffer from soot formation because of its contribution to radiant heat transfer to the combustion chamber walls, and the emissions in the exhaust. Soot formation in gas turbine engines has a negligible effect in the specific fuel consumption in comparison with the heat transfer losses. Radcliffe & Appleton (1971). The design modifications in decreasing the exhaust visibility in such cases is discussed by Faitani (1968) and Sawyer (1970). For such applications it is desired that the carbon formed is also consumed in the medium. In order to check this possibility an acceptable mechanism of oxidation properties must be established. Tu, Davis & Hottel (1934) studied the combustion rate of carbon spheres in flowing gas streams, under conditions in which both the rate of diffusion of the oxidant to the surface



and the rate of chemical reaction at the surface are the controlling factors. Tu et al concluded that, carbon when burnt in a stream of air, is consumed by direct oxidation with oxygen rather than by a mechanism in which oxygen reaches the surface in form of another species. This conclusion was reached from experiments using carbon balls of 2.5 cm in diameter suspended in a stream of nitrogen-oxygen mixture.

Yagi & Kunii (1955) in their studies on combustion of carbon particles in flames and fluidised beds, also considered the two above mentioned steps in the overall rate of reaction. They concluded that especially in the case of combustion in flames and in fluidized beds the overall rate of combustion of carbon particle is a function of not only the chemical reaction rate, but the mass transfer coefficient through the boundary film surrounding it too.

### 3.3.1 THE OXIDATION MECHANISM

In a single spherical carbon particle undergoing oxidation the two main steps that should be considered are:

1. Transfer of the oxidant molecules from the gaseous phase to the particle surface
2. Heterogeneous chemical reaction at the surface.

From these two steps the rate of consumption of carbon

per unit area of the external surface of the particle at any instant can be expressed as

$$1/R_c = (1/R_{MT} + 1/R_{CHEM}) \quad (3-2)$$

where  $R_{MT}$  is the mass transfer controlled rate and  $R_{CHEM}$  is the chemical reaction controlled rate.  $R_c$  is the overall consumption rate of the carbon particle.

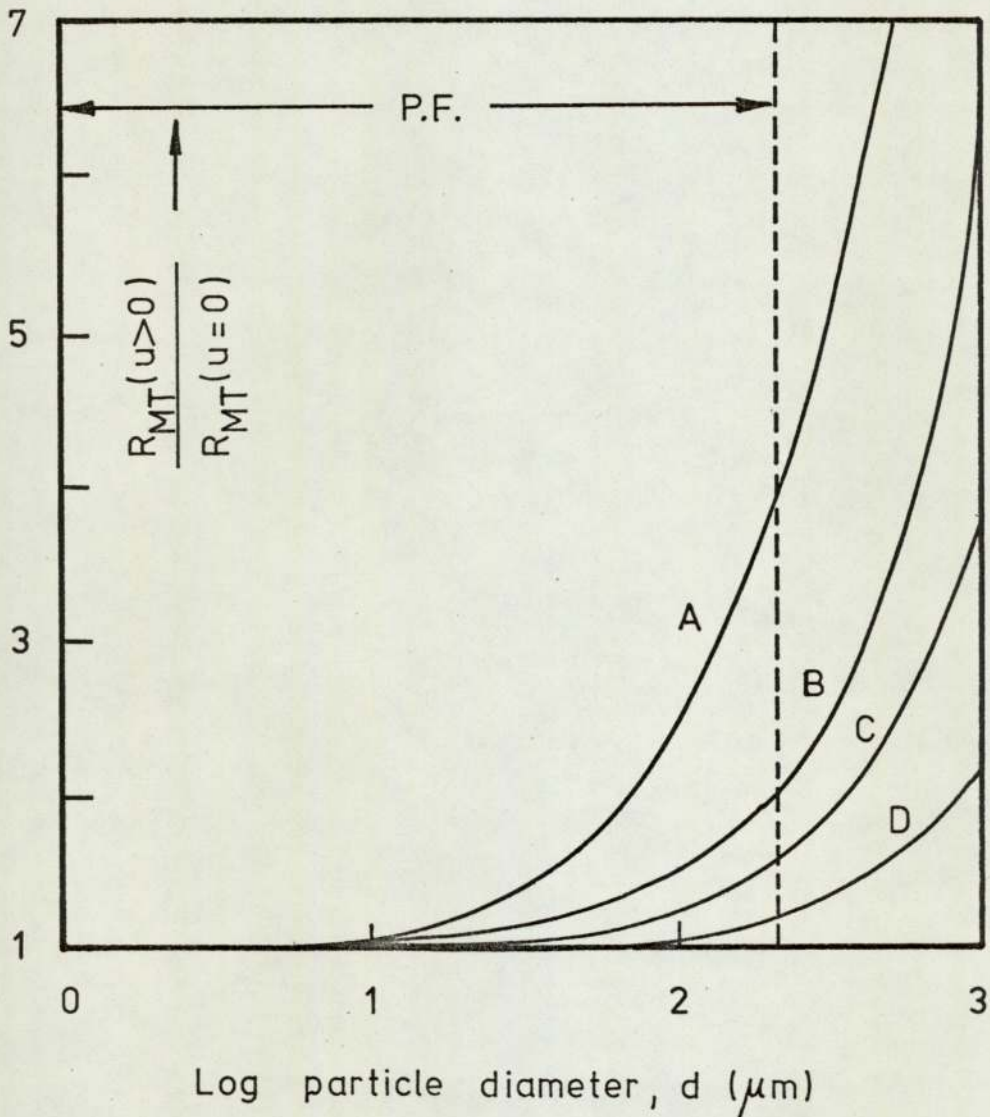
Mass transfer of the oxidising species to the surface of the particle is a function of the flow of gas, i.e. laminar or turbulent. If there is a high relative motion between the particle and the gas, the boundary layer around the particle is reduced. The mass transfer rate under such conditions can be expressed as,

$$R_{MT(u>0)} = R_{MT(u=0)} \left[ 1 + a (N_{Re})^b (N_{Sc})^c \right] \quad (3-3)$$

as a function of  $N_{Re}$  the Reynolds number and  $N_{Sc}$  the Schmidt number where  $a, b, c$  are constants. Bird, Steward & Lightfoot (1960). The effect of the flow rate around the particle to the combustion rate is discussed by Finaev (1965) and by Mulcahy & Smith (1969). Fig.(III-1). They showed that in the pulverized fuel size range little increase in the mass transfer rates occurs even at accelerations of 1000 g. Where the acceleration is expressed in multiples of normal gravity. But



FIGURE III - 1 EFFECTS OF PARTICLE SIZE AND ACCELERATION ON MASS TRANSFER RATES



A, 1000g ; B, 100g ; C, 10g ; D, g  
g, normal gravity

for larger particles of  $\sim 100 \mu\text{m}$  the mass transfer rates were almost doubled. Therefore a decrease in particle size would compensate for an increase in the relative motion between the particle and the gas as far as the mass transfer is concerned.

In the above discussions the difference between the carbon particle and soot was not emphasized. Soot particle having a much smaller diameter than pulverized fuel or the carbon considered by Tu et. al. and Yagi et. al. must behave in a different way to the carbon considered. Mulcahy & Smith (1969) expressed the mass transfer rates in terms of particle size,

$$R_{MT} = -48 \left[ (D_0/d) \rho_0 (T/T_0)^{0.75} \ln\{(1 - \bar{\delta}_{fm})\} / \bar{\delta} \right]^{3/2} \quad (3-4)$$

where  $D_0$  is the diffusion coefficient,  $d$  the particle diameter,  $\rho_0$  gas density (mass units),  $T$  the reaction temperature,  $T_0$  at standard conditions,  $f_m$  is the mass fraction of the oxidant in the gas phase,  $\bar{\delta}$  the dimensionless quantity in terms of diffusion coefficient and radial gas velocity.

The important factor in the above equation is the combustion rate being independent of the system pressure and having a small temperature coefficient (0.75), while it is inversely proportional to the particle diameter. Hence at some critical particle size the mass transfer will become faster than the chemical reaction ( $R_{MT} \gg R_{CHEM}$ ) and from eq. 3-2 the latter will become



the rate controlling ( $R_c = R_{CHEM}$ ) step. This critical diameter limit is given as  $100 \mu m$  in the literature. Magnussen (1971) studied the combustion of soot in turbulent flames and showed that the specific surface reaction rate of soot is one hundred times smaller than that of carbon, when compared with the results of Tu et al (1934), Field et al (1967) & Nagle et al (1962). Magnussen reached this conclusion by taking the characteristic soot particle dimension as 20 nm and comparing this dimension with the gas mean free path and his subsequent argument was that soot particles have no boundary diffusion film around them. It can be argued against his statement that from the electron micrographs it is known that the soot particles are in the form of agglomerates, hence the characteristic length is increased considerably. Under these conditions the appropriate length would be the one characterising the agglomerate as a whole, not of the individual particle since the gas must flow around the whole bulk volume. This might lead to a presence of a boundary layer around the particles and may contribute to the effectiveness of the mass transfer controlled rate as well as the chemical one. But as discussed in the previous chapter even though the agglomerates are present in the flame besides being in a small proportion they are also about 200 nm in size. Magnussen's mean free path at flame conditions was  $\sim 500$  nm, so even accounting for the agglomerates, as the gas cannot be treated as a continuous medium, there can be no boundary layer. Another important observ-

ation in the above mentioned paper was that there was a reduced reaction rate in turbulent flow when it would be expected that a boundary layer of sufficient thickness would reduce the reaction rate and the effect of turbulence being an increase in the mass transport the reaction rate would be increased. Consequently the existence of boundary layer around the soot particle in the flame cannot account for this observation.

In the oxidation mechanism of soot particles in flames it is generally agreed in the literature that;

1. Particles burn uniformly at their external surface only. Models based on pore expansion is incorrect. (Mulcahy & Smith (1969) )
2. Due to their small size, soot particles generated in the flame have no diffusion boundary layer
3. Following the above argument, the oxidation rate is not limited by the diffusion of the oxidant to the surface, i.e. mass transfer, but by the rate of heterogeneous chemical reaction at the surface.

### 3.3.2. THE NATURE OF THE SOOT OXIDANT

There is no generally agreed acceptable definition of the oxidising species in the literature which would cover the whole combustion process of soot particles in flames. The early workers, Tu et al (1934), argued that oxygen is the attaching oxidant



following their experiments on 2.5 cm carbon balls suspended in a flow of nitrogen/oxygen mixture. Under these conditions diffusion and chemical reaction rate both being effective in the rate control they concluded that the rate varies linearly with the partial pressure of oxygen in the ambient medium and named  $O_2$  as the direct oxidant. This argument was far from being able to explain the conditions discussed in the previous section when applying it to the oxidation of soot particles.

Lee et al (1962) studied the rate of combustion of soot in a laminar hydrocarbon flame. They proposed a semi empirical rate equation with an activation energy of 39 Kcal/mole. Samples of the gas and soot particles were collected at 1 cm intervals from the beginning of the soot column to 6 cm downstream. Size measurements were based on electron microscopy. The semi empirical rate equation is given as,

$$1.085 \times 10^4 P_{O_2}^4 T^{-\frac{1}{2}} \exp(-39.3 \text{Kcal/RT}) \text{ gr cm}^{-2} \text{sec}^{-1} \quad (3-5)$$

with  $P_{O_2} = 0.05 - 0.10$  atm and  $T = 1350 - 1650$  K. They have accepted  $O_2$  as the only important oxidant when  $P_{O_2}$  was considerable. The workers themselves, however, concluded that the validity of the above equation should be checked against other variables. Their results might be effected firstly by a narrow range of  $P_{O_2}$ , secondly by not eliminating the possible experimental limitations. Later Magnussen (1971) extended Lee et

al's (1962) work to turbulent flames and compared his results with the case of laminar flames. Magnussen's modified rate equation fits Lee et al's results with better correlation and it is argued that it will satisfy experimental data outside the experimental range of Lee et al better than eq. (3-5).

In addition he argued that from the experiments there was good reason to believe that combustion is effected with oxygen partial pressures of below 0.05 atm. Radcliffe & Appleton (1971) in their studies of soot oxidation rates in gas turbine engines followed a different experimental approach, since the previous measurements had been made at pressures and temperatures well below those encountered in these engines.

They followed the pyrographite oxidation rates and argued that within experimental uncertainty, the soot oxidation rate measurements correlate with the measurements of the surface oxidation rates of macroscopic sized samples of pyrographite. Following this argument they have related Lee et al's (1962) rate equation (eq. 3-5) to Nagle & Strickland - Constable's (1962) correlation formula and suggested a rate relation based on oxygen being the oxidising species. Later, Park & Appleton (1973) studied the surface oxidation rates of carbon black, representing the soot formed during the combustion of hydrocarbons. Their measurements were made within the range of 1700-4000 K and  $P_{O_2}$  was 0.05-13 atm., in a shock tube. They concluded that for a fixed



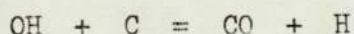
temperature and low oxygen partial pressures, the surface oxidation rate is first order in the oxygen partial pressure and at high pressures approaches to a zero-order limit. Their results were evaluated by comparing with Nagle & Strickland-Constable (1962) formula, in the same way as Radcliffe & Appleton (1971).

The fact that Magnussen (1971) based his argument on Lee et al's (1962) pioneering work undoubtedly leads to a conclusion that oxygen is the attacking species in oxidation of soot particles as in Lee et al (1962). Radcliffe & Appleton (1971) and Park & Appleton (1973) both related the soot oxidation process to an event which does not actually take place in the flame and argued that pyrographites and carbon black oxidations respectively could be related to soot oxidation rates in flames. This argument leaves room for doubt. Also Nagle & Strickland-Constable (1962) correlation formula being used in both cases may indicate the non independence of the two works. The lack of in situ measurements in the above works is another important factor effecting the result of indicating oxygen as the responsible oxidant.

Other possible attaching species such as O, OH and H are studied by Rosner & Allendorf (1968), (1970), in their studies on the experimental rates of attack of these species on graphite surfaces.

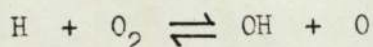
### 3.3.3. HYDROXYL RADICALS AS THE OXIDISING SPECIES

The role of hydroxyl radicals in the oxidation of carbon is first reported by Graham et al (1957), following their studies on reaction rates of high temperature pyrolytic carbons. OH radicals in their report is taken to be the product of dissociation of water at high temperatures, from their experimental results it was argued that at 2600K the rate of reaction may be governed almost entirely by the reaction,

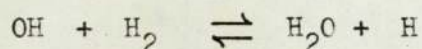
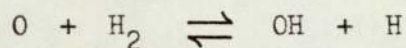


the attribution of the reaction to OH radicals followed the reaction rate being  $10^2$  greater than at low temperatures.

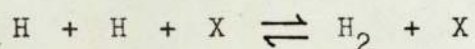
Hydroxyl radicals as the oxidising species in the oxidation of soot particles and their dominance over much larger concentrations of  $\text{CO}_2$  or  $\text{H}_2\text{O}$  was pointed out by Millikan (1962). Later Fenimore & Jones (1967) argued that at wider limits than Lee et al (1962) of  $P_{\text{O}_2} = 10^{-4} - 0.3$  atm and  $T = 1530 - 1890\text{K}$  soot oxidation does not in fact depend very strongly on  $P_{\text{O}_2}$ , an additional mechanism besides oxidation by  $\text{O}_2$  was important and OH radicals were named as the oxidising species. The nature of OH radicals is from the following principal reactions in flames of  $\text{H}_2/\text{O}_2$ ,



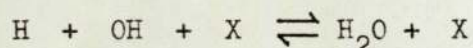




once a hydrogen atom is present in the system, it acts as the initiator, the propagation and the branching steps of the chain reaction then follows. Since the radicals are only changed from one to another in this way, the reaction could never approach a final state of chemical equilibrium, by the function of these bimolecular steps above, unless terminated by another process. The only mechanism that could establish a final state of equilibrium must be by way of radical recombination reactions involving a third body, like



or



where X is any third body molecule. The nature of this third body and its various characteristics is studied by Padley & Sugden (1959). They showed that while silver was acting as intermediate, lead favoured the H + OH recombination and sodium the H + H recombination, even though both of the processes were operative for Na. The radiative recombination of H + OH is also studied by Padley (1960). Other recombination reactions studies are reported by Jensen & Padley (1967), Kelly

& Padley (1969), Jensen & Padley (1966). It should be pointed out at this stage, that the free radical concentrations in the reaction zone of flames are in excess of their thermodynamic equilibrium values at lower temperatures Bulewicz, James & Sugden (1956). This phenomena will be discussed in section (5.2), in detail.



## CHAPTER 4

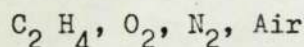
### 4. APPARATUS

In following the oxidation mechanism of soot particles in flames the importance of in situ measurements and the flame disturbance was discussed in the previous chapters. As a result of these arguments in situ measurements were the basis of the detecting system. Light scattering technique has this advantage in flame studies over the other possible methods. In order to carry out the experiments on actual flame soot, instead of a correlation with an external process, the particles were produced within the system, and carried pneumatically to the oxidation medium. The burner, light scattering system, and the other features of the apparatus will be discussed in the following sections.

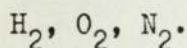
#### 4.1. THE BURNER SYSTEM

The generation and oxidation of soot particles take place in two different sections of the burner system. The unit is essentially composed of two burners with similar characteristics:

1. PRIMARY BURNER: for the production of soot, using



2. SECONDARY BURNER: for the oxidation of soot, using



Both flames are premixed laminar flames with additional shields around for different purposes. (Fig. IV-1).

#### 4.1.1. PRIMARY BURNER

Burner design is shown in Fig. (IV-2). It is made out of two parts, The burner barrel and the internal tubular section. The gas inlets are from the main burner barrel body, air inlet is placed tangential to the barrel. Tubular section has three compartments, the top one is for cooling water, middle compartment is for introducing air, for shielding purposes. From the flame stability experiments it is found that an additional air jacket is necessary to keep the flame, in the experimental conditions, stable in the closed medium. The lower section acts as a mixing chamber for the fuel and oxygen, as well as the gas inlet for the actual soot generator. The metal discs used to separate the three sections, have appropriate number of holes drilled through for the hypodermic tubes to penetrate. The inner flame where  $C_2H_4$ ,  $O_2$ ,  $N_2$  is fed burns on 19 of the hypodermic tubes arranged with hexagonal symmetry; there is an extra 18 for the air shield. The tubes were supplied by Cooper's Needle Works and are 18 gauge, with an internal diameter of  $8.4 \times 10^{-4}$  m. All the parts of the burner are made out of brass except the stainless steel hypodermic tubes and the rubber 'O' rings for separating the compartments. The tubes are soldered together by using ordinary soft solder. With the help of



FIGURE IV-1 THE BURNER SYSTEM

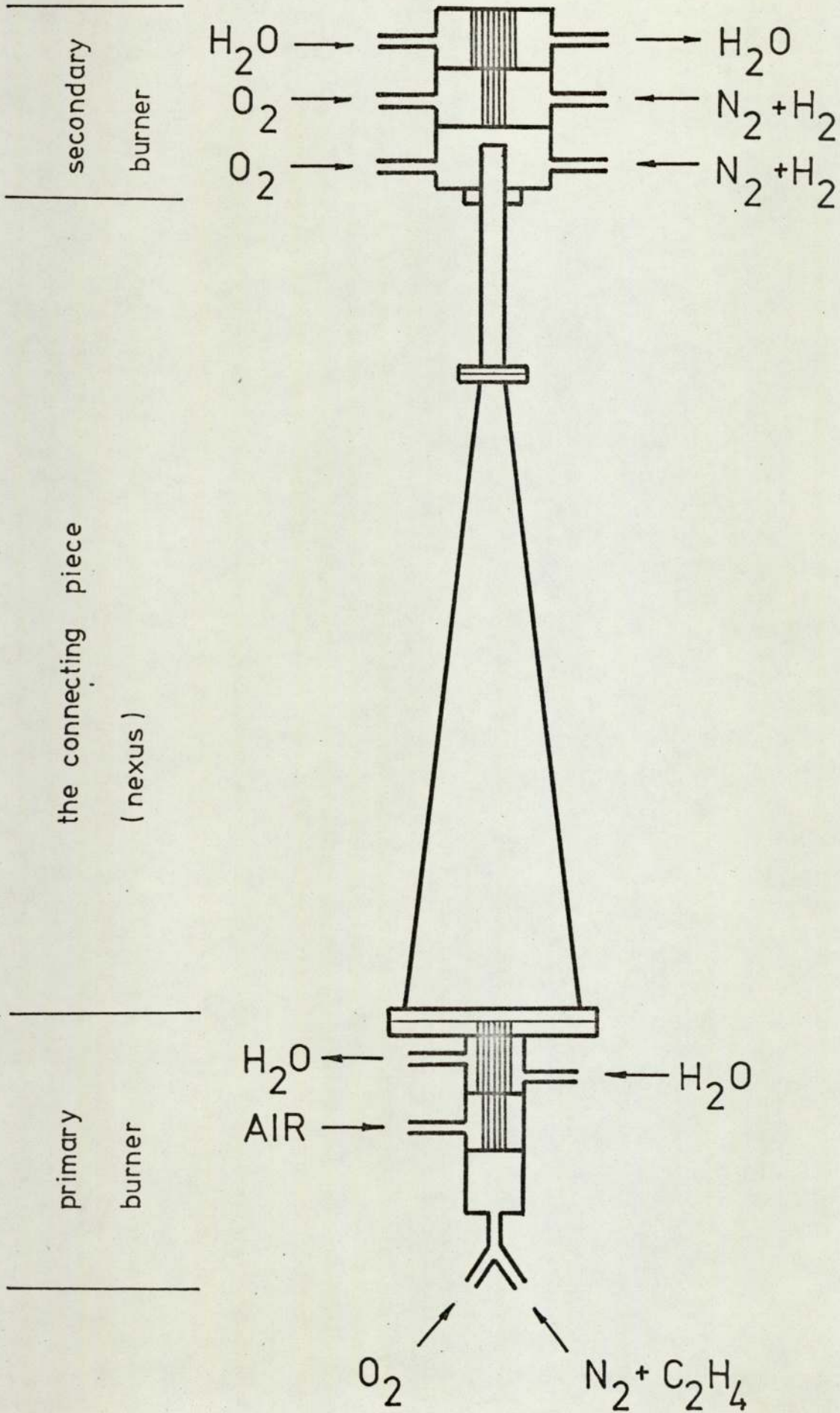
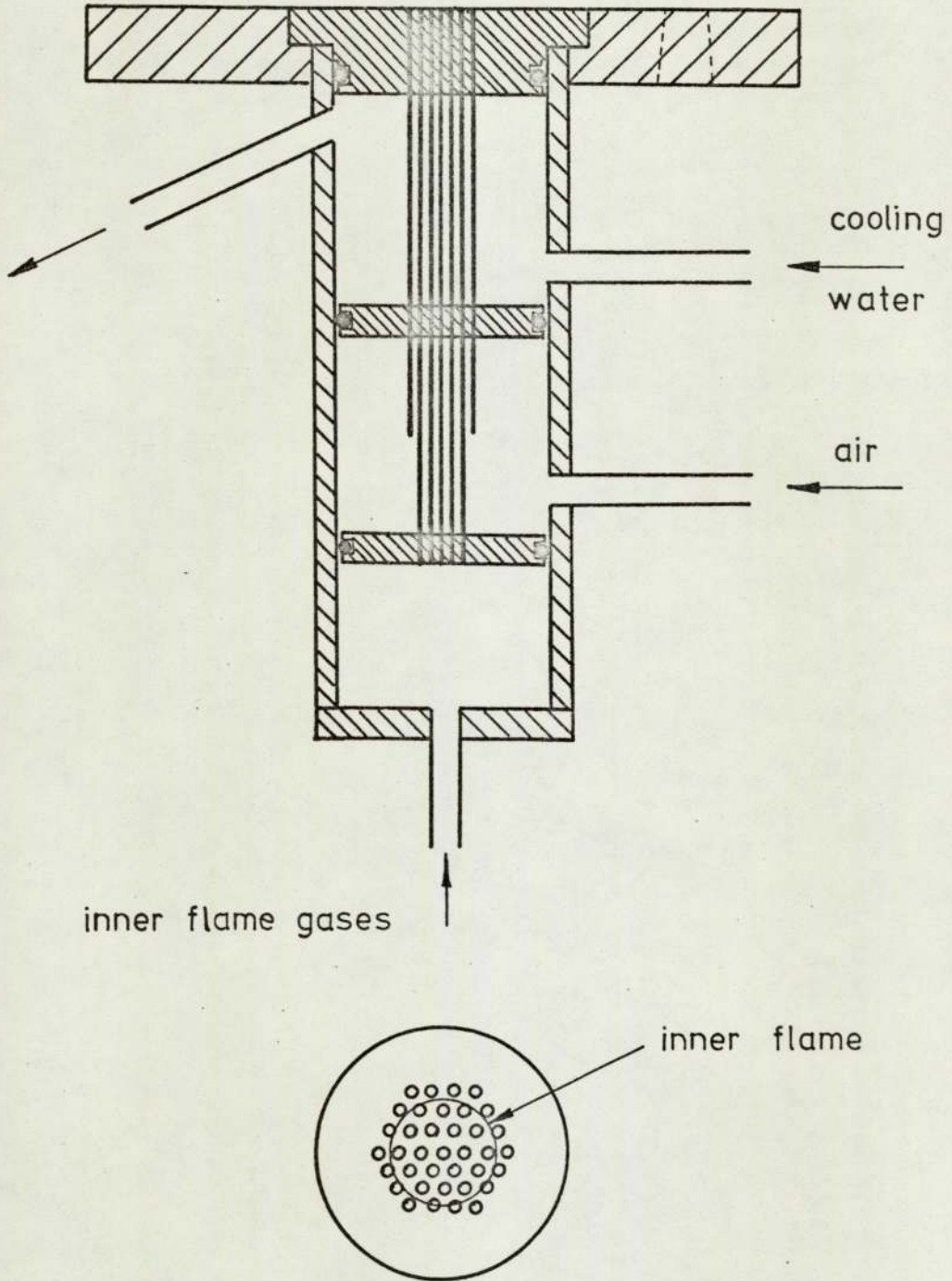


FIGURE IV - 2 PRIMARY BURNER



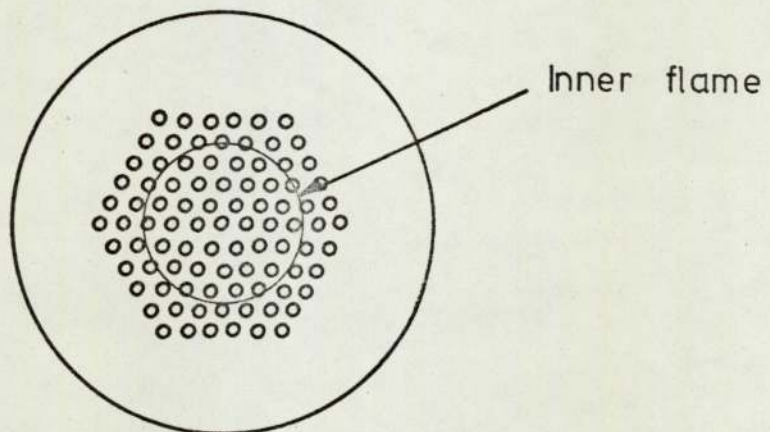
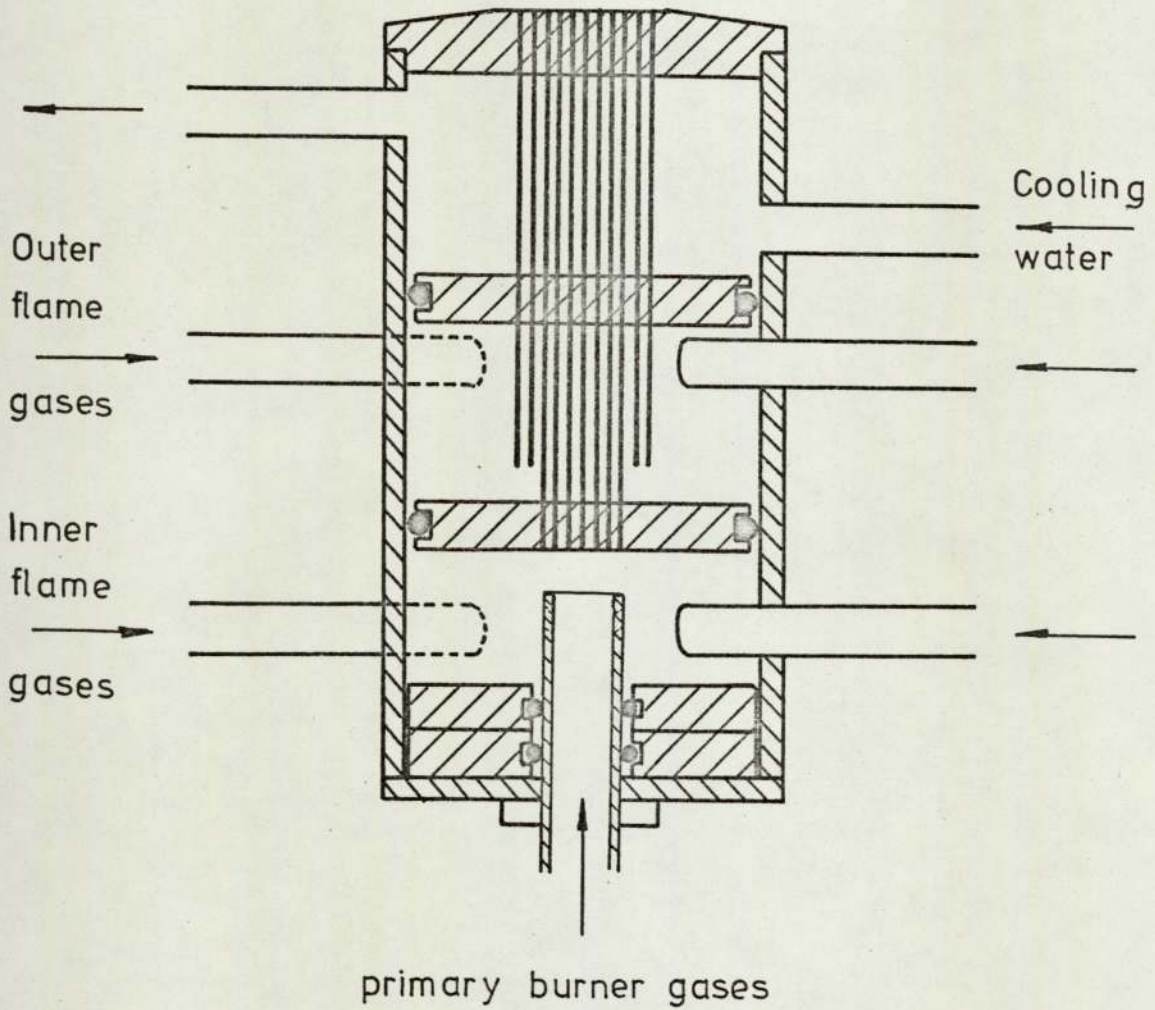


the cooling water circulation it is possible to keep this arrangement below the melting point of the solder used. The internal tubular section is fixed to the burner barrel with six screws from the top. There is a flange on the top of the burner for connections with the conical connector piece, equipped with six 2BA screws. The flange disc has an ignition inlet, plugged with a tapered metal to glass seal nut having a platinum wire of  $\sim 3$  cm protruding to the centre of the burner with the other end connected to a high voltage spark source. (H.F. TESTER Model T.1). This permits ignition of the flame from outside without disconnecting the flange. All the gas tubes were  $\frac{1}{2}$ " copper tubes with additional plastic tubes where necessary and  $\frac{1}{4}$ " knots fittings were used throughout.

#### 4.1.2 SECONDARY BURNER

The secondary burner shown in Fig. (IV-3) is of the water cooled Meker type and similar to the primary burner, made for a premixed hydrogen oxygen flame. A hydrogen flame has the advantage of possessing a very low level of natural ionisation. As in the primary burner the secondary one has a main burner barrel and an inner tubular section. Cooling water in the top compartment is for the same purpose described in section (4.1.1.). The middle section is for providing a shield flame around the actual flame where the oxidation process being followed takes place. Cooling effects by the surrounding air and the

FIGURE IV - 3 SECONDARY BURNER





external limitations can be greatly eliminated by this additional flame mantle as shield.

Internal tubular section is composed of  $8.4 \times 10^{-4}$  m internal diameter stainless steel hypodermic tubes soldered together and individually located in the separating brass discs with hexagonal symmetry. Tube spacing is arranged to allow for the expansion in a horizontal plane by a factor of  $7^{(2/3)}$  (Miller 1969). The middle section is for outer flame inlets and the bottom part is for the inner flame. Fuel and oxygen inlets are placed tangential to the main burner barrel for providing a swirling motion, which is particularly important in the inner flame case. While the bottom section acts as inner flame inlet, it also provides a mixing chamber for the primary burner product soot before entering the tubes. The swirling motion provided by the tangential inlets contributes greatly to the uniform distribution of soot particles amongst the hypodermic tubes. Soot inlet to the secondary burner's bottom compartment is specially designed to overcome the distribution problem and will be discussed in the following section.

Internal tubular part of the secondary burner when inserted into the burner barrel is held in position by small bolts through the upper disc and by the rubber 'O' rings on the other two. Similar to the primary burner all parts except the stainless steel tubes and rubber 'O' rings of the secondary burner is

made out of brass. Small combustion zones were maintained above each tube to a height of  $\sim 1-2 \times 10^{-2}$  m, providing a flat reaction zone, important in flame reactions studies.

#### 4.1.3. THE CONICAL NEXUS

*The basic design of the apparatus may be divided into three parts, two burners and a connecting piece which should be a closed chamber transferring the soot from the primary burner where it is produced, to the fuel inlet of the secondary burner.*

Following this argument a simple soot generator was designed, using  $\frac{3}{4}$ " ID brass tube as the burner body with a nozzle at the mouth covered with a wire gauze. The burner mouth and the fuel inlets were  $\frac{1}{4}$ " ID. In the construction of this burner  $\frac{3}{4}$ " ID brass tube and appropriate sizes of Enots fittings were used. The connecting piece was also a brass tube of  $\frac{3}{4}$ " ID and  $\sim 60$  cm long which could be screwed on top of the burner after ignition, and wound with a  $\frac{1}{4}$ " ID copper tube for cooling. Different fuel inlet arrangements were used to get a stable flame. The nozzle size was varied between  $1/8$ " -  $1/4$ ", fuel and oxidant were pre-mixed, a diffusion flame arrangement was also tried but it was not possible to keep the flame steady and going inside the nexus. A wider connecting piece was also tried. Following these findings a primary burner as described in sec.(4.1.1.) was constructed.

The link between the primary and secondary burners was

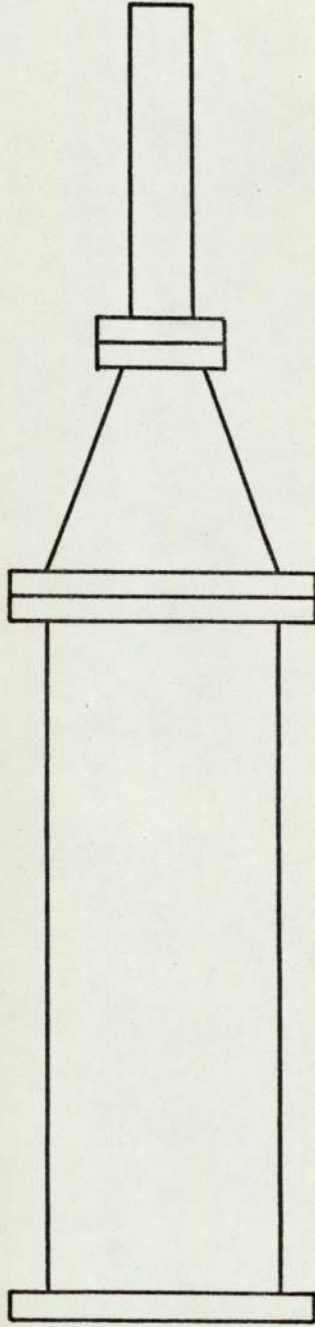


initially made out of three units as in Fig. (IV-4). Starting from the soot generator a cylindrical section of  $\sim 30$  cm long and  $2\frac{1}{2}$ " ID is followed by a small conical unit of 9.5 cm high and having a diameter of  $2\frac{1}{2}$ " ID to  $\frac{1}{2}$ " ID on each end. After reducing the initial diameter from  $2\frac{1}{2}$ " to  $\frac{1}{2}$ " a straight tube of 22 cm with  $\frac{1}{2}$ " ID was the final path in the soot flow. The three units were connected together by their flanges at the ends.

Secondary burner was standing on this  $\frac{1}{2}$ " tube which protrudes about 8 mm into the mixing chamber. The base of the burner, is held on the tube by two 'O' rings as a safety measure in case of flame flash back. From the preliminary runs it was found that, soot particles, when introduced to the mixing chamber of the secondary burner tend to concentrate around the central hypodermic tubes. Hence the soot inlet mouth is modified into a form of distributor, to overcome this. Fig. (IV-5).

The distributor is made by plugging the  $\frac{1}{2}$ " inlet tube, with a double sloped cone, from the top and drilling 12 oval holes all around with walls following the initial slope of the cone towards the inside and 4 mm from the top with a diameter of 3 mm. By this arrangement it was possible to divide the initial soot stream to 12 and obtain a flow, like a saucer, of soot. This flow, by the help of tangential fuel and oxygen

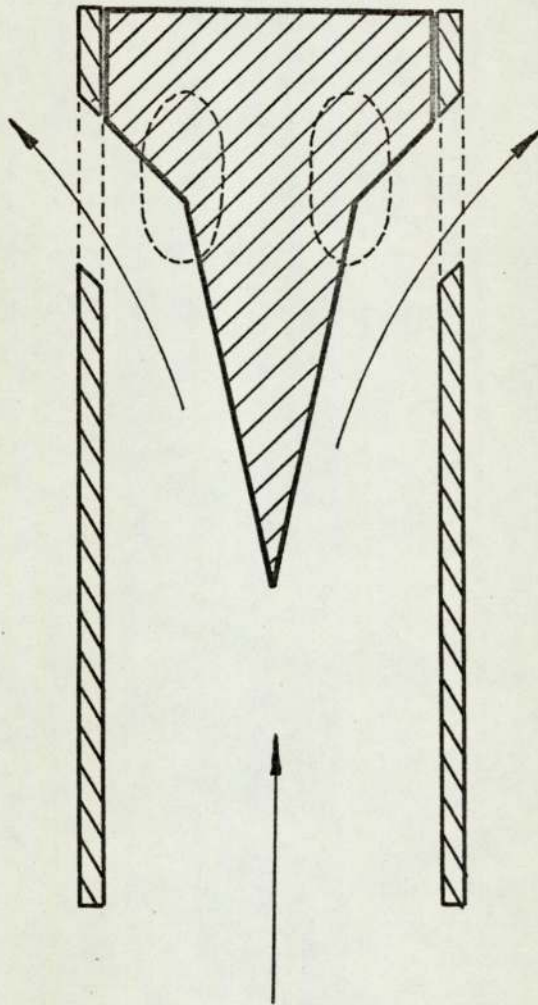
FIGURE IV-4 INITIAL NEXUS DESIGN



primary burner  
connection



FIGURE IV-5 THE SOOT DISTRIBUTOR



primary burner products  
(SOOT)

inlets into the chamber, undergoes a swirling motion, hence, a better distribution of soot amongst the hypodermic tubes. The selective distribution of soot particles, especially to the central tubes, was not recorded when using the above mentioned distributor.

Combustion products of the primary burner, when the three member nexus was used, caused clogging problems. Water vapour condensation and sludge formation with the soot, restricted the working time of the burner system and caused variations in the soot delivery. Therefore it was necessary to keep both the nexus and the secondary burner at a high temperature where condensation would not take place. The sudden decrease in the diameter of the three member connector was also a limiting factor, as far as the deposition of soot on the inner walls and especially at the  $\frac{1}{2}$ " ID side of the cone is concerned. Hence a conical vessel of  $\sim 50$  cm long and rolled from copper sheet was used (supplied by R.P.E. Westcott). The diameter was  $2\frac{1}{2}$ " and  $\frac{1}{2}$ " at each end. Distributor head with  $\frac{1}{2}$ " ID tube was mounted on the conical nexus and the whole unit is wrapped with a heating tape. The temperature was held at a point, where the condensation of the combustion product water vapour, would not take place during the runs. General layout of the final primary and secondary burners and the nexus arrangement which was used in the experiments throughout, is shown in Fig. (IV-1).



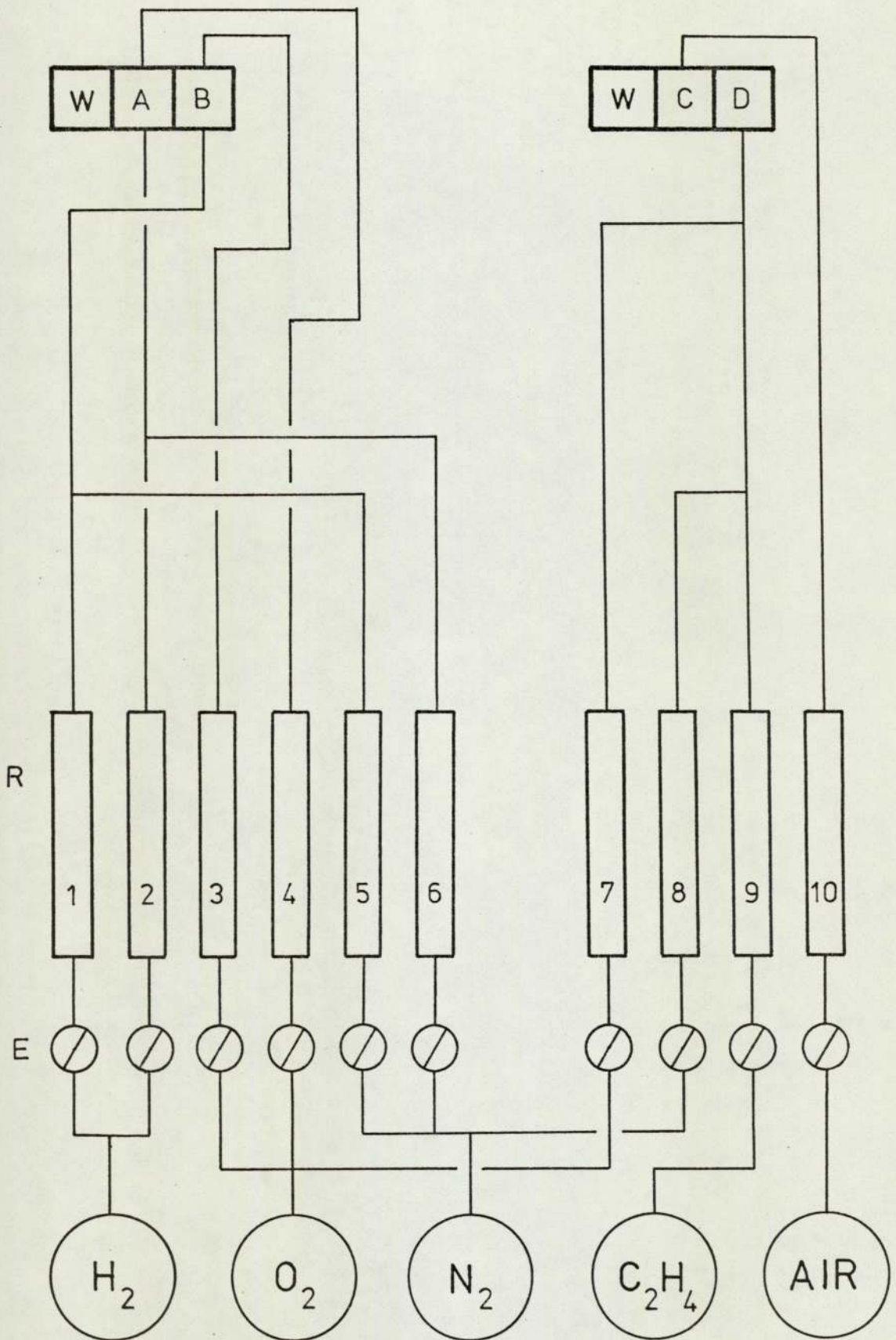
#### 4.2. GAS SUPPLY SYSTEM

The unburnt gases used in the primary and secondary burners, were  $C_2H_4$ ,  $N_2$ ,  $O_2$ , AIR and  $H_2$ , and were obtained from commercial cylinders (British Oxygen Co.). Nitrogen was from "white spot" purity cylinders. Gas supply arrangement is shown in Fig.

(IV-6). The flow rates were controlled by "Clockhouse" Needle valves which were placed on each of the ten feed lines. Measurements of the flow rates were made by pre-calibrated Rotameters. Calibrations were carried out by using soap bubble technique for the small rates and wet-gas meter (Parkinson Cowan meter) for flows bigger than 1.5 lt/min. As a minimum safety measure hydrogen and oxygen supplies were only mixed at the appropriate mixing chambers of the secondary burner. Flow rates for the inner and outer flames were arranged to be such that, both would have the same convective velocity. The tubes used on the supply lines were plastic, except the lines from the cylinders to the flow meters and the appropriate inlets on the burners.

Rotameters 5 and 8 which are the controls for the nitrogen supply to primary and secondary inner flames were also used for cleaning the hypodermic tubes where the soot causes the clogging. This is achieved by passing a very high flow of nitrogen through the tubes and tapping the burner slightly when necessary.

FIGURE IV - 6 GAS SUPPLY SYSTEM





A : secondary burner outer flame

B : secondary burner inner flame

C : primary burner outer flame

D : primary burner inner flame

E : control valves

W : cooling water

R : rotameters

During the temperature measurements a slightly different gas supply arrangement was adopted, which will be discussed in the following sections.

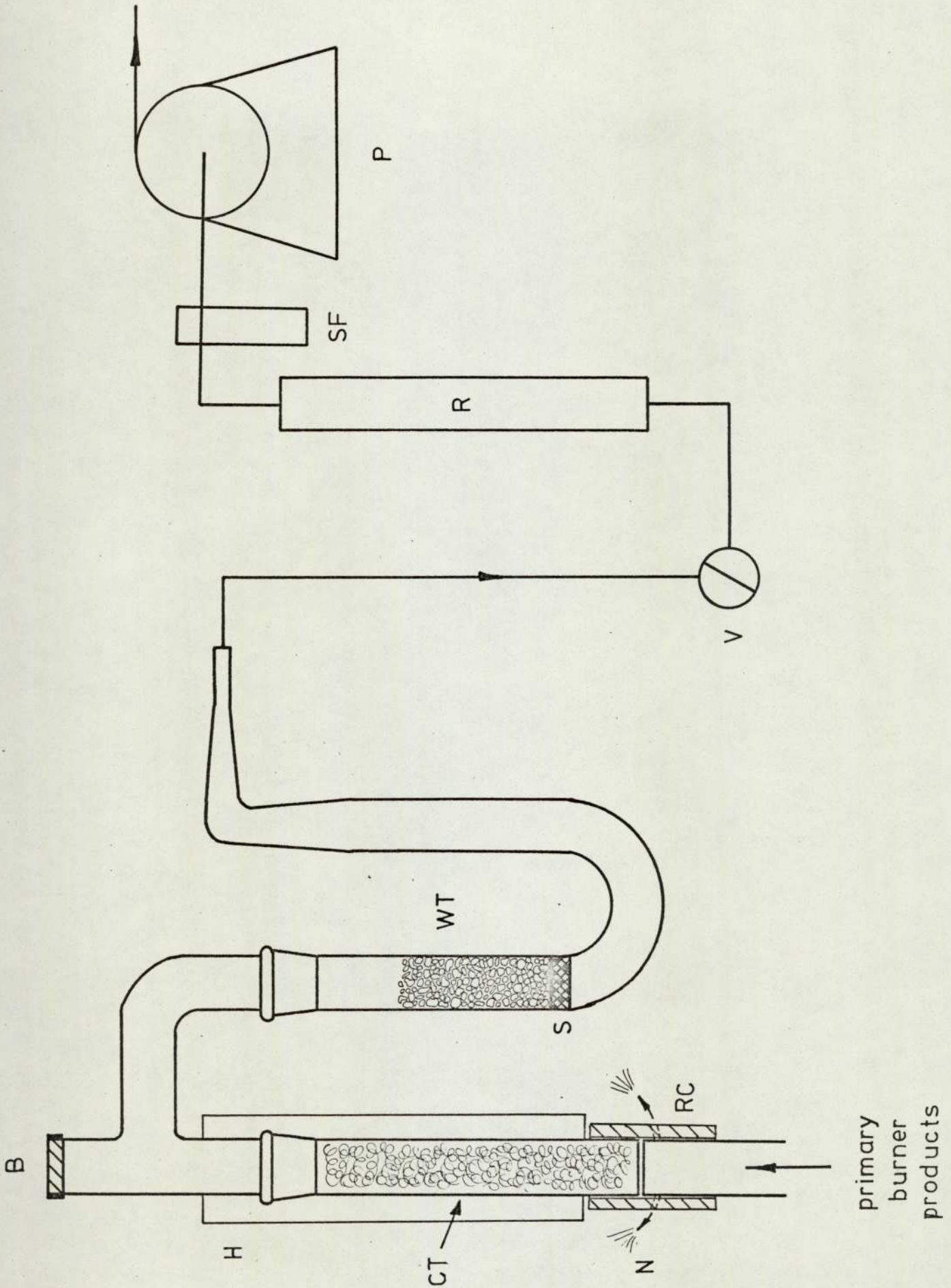
#### 4.3. GAS ANALYSIS ARRANGEMENTS

##### 4.3.1. GAS SAMPLING SYSTEM

In determining the composition of the primary burner combustion products, which is the feed for the secondary burner inner flame, a gas chromatographic technique is used in conjunction with direct weighing. The two major products, being soot and water vapour, created similar problems by forming sludge as mentioned in section(4.1.3.) On these grounds, the first step in sampling is to keep the soot and water vapour separate, that is, in vapour form and prevent sludge formation. In order to achieve this a sampling system as shown in Fig. (IV-7) is designed. The carbon trap is basically a glass wool medium, placed in a tubular oven, to keep the temperature high enough for water vapour. The trap is secured on the distributor head after removing the conical stopper. A ~ 3 cm long rubber tube was used as a seal, the outlets around the seal was for pressure release purposes. Water trap is a glass U tube with a sintered glass disc on one side and filled with self indicating silica gel. A 'Meterate' flow meter for control is followed by a safety flask. The whole unit is connected to a diaphragm suction pump, and the suction rate is maintained at



FIGURE IV - 7 GAS SAMPLING SYSTEM



CT : carbon trap

WT : water trap

V : control valve

R : flow meter

P : suction pump

S : sintered glass stopper

H : heating tube

B : sampling bung

RC : rubber connector

N : pressure release nozzles

SF : safety flask



relative gas flow rates.

Sampling is done by hypodermic gas syringes, and samples drawn from the rubber plug situated before the water and after the carbon trap.

The amount of soot and the water as combustion product is determined by direct weighing of the traps before and after the runs. Particular attention was given to changes in flow through the system, and pressure release nozzles, by monitoring the rate. This is caused by blockage due to prolonged runs.

#### 4.3.2. ANALYSIS BY GAS CHROMATOGRAPHY

Gas chromatography is an analysis technique which can be used for continuous or batch chemical analysis and separation. It is based on the preferential adsorption of different components of a gas mixture as it contacts an adsorbent medium. Each component appears at a different time in the flow process as a result of this selectivity. The choice of the adsorbent medium is the major step in adopting such an analysis technique. A chromatograph consists of a column packed with the suitable adsorbent, a flow system, a sample introduction system and a detector. Advantages of using such a technique for analysis of flame gases are high selectivity, high sensitivity,

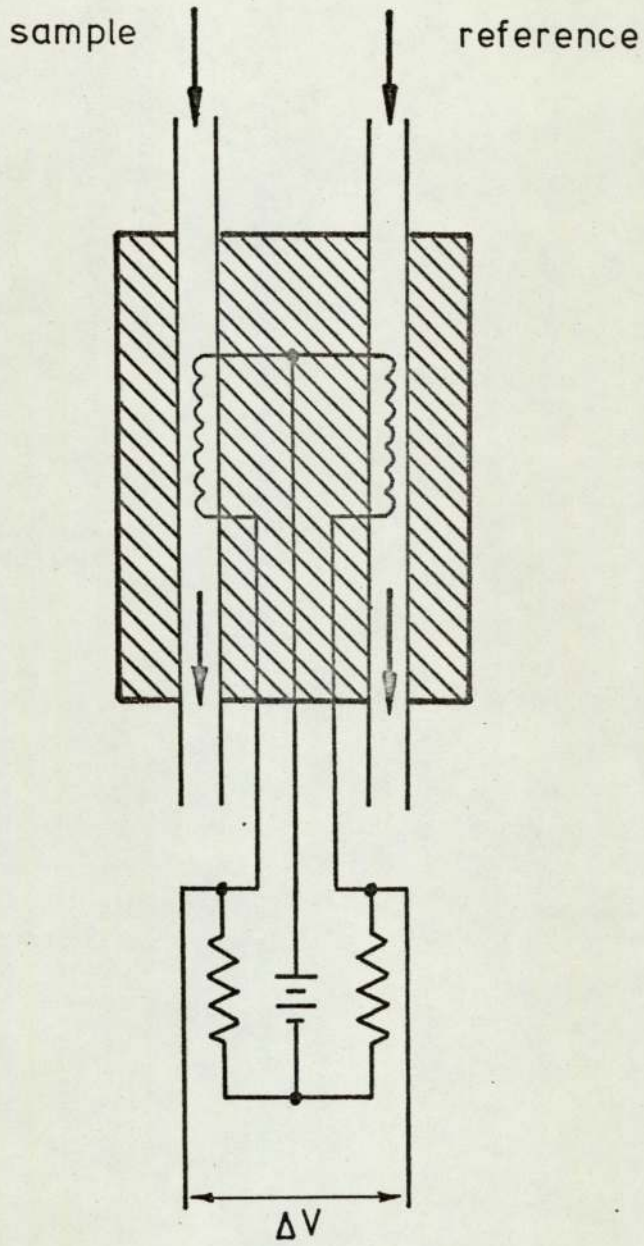
analytical accuracy, need for a small sample size and the rapidity.

Primary burner combustion products include  $\text{CO}_2$ ,  $\text{CO}$ ,  $\text{N}_2$ ,  $\text{CH}_4$  and  $\text{C}_2\text{H}_4$  as major components, as determined by mass spectrometer, others being  $\text{C}$  and  $\text{H}_2\text{O}$  are based on the traps arrangement. The choice of detectors is between flame ionisation detector (FID) and thermal conductivity detector (TCD) for the above mentioned combination of gases. TCD would be the detector of choice from ppm levels to percentage quantities, and because of its sensitive response to all component gases involved (except  $\text{C}$  and  $\text{H}_2\text{O}$ ). Whereas FID do not respond to permanent gases such as air, carbon monoxide and carbon dioxide. Grune (1962), Hammarstrand (1974).

TCD, which is also referred to as the Katharometer, consists of a wire heated by a stabilised electric current and placed in the cell through which the gas mixture to be analysed is passed. In the detector head the cell has two chambers, one through which only the carrier gas passes as reference and the other for the carrier gas and the sample of mixture for analysis. The system is balanced by a Wheatstone bridge arrangement as shown in Fig. (IV-8). The equilibrium temperature of the wire and therefore its resistance, keeping the variables as temperature of the gases, pressures and flow as equal, depends only on the thermal conductivity of the gas, flowing.



FIGURE IV - 8 TCD



Hence in the presence of a different gas, than the carrier gas, in the cell, there will be a change in the resistance, and this change is then converted to potential difference. Therefore the apparatus will be more sensitive, if the difference between the thermal conductivity of the carrier gas and the constituents in question is greater. Helium or hydrogen would be the choice because of their very high conductivity, in comparison with the rest of the gases.

There is no single column that will separate all the gases mentioned at ambient or high temperatures. A more complex system would be required. The method recommended by Hammarstrand (1974) involves a dual column system with a column switching valve. The column arrangement is shown in Fig. (IV-9). Molecular sieve 5A separates  $O_2$ ,  $N_2$ ,  $CH_4$ , CO however  $CO_2$  is irreversibly adsorbed on molecular sieves and do not desorb at high temperatures that can be involved in gas chromatographic analysis. However porous polymers, such as Poropak Q and chromosorb 102, will not separate  $O_2$ ,  $N_2$ ,  $CH_4$  and CO which will appear as a composite peak, but are capable of separating  $CO_2$  and higher

Therefore the use of chromosorb 102 column in conjunction with a molecular sieve 5A column would be the solution for the complete analysis of the gas mentioned. As in Fig. (IV-9) 10' x 1/8" stainless steel column packed with 80/100 mesh chromosorb 102 and 5' x 1/8" stainless steel column packed with 30/60 mesh molecular sieve 5A connected by a four way



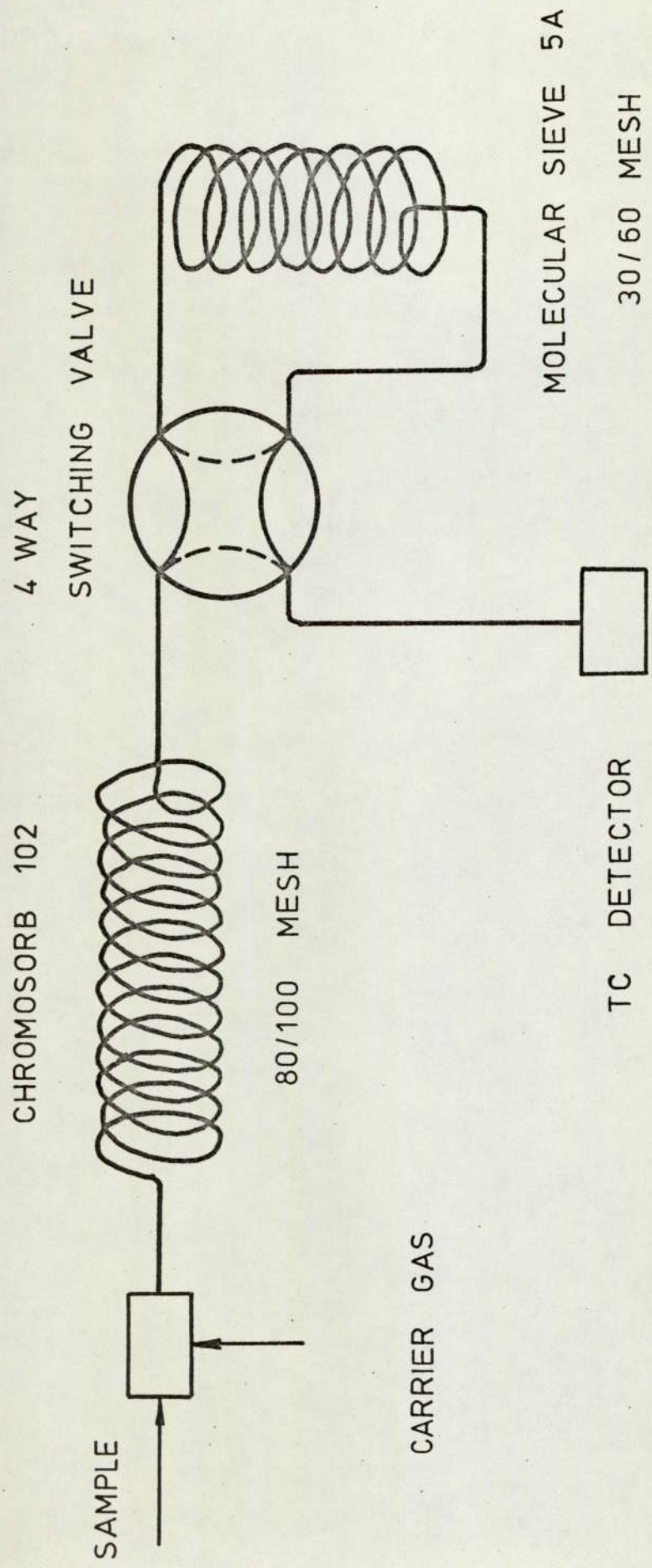


FIGURE IV - 9 GAS ANALYSIS COLUMN SYSTEM

rotary column switching valve forms the separating system. The four way switching valve allows the carrier gas to flow through both columns to the detector or through the porous polymer to the detector. During the single column case, the molecular sieve column is in a closed loop with no flow. Pye 104 series chromatograph coupled with a TCD detector head is used throughout, output was recorded on a Honeywell vertical chart recorder. A typical chromatogram achieved by this principle is shown in Fig. (IV-10). Even though a temperature programming is useful to reduce the time required for complete analysis, it wasn't found practical in the experiments carried out.

The detector and column conditions during the analysis were as follows:-

Column Temperature	:	52C
Column Pressure	:	45 psi
Bridge Current	:	150 mA
Carrier Gas Flow	:	30 ml.min <sup>-1</sup> (He)
Sample Volume	:	1 ml

A reference column with the same conditions is also used in conjunction with the separating column, as described in the TCD principles. A typical composition of the primary burner gas analysed by this technique is given in Table (IV-1). The amount of unburnt ethylene is calculated from mass balance, and the air entrapment during the sampling process is eliminated



TABLE (IV-1) TYPICAL COMPOSITION OF PRIMARY BURNER GASES AND FLAME CONDITIONS.

1° Burner feed	lt/min	% (vol)	% (weight)
O <sub>2</sub>	0.45	29	33
N <sub>2</sub>	0.30	40	38
C <sub>2</sub> H <sub>4</sub>	0.61	31	29
AIR	0.64		

1° Burner gas	% (weight)	% (vol)
CO	21.7	18.9
CO <sub>2</sub>	5.4	3.0
CH <sub>4</sub>	2.5	3.8
C <sub>2</sub> H <sub>4</sub>	10.5	9.1
H <sub>2</sub> O	18.2	24.6
C	3.7	(*) 7.5
N <sub>2</sub>	38.1	33.1

\* C assumed to be in gas form

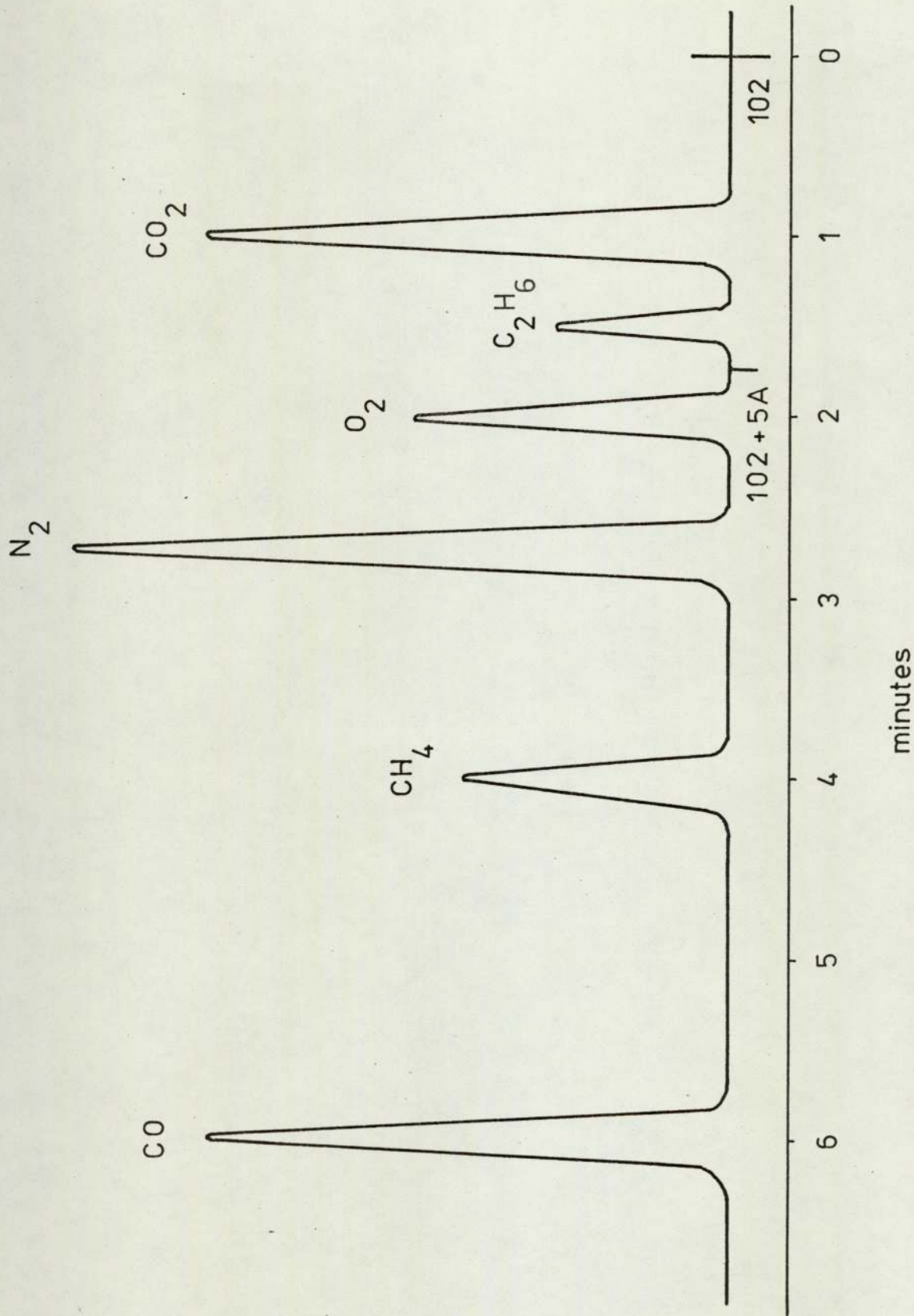


FIGURE IV - 10 A TYPICAL CHROMATOGRAM



in the calculations. The amount given for carbon in the table is derived assuming C to be in gas form.

#### 4.4. DETERMINATION OF FLAME TEMPERATURES

##### 4.4.1. METHOD

Flame temperatures have been determined by using the sodium - D - line reversal method. The technique is well established in the literature, Griffiths & Awbery (1929), Lewis & von Elbe (1963), Gaydon & Wolfhard (1970). The principle advantage of this technique is that it does not disturb the system being studied, and has no higher temperature limit applicable in normal flame studies. The method gives the electronic excitation temperature for sodium and as shown by Griffiths & Awbery (1929) can be taken as the true thermodynamic temperature of the system.

It is well known that, when sodium is introduced into the flame it emits two yellow D - lines at 589 and 589.6 nm. The comparison of these two yellow lines with a background source is the basis of the technique. Fig. (IV-11) shows the arrangement used. A tungsten strip filament lamp (Phillips) was used as the background source. The light from the lamp (S) is focused with the lens ( $L_1$ ), on the flame to give an image of the filament. The image of both the flame and the filament is then focused by the second lens ( $L_2$ ) on to the slit of a Hilger constant deviation spectrometer. An aperture stop in front

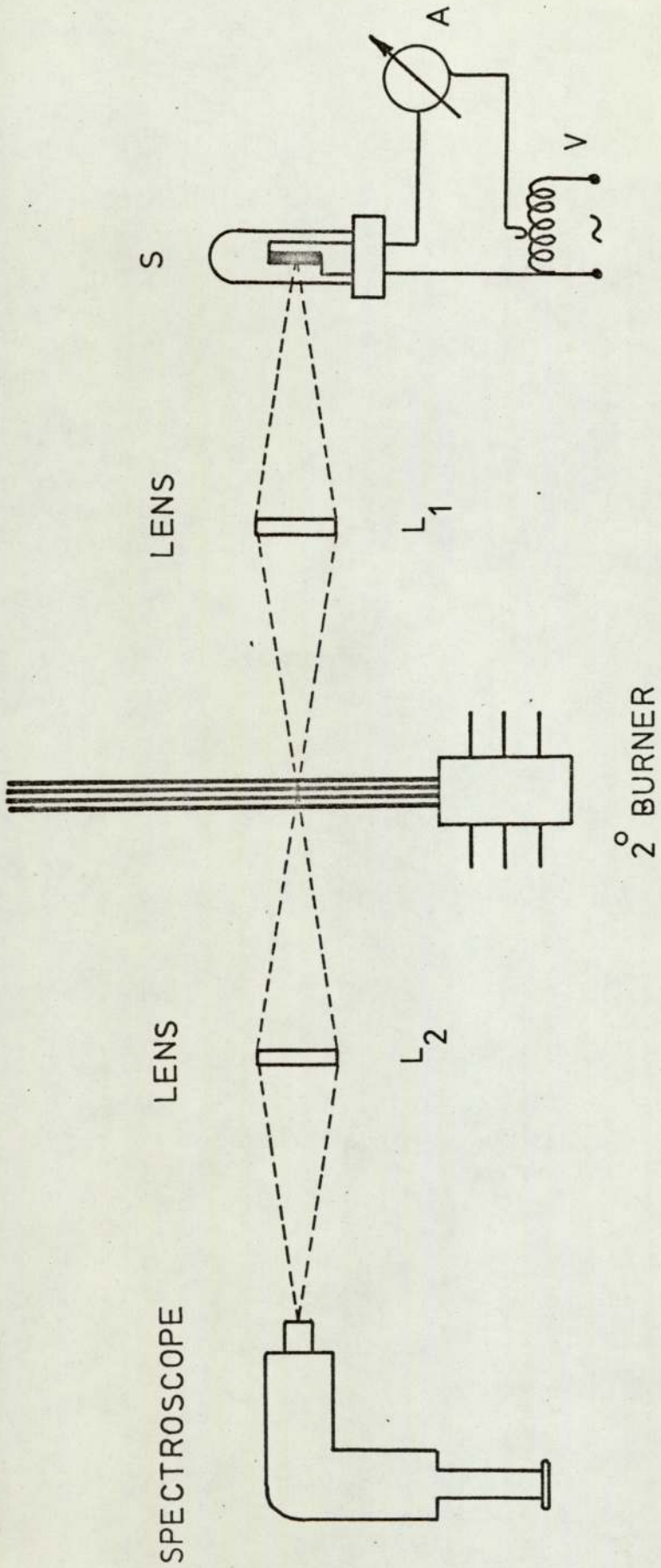


FIGURE IV - 11 TEMPERATURE MEASURING SYSTEM



of the spectrometer slit restricts the aperture opening so that the solid angle of light from the flame is same as that from the filament of the lamp.

As the light from the background source is passed through the flame containing sodium vapour, the two D - lines appear either in absorption as dark lines against the continuum, or in emission as bright lines, when the brightness temperature of the background source is higher or lower than the flame temperature respectively. The background intensity can be varied with the arrangement as shown in Fig. (IV-11). When the brightness temperature of the background and the flame temperature are exactly the same, the lines are invisible, this is called the reversal point. At this point the amount of light absorbed by the sodium atoms from the lamp is compensated by their emission, such that by Kirchoff's law the flame temperature is equal to the brightness temperature of the filament. Calibration of the lamp is made at 655 nm by using a Leeds Northorp optical pyrometer, itself having been calibrated against a black body radiator.

Under the above mentioned conditions there are two corrections to be made. Since the calibration of the filament is made at 655 nm, which is in the red, the true temperature of the filament is higher than the measured brightness temperature. A relation between the two temperatures exists knowing

the emissivity of the filament at both wavelengths, and is given by Wien's law,

$$\frac{1}{T_{\lambda'}} = \frac{2.303}{C_2} \left( \lambda \log e_{\lambda} - \lambda' \log e_{\lambda'} \right) + \frac{1}{T_{\lambda}} \quad (4-1)$$

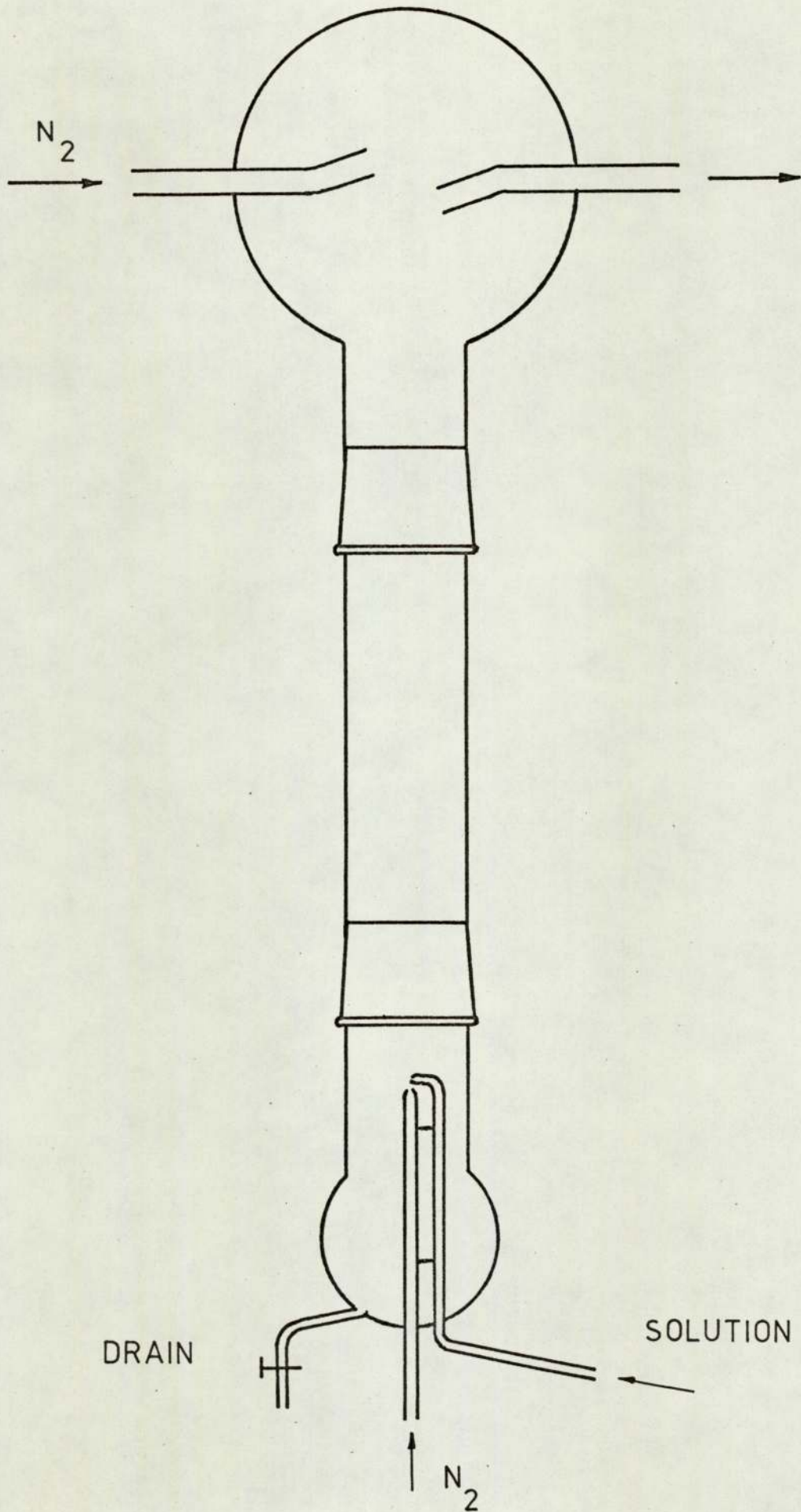
where  $T_{\lambda'}$  and  $T_{\lambda}$  are the brightness temperatures in K at  $0.655 \times 10^{-4}$  and  $0.589 \times 10^{-4}$  cm with  $e_{\lambda'}$  and  $e_{\lambda}$  the corresponding emissivities  $C_2$  is a second radiation constant equal to 1.439 cm. deg. The background source is weakened when passing through the lens  $L_1$ , whereas the light from the flame does not; a second correction should consider these reflection losses. In fact Gaydon & Wolfhard (1970) showed that, this reflection loss almost exactly compensates the brightness temperature correction, in the case of sodium within the experimental limits of the method.

#### 4.4.2. APPLICATIONS

Temperature measurements were made under two conditions. First being in the absence of primary burner product soot and secondly in the presence of soot particles in the secondary flame, that is when both burners are in operation. The introduction technique of sodium in both cases were different, due to experimental limitations. In the absence of primary burner products a spraying method was used. A right-angle external atomizer as shown in Fig.(IV-12) provided the atomized



FIGURE IV - 12 THE ATOMIZER



droplets for the flame, the nitrogen flow at the top flask, is for carrying the droplets to the feed line. M/100 NaCl solution was used; with concentrations above this level, the atomiser nozzle does not function properly.

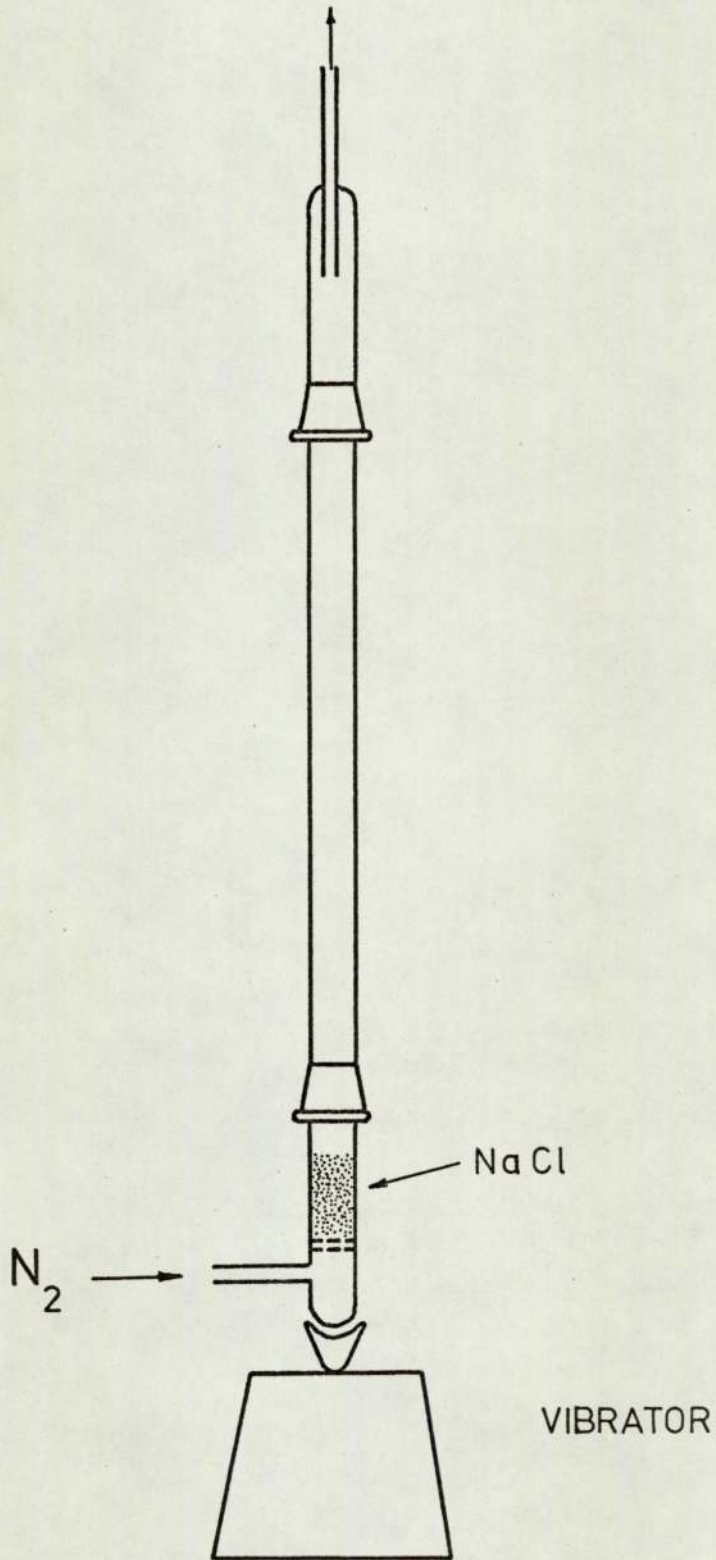
In the presence of primary burner products in the secondary flame, sodium introduction presents different problems. Due to the presence of water, if a spraying method is used, similar clogging problems as described in Section (4.1.3.) do arise. Therefore a method of introducing sodium chloride in solid form had to be adopted. For this an elutriator as shown in Fig. (IV-13) was used. Very finely ground sodium chloride crystals are placed on the sintered glass stopper. With the flow of nitrogen from the bottom these particles are suspended in the flowing fluid. From Stoke's Law,

$$U_{tf} = \frac{g d^2 (\rho_p - \rho)}{18\eta} \quad (4-2)$$

the terminal falling velocity,  $U_{tf}$ , of the particle must be smaller than the velocity of the fluid, so that the particles could be suspended in the flowing gas. In the above equation  $d$  is the particle diameter,  $g$  the acceleration due to gravity,  $\rho_p$  and  $\rho$  are the densities of the particle and gas respectively, where  $\eta$  is the gas viscosity.



FIGURE IV - 13 THE ELUTRIATOR



The NaCl powder in the bottom container was kept in constant motion by a vibrator which also helps the powder sticking on the walls, to return to the container. By this technique only the finest particles are carried through.

The interference by flame luminosity, in the presence of primary burner products, did not prevent the use of sodium D - line reversal technique, but did make these measurements difficult. Fig. (IV-14) shows the flame temperatures in both cases. Addition of primary flame gases lowered the temperature by about 100K.

Theoretical flame temperatures were also calculated for comparison. The method and the computer program developed for this purpose is discussed in the following section.

#### 4.4.3. THEORETICAL FLAME TEMPERATURES

The calculations of flame temperatures were based on a trial and error method, involving mass and heat balance equations as well as the principle reactions in the flame. In the case of the absence of primary burner products, the principle reactions considered included,

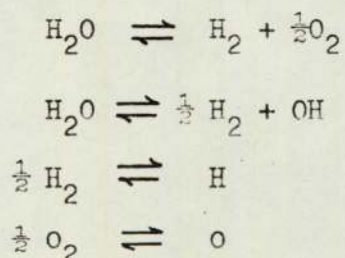
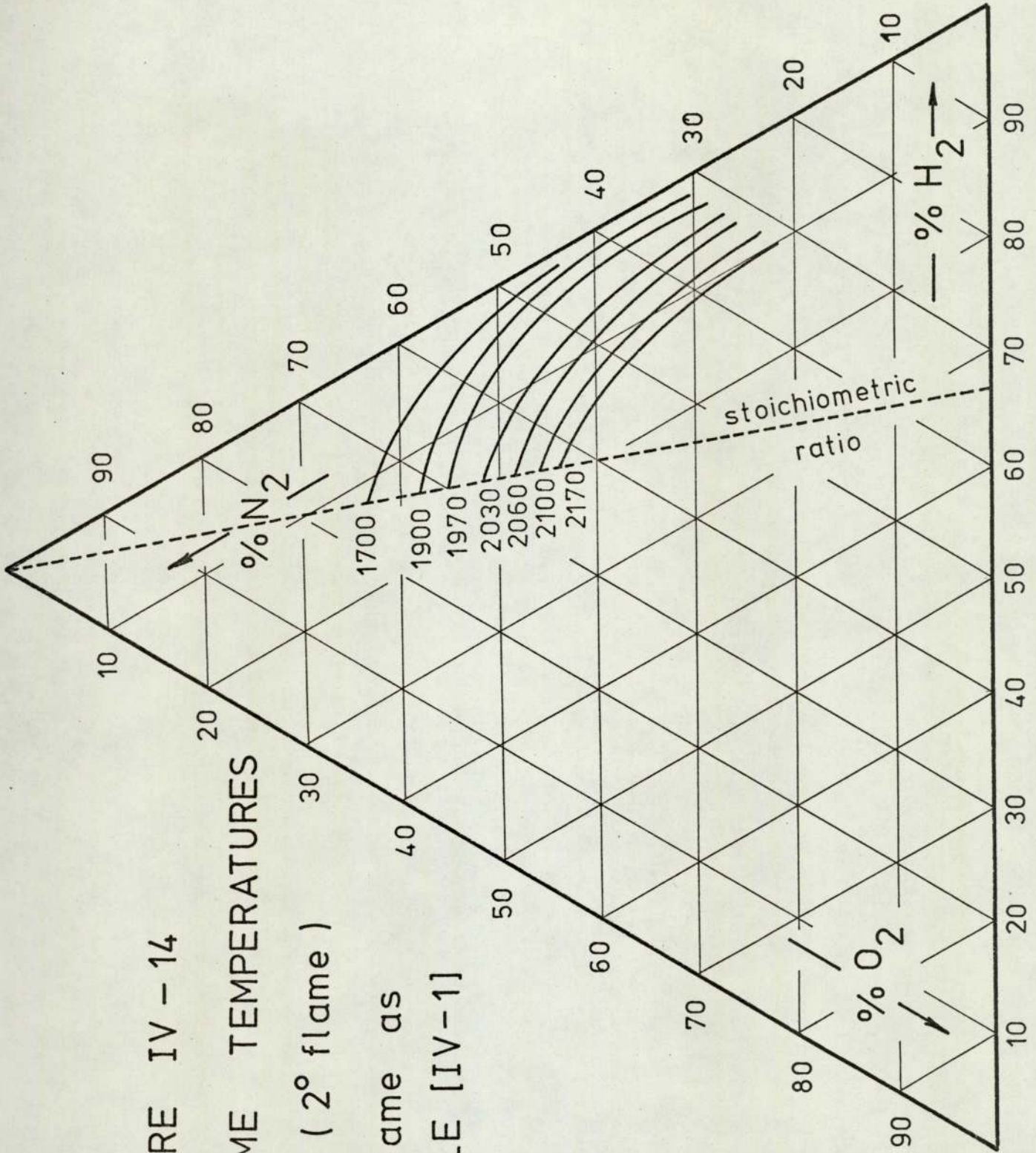




FIGURE IV - 14  
FLAME TEMPERATURES  
[K] ( 2° flame )  
1° flame as  
TABLE [IV-1]



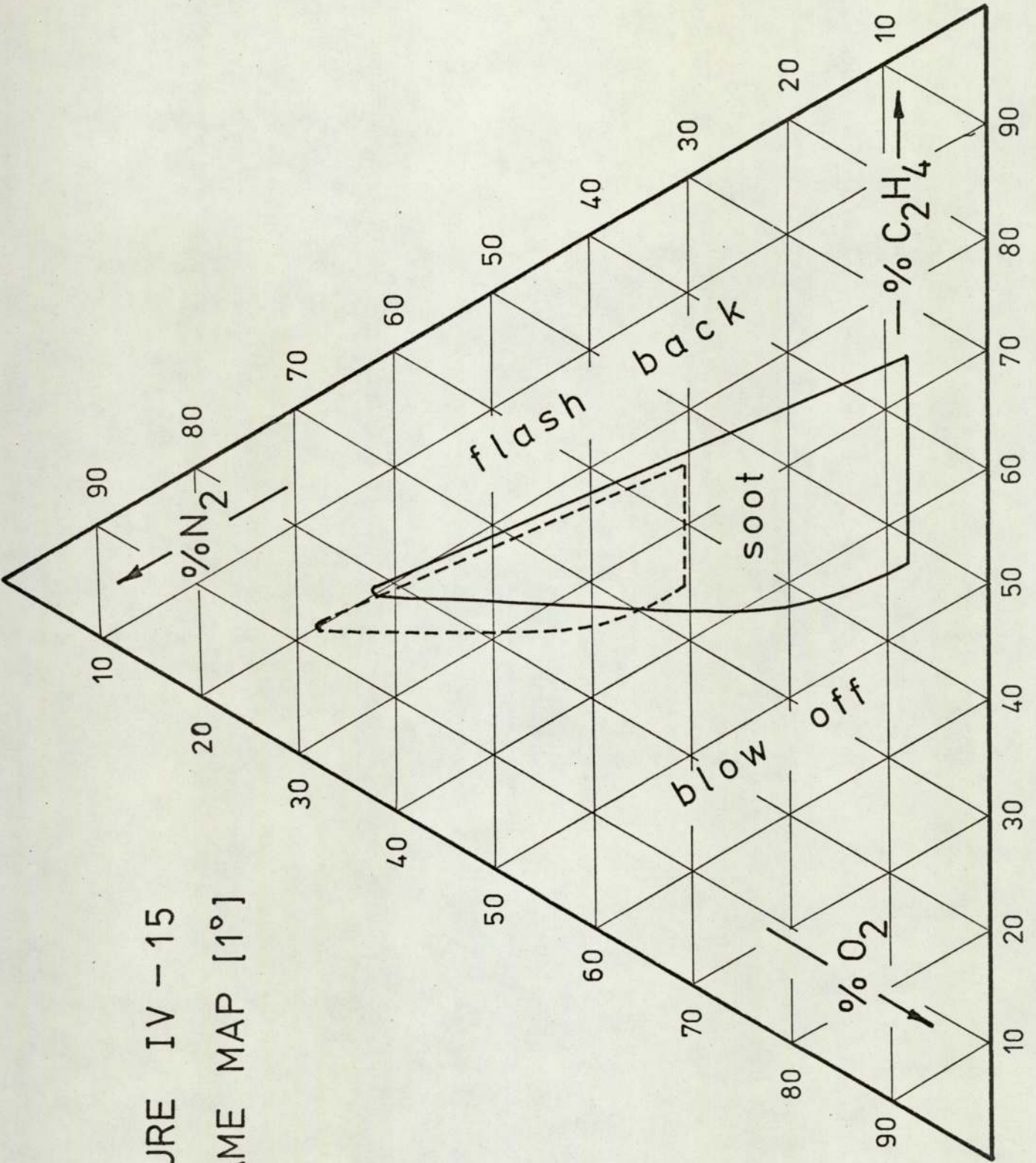
equilibrium constants were taken from Gurvich et al(1962) and tabulated for the above cases by Gaydon & Wolfhard (1970). The computer program developed and based on a trial and error method, using Fortran 1900, is described in Appendix I. For the case of primary burner products being present in the secondary flame, temperature values were computed at R.P.E. Westcott, by the courtesy of Mr G Jones. The results do agree with the measured temperatures, and the 100K decrease in the flame temperature by the introduction of primary burner products is persistent.

#### 4.5. FLAME MAPPING FOR SOOT

Primary flame is mapped for sooty compositions by visual inspection. A suitable mirror arrangement was placed on top of the conical nexus after removing the secondary burner mounting attachments. Keeping the total gas flow rate constant, and only varying the composition of the three major constituents, ethylene, oxygen and nitrogen the shaded area in Fig. (IV-15) shows the region where a sooty flame could be obtained. The two boundaries are the flash back limit on the fuel rich side and the blow-off limit on the fuel lean side. As far as the nitrogen limit is concerned the restriction is from the experimental settings. The flow rate of air around the flame is kept constant during the process, and when the 21% oxygen of the air is included in the overall composition, the limits are



FIGURE IV - 15  
FLAME MAP [1°]



shown in Fig. (IV-15) by the broken lines. It is always best to ignite the flame initially at a fuel rich mixture then set the composition required, within the sooty limits.

#### 4.6. THE LIGHT-SCATTERING SYSTEM

The main features of the light-scattering system are shown in Fig. (IV-16). A Ferranti DC-excited gas laser type SL3 at 632.8nm was used as the light source. The scattered light intensity was measured with a photo-multiplier (E.M.I. 9658B) system, placed at an angle of  $32^{\circ}$ . Radiation from the flame is isolated by a Grubb Parson interference filter tuned to 632.8 nm by mounting at  $15^{\circ}$ . To minimize the unwanted output of the photo-multiplier tube, due to the flame light, a reference signal chopped with the same frequency as the incident light is used in conjunction with a Brookdeal 9412 phase sensitive detector (PSD). The output of the PSD is recorded on a Servoscribe IS potentiometric flatbed recorder. An oscilloscope and a digital voltmeter were also connected, in order to follow the instant output value and the synchronisation of the reference and the signal inputs. Details of the PM circuit is shown in Fig. (IV-17). The burner system Fig. (IV-1) is mounted on a platform which enables the measurements to be carried out at various heights in the flame. The secondary flame is covered with a metal shield with openings at the incident beam inlet and at  $32^{\circ}$  outlet, acting as a wind shield.



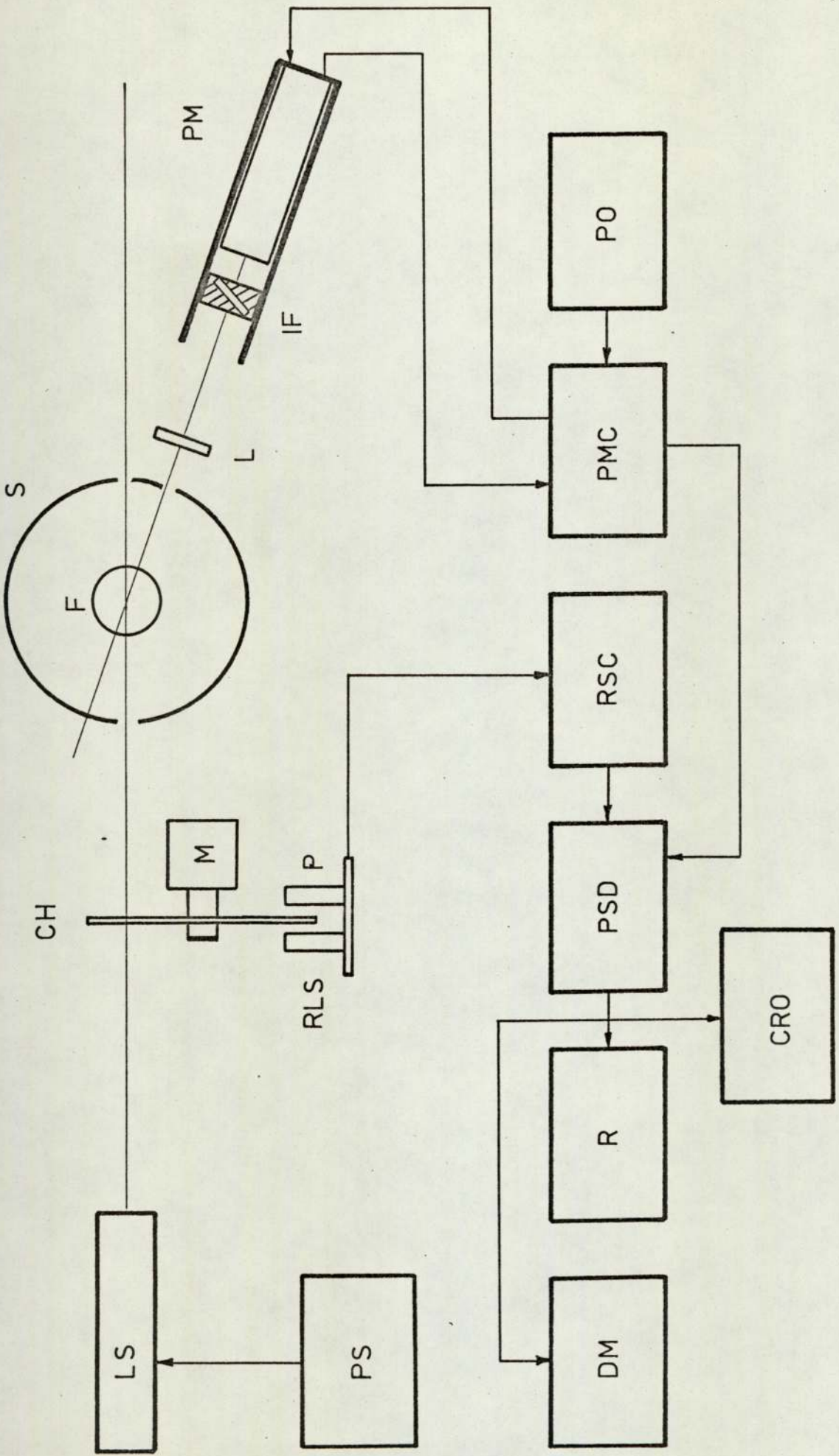
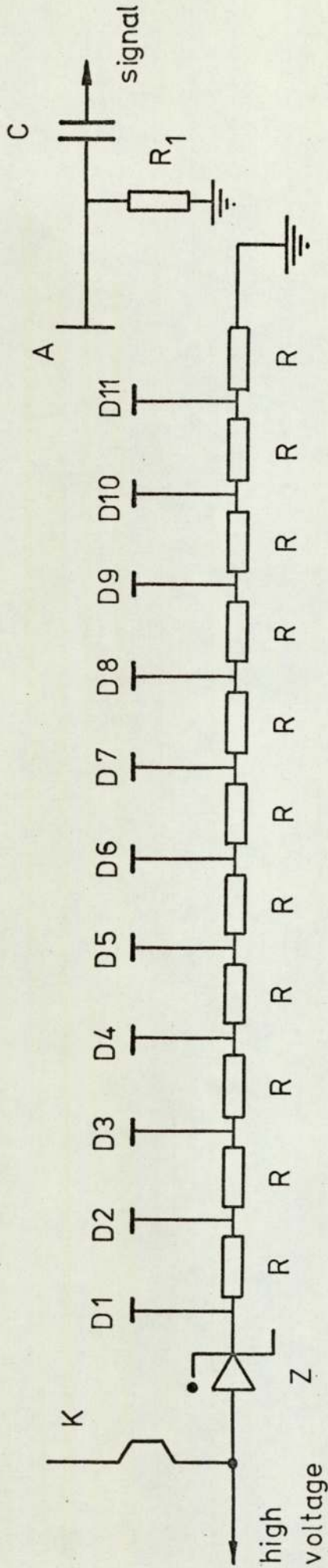


FIGURE IV - 16 THE LIGHT SCATTERING SYSTEM

LS : laser source  
CH : beam chopper  
M : chopper motor  
S : flame shield  
F : flame  
L : lens  
IF : interference filter  
PM : photomultiplier tube  
PS : laser power source  
RLS : reference light source  
P : photocell  
DM : digital meter  
R : chart recorder  
CRO : oscilloscope  
PSD : phase sensitive detector  
RSC : reference signal circuit  
PMC : photomultiplier circuit  
PO : D.C. power source





K : cathode , Z : 1S4150A , R : 100K $\Omega$ , R<sub>1</sub> : 520K $\Omega$ , C : .33 $\mu$ F

A : anode

FIGURE IV - 17 PM CIRCUIT [EMI 9658B]

CHAPTER 5

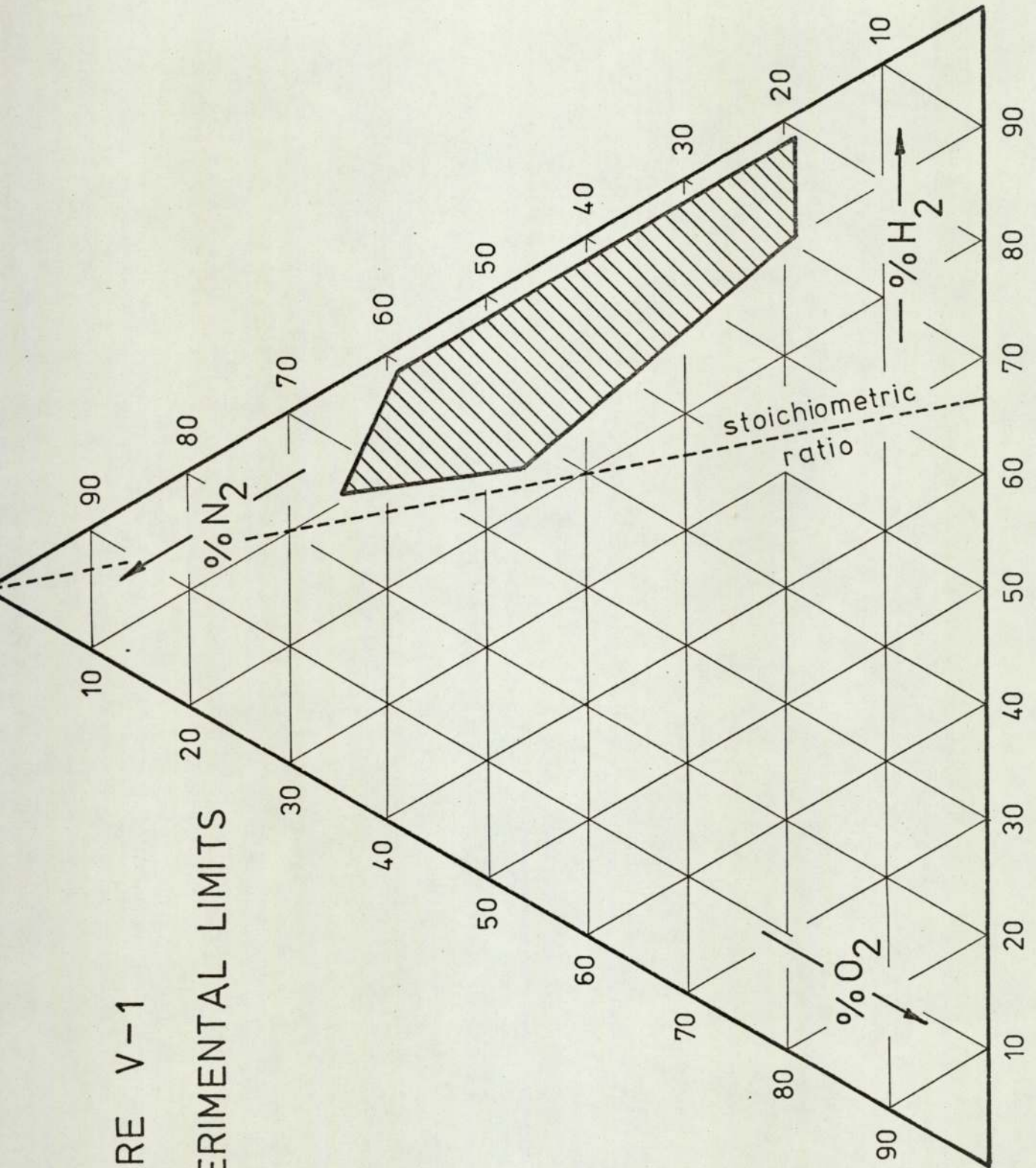
5. LIGHT SCATTERING STUDIES OF SOOT OXIDATION IN FUEL-RICH FLAMES

The oxidation of soot has been studied by various workers, as described in section 3.3., and a variety of techniques have been applied to find out the oxidation mechanism. As far as any one mechanism applicable to all flames is concerned no firm conclusion has yet been reached. Contrary to the fact that most of the previous work being carried out in fuel lean flames, where the oxidation is rapid, fuel-rich hydrogen flames are used in this work. Fig. (V-1) shows the experimental limits. Flames, having the advantage of being time invariant, when compared to shock-tube studies, do suffer from the difficulty of maintaining stability over a wide range of fuel/oxidiser ratio and percentage dilution by inert additives. The direct relationship between the initial composition and the flame temperature is also a restricting factor in the choice of experimental conditions.

Previous workers do agree that in the oxidation of soot particles in flames, the principal change is in the particle diameter as the oxidation proceeds, while the number density only changes slowly. The flame height is used in this study as the time parameter in following this change. The experimental variables chosen were the flame temperature and



FIGURE V-1  
EXPERIMENTAL LIMITS



composition. Measurements were made at varying flame compositions while keeping the temperature constant. Unfortunately as mentioned above there is little room for temperature variations at constant compositions. All the runs were made at a fixed primary burner composition.

## 5.1. EXPERIMENTAL

Experimental procedure followed in this study can be grouped as, the settling time of the system, working time limitations and finally, following the light scattered with respect to the flame height.

### 5.1.1. THE SYSTEM SETTLING TIME

Preliminary investigations showed that the relationship between the flame height and PSD output, which was used as a measure of scattered light, was not reproducible. A decrease in the output (PSD) with time was the significant character. The inner walls of the conical nexus and the straight piece following, as well as the mixing chamber of the secondary burner are covered with a layer of soot during the runs. When the clean system is used it is possible to follow the decrease in PSD output with time. This is shown in Fig. (V-2). After a period of about 50 minutes the drop in the output comes to a steady level, the readings taken from them



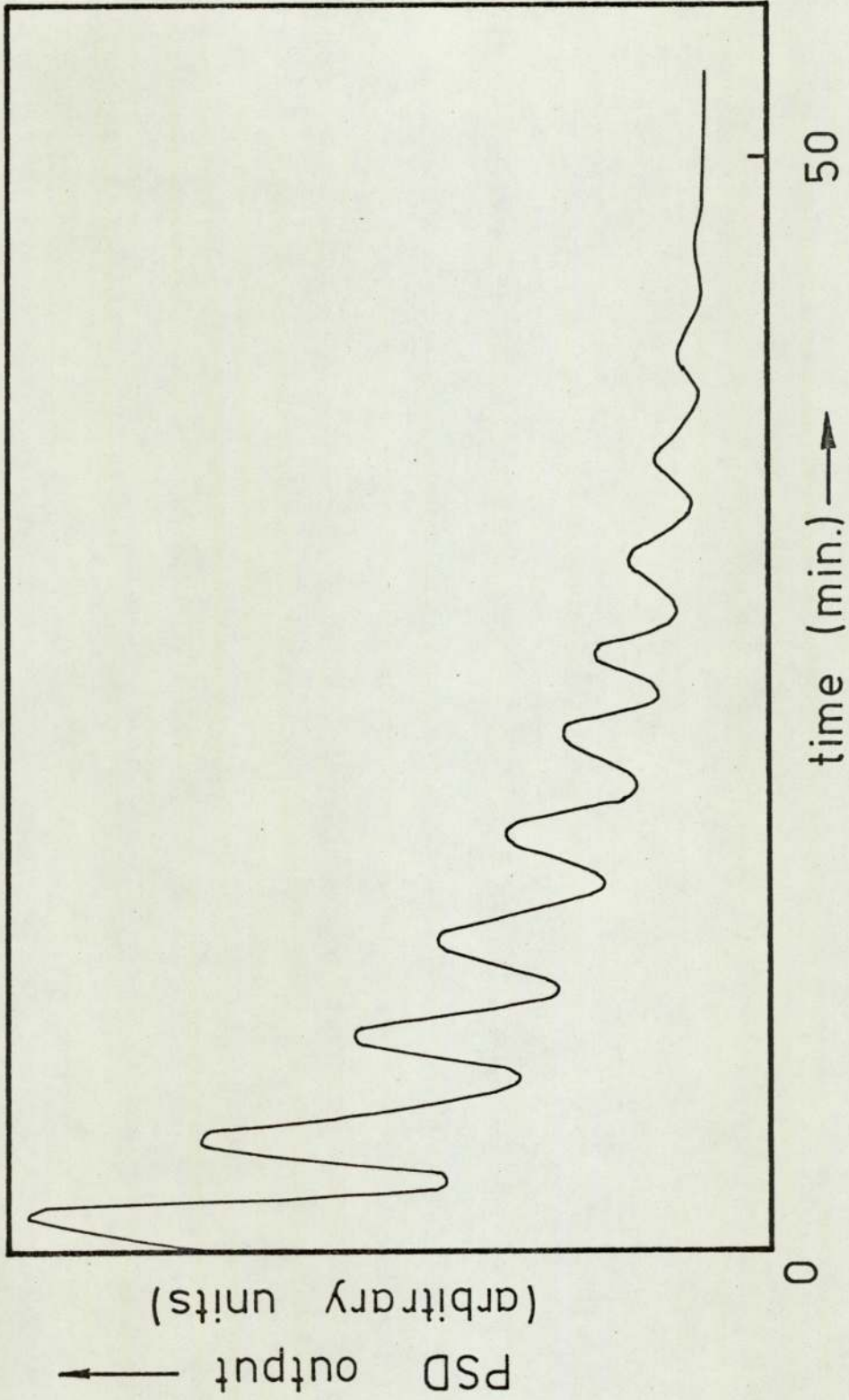


FIGURE V-2 SYSTEM SETTLING TIME

onwards do agree as far as the reproducibility is concerned. The ripples in the initial state also fade as settling proceeds. Temperature of the nexus and the secondary burner circulation water should also be kept constant.

Fluctuations in the output are mainly due to changing flow of soot from the primary burner. Deposition on the system inner walls is a big contributor. Once a sufficient deposit layer on the walls, is formed and a steady temperature of the nexus is reached the system is settled. Therefore, primary and secondary flames should be set at a desired temperature and composition, the heating of the conical nexus and secondary burner circulation should be at a constant level, and a period of 50 minutes should be completed under these conditions, before an acceptable reading is taken.

#### 5.1.2. WORKING TIME LIMITATIONS

There also is an upper limit as far as the duration of the runs are concerned. Once the settling is completed the deposition on the inner walls does not stop, but there is enough time for a number of acceptable runs to be completed before the soot path is blocked, because of further deposition. These limits are set by observation and averaging individual runs. In fact going beyond these limits produce



poor results and larger variations. The time gap after the initial settling process is about 65 minutes, then it is necessary to dismantle the burners and the nexus for cleaning. Working time is also a factor of primary burner feed composition, from Fig. (IV-15) if the composition is set at near the blow off limit the working time gap can be increased. While at the flash back limit it decreases. The figure given above is a rough limit which is within the safe restricted period, and was used in the experiments carried out.

#### 5.1.3. LIGHT SCATTERING AS A FUNCTION OF FLAME HEIGHT

When the conditions in section 5.1.1. and 5.1.2. are met, the light scattered by the soot particles in the flame falls on to the photomultiplier tube arrangement as mentioned in section 4.6. The signal is chopped and fed into the PSD with a reference signal, which is also chopped at the same frequency, and synchronised with the actual signal. The synchronisation is followed on the CRO. PSD filters are set at an acceptable noise level. The PSD output level is related to the size of the particles according to the relation between the scattered intensity  $I$  and the particle radius  $a^6$ , other terms being constant throughout the flame.

The amount of soot in the secondary flame was recorded at various heights, and as expected, a steady decrease in the intensity of the scattered light, was observed. The

height at which no more scattering is recorded, as far as the apparatus is concerned, is a function of flame temperature. In fact, this characteristic also restricts the working area as shown in Fig. (V-1). For the high temperature flames, that is with high oxygen percentage, it is only possible to follow the scattered light up to a height of about 70 mm from the burner top. In these flames, the flame luminosity also makes the measurements difficult. It was not possible to detect the scattered light from the soot particles in flames of higher temperatures. As one approaches the stoichiometric mixture, the flames tend to get very small and very luminous with a height of about 10 cm. The situation is even worse at and below the stoichiometric  $H_2:O_2$  ratio, where no scattering could be followed. However at the higher  $H_2:O_2$  ratios, where the diluent  $N_2$  is very small in quantity, flames do tend to be broader and begin to lose their thin long shape. This characteristic of being unsteady restricts the upper height limit of reliable measurements. Whereas within these limits a variation of about 500K in temperature and 40% in  $H_2$  percentage as fuel inlet is possible.

The purpose of this study on soot particles in flames, is to identify the oxidising species, and the oxidation process of these particles. The history of soot in flames, its formation and the proposed mechanisms are discussed in



Chapter 3. The current argument on the nature of the oxidant is between the oxygen atoms and the hydroxyl radicals, which is known to be a very active oxidant. In flames of  $H_2-O_2-N_2$  the individual species present in flame gases can commonly be classified as molecules, free radicals, atoms and ions. Before any further analysis of these species is made the kinetic behaviour of the flame should be analysed.

## 5.2. CHEMICAL KINETIC ANALYSIS OF THE FUEL-RICH $H_2-O_2$ FLAME

From the classification of the individual species in the flame gases (Section 5.1.3.), the term molecule generally refers to a stable enough polyatomic species such as  $H_2O$ ,  $H_2$ , etc. The molecular fragments from the free radicals class, although electrically neutral are characterised by one or more unpaired electrons. Thus the free radicals are highly unstable and reactive, eg OH. The term atom, in the above mentioned classification refers to free radicals having a single atom, these are also unstable, eg H, O. Finally the species carrying a net charge, which is also unstable are referred to as the ions.

### 5.2.1. BIMOLECULAR RADICAL REACTIONS

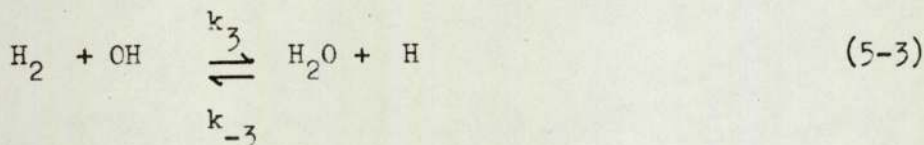
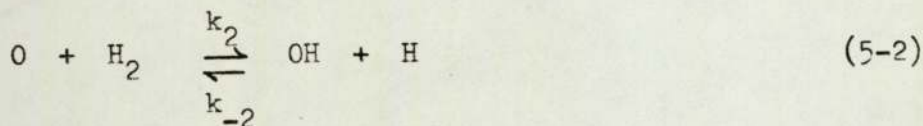
The combustion process in the reaction zone of a  $H_2-O_2$

flame is a branched chain reaction. Formation of a free hydrogen atom is the initiation step. The reaction,



which is the branching step in the mechanism, is extremely important in many high temperature combustion systems. It is endothermic and too slow to play a role at room temperature, Warren (1952). In hydrogen/oxygen flames, reaction (5-1) is the principal mode of removal of  $\text{O}_2$  in the reaction zone, Fenimore & Jones (1958), (1959). Reaction (5-1) has been studied extensively and with various techniques. Fenimore & Jones (1969) used high-temperature flames whereas shock tube studies reported by Schott & Kinsey (1958), and Strehlow & Cohen (1962).

Propagation step of the chain reaction is characterised by the following two reactions.





In the reaction zone of any hydrogen oxygen flame it is likely that only the species  $H_2, O_2, H_2O, OH, H$  and  $O$  need be considered. Other possibilities such as  $HO_2, H_2O_2$  and  $O_3$  would be negligible at high temperatures, which is the case in such flames, Kaskan (1958). For these main species and from the eq. 5-1, 2&3 the time rate of change of all six species may be expressed as,

$$\begin{aligned} \frac{dN_H}{dt} = & -k_1 N_H N_{O_2} + k_{-1} N_{OH} N_O + k_2 N_O N_{H_2} - k_{-2} N_{OH} N_H \\ & + k_3 N_{H_2} N_{OH} - k_{-3} N_{H_2} O N_H \end{aligned} \quad (5-4)$$

$$\frac{dN_{O_2}}{dt} = -k_1 N_H N_{O_2} + k_{-1} N_{OH} N_O \quad (5-5)$$

$$\begin{aligned} \frac{dN_{OH}}{dt} = & k_1 N_H N_{O_2} - k_{-1} N_{OH} N_O + k_2 N_O N_{H_2} - k_{-2} N_{OH} N_H \\ & - k_3 N_{H_2} N_{OH} + k_{-3} N_{H_2} O N_H \end{aligned} \quad (5-6)$$

$$\frac{dN_O}{dt} = k_1 N_H N_{O_2} - k_{-1} N_{OH} N_O - k_2 N_O N_{H_2} + k_{-2} N_{OH} N_H \quad (5-7)$$

$$\frac{dN_{H_2}}{dt} = -k_2 N_O N_{H_2} + k_{-2} N_{OH} N_H - k_3 N_{H_2} N_{OH} + k_{-3} N_{H_2} O N_H \quad (5-8)$$

$$\frac{dN_{H_2O}}{dt} = k_3 N_{H_2} N_{OH} - k_{-3} N_{H_2} O N_H \quad (5-9)$$

In fuel rich flames of hydrogen and oxygen,  $N_{H_2}$  and  $N_{H_2O}$  can be taken as essentially constant. With suitable arrangements of eqs. (5-4) - (5-7) it can be shown that,

$$\frac{dN_H}{dt} + \frac{dN_{OH}}{dt} + 2\frac{dN_O}{dt} + 2\frac{dN_{O_2}}{dt} = 0 \quad (5-10)$$

therefore the number of free valencies will remain constant and reactions (5-1) - (5-3) cannot lead to a final state of chemical equilibrium but to a condition where eq (5-10) is valid.

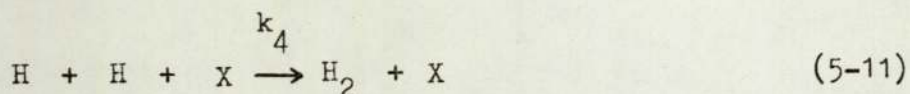
Reaction (5-2) has been studied by Clyne & Thrush (1963), Hoyerman et al (1967), Browne et al (1969) and Brabbs et al (1971). Jensen & Kurzius (1967) reported the  $k$  value for reaction (5-3) as  $2.4 \times 10^{13} \exp(-2770/T) \text{ cm}^3 \text{ mol}^{-1} \text{ s}^{-1}$  which is an evaluated result for temperatures of 300-2000K for their calculations on nozzle and rocket exhaust flow fields.

### 5.2.2. THREE-BODY RADICAL RECOMBINATION REACTIONS.

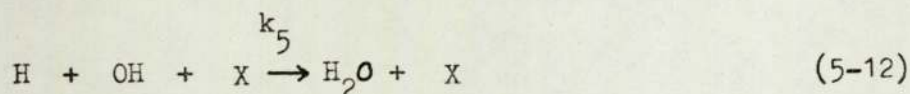
The nonequilibrium state mentioned in section 5.2.1. shows that by a function of the three (5-1) - (5-3) bimolecular steps alone a final state of chemical equilibrium cannot be reached, unless some other reaction terminates the



process. The only mechanism, for the establishment of final equilibrium, must be by way of a radical recombination reaction, involving a third body. This can be any third body molecule or the system walls. In the case of open flames, system walls cannot be mentioned. Therefore reactions such as,



or



where X is any third body molecule, would act as the termination step of the chain reaction in the combustion system, as far as the final state of chemical equilibrium is concerned. Padley & Sugden (1958) studied the above two reactions by following the intensity of the emission of sodium D - lines as a function of distance (time) in the flames of  $\text{H}_2 + \text{O}_2 + \text{N}_2$  at temperatures of 1400 - 2500K. In their hydrogen rich flames where there is little O atom, they found that reaction (5-12) was the dominant one when compared with (5-11), which is the faster of the two. It is important that, all the recombinations are strongly exothermic and require third bodies to accept part of their reaction energies. In the literature the relative importance of H and  $\text{H}_2$  as the third body in reaction (5-11) was a source of controversy. Where

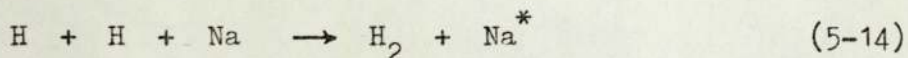
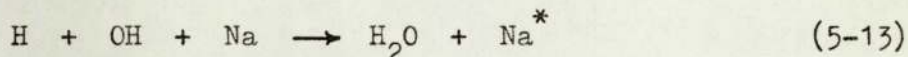
the purity of  $H_2$  is in doubt it is necessary to ignore the work, because of the interference with the decay of hydrogen atoms. The flame studies and works on shock tube for reaction (5-11) is also reported by Schott (1960), Schott & Bird (1964), and Getzinger & Blair (1969) where reliable data were quoted. It is difficult to derive the precise values of  $k$  from such studies for two reasons;

- (a) At least two of the termolecular (5-11) - (5-12)  
(where the third one is  $O_2 + H + X \rightarrow HO_2 + X$ )  
do control the decay of radicals and atoms in the recombination zone of flames and shock tubes.
- (b) The species  $H$ ,  $O$  and  $OH$  are in a state of partial equilibrium (section 5.2.3.) at these temperatures, the decay towards complete equilibrium is governed by the reactions (5-11) - (5-12).

In fuel rich flames (5-11) becomes of increasing importance while (5-12) tend to predominate in fuel lean mixtures. The uncertainties in studies on (5-12) are due to the reaction (5-3). In flames and shock tubes the balanced reaction is quickly attained where  $H$  and  $OH$  are present, and the overall decay proceeds by the recombination reaction (5-11) & (5-12). Padley & Sugden (1958) in their Na - seeded fuel rich  $H_2/O_2/N_2$  flames determined the  $k$  (5-12) from rate of heat release in post flame zone assuming  $H_2O$  being the only effective third



body, and concluded that in low temperature flames the Na emission is due to the chemiluminescent reactions,



the decay of chemiluminescence with height in the flame accorded with the known decrease of atomic hydrogen and hydroxyl concentrations. Padley & Sugden extended their observation to other elements and showed that lead favoured the H + OH recombination while sodium catalysed the H + H recombination. Other studies on ion recombinations are reported by Jensen & Padley (1967).

### 5.2.3. PARTIAL EQUILIBRIUM

Following Sugden, a reaction which is in equilibrium with its reverse is called a balanced reaction. The bimolecular reactions (5-1) - (5-3) are faster than the recombination reactions (5-11) & (5-12), hence it should be expected that a step would be reached where the bimolecular radical reactions are approximately equilibrated even though the system as a whole was not. This state of equilibrium is called the partial equilibrium, Schott (1960). At this stage

the equilibrium relations can be expressed by,

$$K_1 = \frac{N_{OH} N_O}{N_H N_{O_2}} \quad (5-15)$$

$$K_2 = \frac{N_{OH} N_H}{N_O N_{H_2}} \quad (5-16)$$

$$K_3 = \frac{N_{H_2O} N_H}{N_{H_2} N_{OH}} \quad (5-17)$$

It should be noted that the above relations hold at true chemical equilibrium, but at partial equilibrium, even though the absolute concentrations are different, various concentration ratios will be the same. In the case of hydrogen-rich flames neither O nor O<sub>2</sub> is present in sufficiently large quantities. From eq (5-10) it can be shown that,

$$(N_H + N_{OH} + 2N_O + 2N_{O_2}) = \text{constant}$$

this is so, as far as the first three reactions are involved, and the three-body recombinations should decrease this sum rather than any single member of it, Kaskan & Schott (1962)



showed that when a system containing H, OH, O, H<sub>2</sub>, O<sub>2</sub> and H<sub>2</sub>O decays to form H<sub>2</sub> and H<sub>2</sub>O, which is the case in fuel-rich mixture, the conservation requires that,

$$- \left[ \frac{dN_H}{dt} + \frac{dN_{OH}}{dt} + 2 \frac{dN_O}{dt} + 2 \frac{dN_{O_2}}{dt} \right] = \begin{array}{l} \text{recombination} \\ \text{rate} \end{array} \quad (5-18)$$

assuming that N<sub>H<sub>2</sub></sub> and N<sub>H<sub>2</sub>O</sub> are constant, it can be shown that,

$$- \left( 1 + K_3 \frac{N_{H_2}}{N_{H_2O}} \right) \frac{dN_{OH}}{dt} = 2 k_4 \left( K_3 \frac{N_{H_2}}{N_{H_2O}} N_{OH} \right)^2 N_M + 2 k_5 \left( K_3 \frac{N_{H_2}}{N_{H_2O}} N_{OH} \right) N_M \quad (5-19)$$

and the relation between N<sub>OH</sub> and time can be expressed as,

$$\frac{1}{N_{OH}} = \frac{2K_3 N_{H_2} N_M}{K_3 N_{H_2} + N_{H_2O}} \left( k_4 K_3 \frac{N_{H_2}}{N_{H_2O}} + k_5 \right) t + c \quad (5-20)$$

which would lead to an important conclusion and experimentally confirmed by Kaskan (1958). A similar analysis in terms of H is carried out by Bulewicz, James and Sugden (1956), which leads to the concept of disequilibrium state.

#### 5.2.4. THE STATE OF DISEQUILIBRIUM

Arthur (1949) argued that in burner flames at atmospheric pressures the free radical concentrations are above the expected thermodynamic full equilibrium level, following his studies on hydrogen atom concentrations in H<sub>2</sub>/air and other flames with molybdenum oxide. From the balanced reaction (5-3) & (5-17) it could be shown that,

$$\frac{N_H}{N_{OH}} = K_3 \frac{N_{H_2}}{N_{H_2O}} \quad (5-21)$$

The experimental behaviour observed by Bulewicz, James and Sugden (1956) showed that a similar analysis for  $N_H^{-1}$  could be carried as in eq (5-20), and it would be a linear function of time too. Their studies confirmed Arthur's suggestion that, while the free radical concentrations are very close to the actual thermodynamic equilibrium levels at high temperatures, they tend to deviate from these values as the temperature decreases. This behaviour is shown in Fig. (V-3).

Bimolecular exchanges will ensure that, the excess radicals over the equilibrium concentrations, would reach a common level that,



$$\frac{N_H}{N_{OH}} = \left[ \frac{N_H}{N_{OH}} \right]_e \quad (5-22)$$

and

$$\frac{N_H}{N_{H_e}} = \frac{N_{OH}}{N_{OH_e}} = \delta \quad (5-23)$$

where  $\delta$  signifies the disequilibrium parameter and  $e$  for the equilibrium concentrations. For the other free radicals similar arguments can be made and in the case of  $N_O$  it could be shown that the actual concentration and the equilibrium levels are related by  $\delta^2$ , where, from. (5-16)

$$\frac{N_H}{N_O} = K_2 \frac{N_{H_2}}{N_{OH}} \quad (5-24)$$

and

$$N_O = N_H^2 \frac{N_{H_2O}}{K_2 K_3 N_{H_2}^2} \quad (5-25)$$

$$\frac{N_O}{N_H^2} = \left[ \frac{N_O}{N_H^2} \right]_e \quad (5-26)$$

where

$$\frac{N_O}{N_{O_e}} = \frac{N_H^2}{N_{H_e}^2} = \delta^2 \quad (5-27)$$

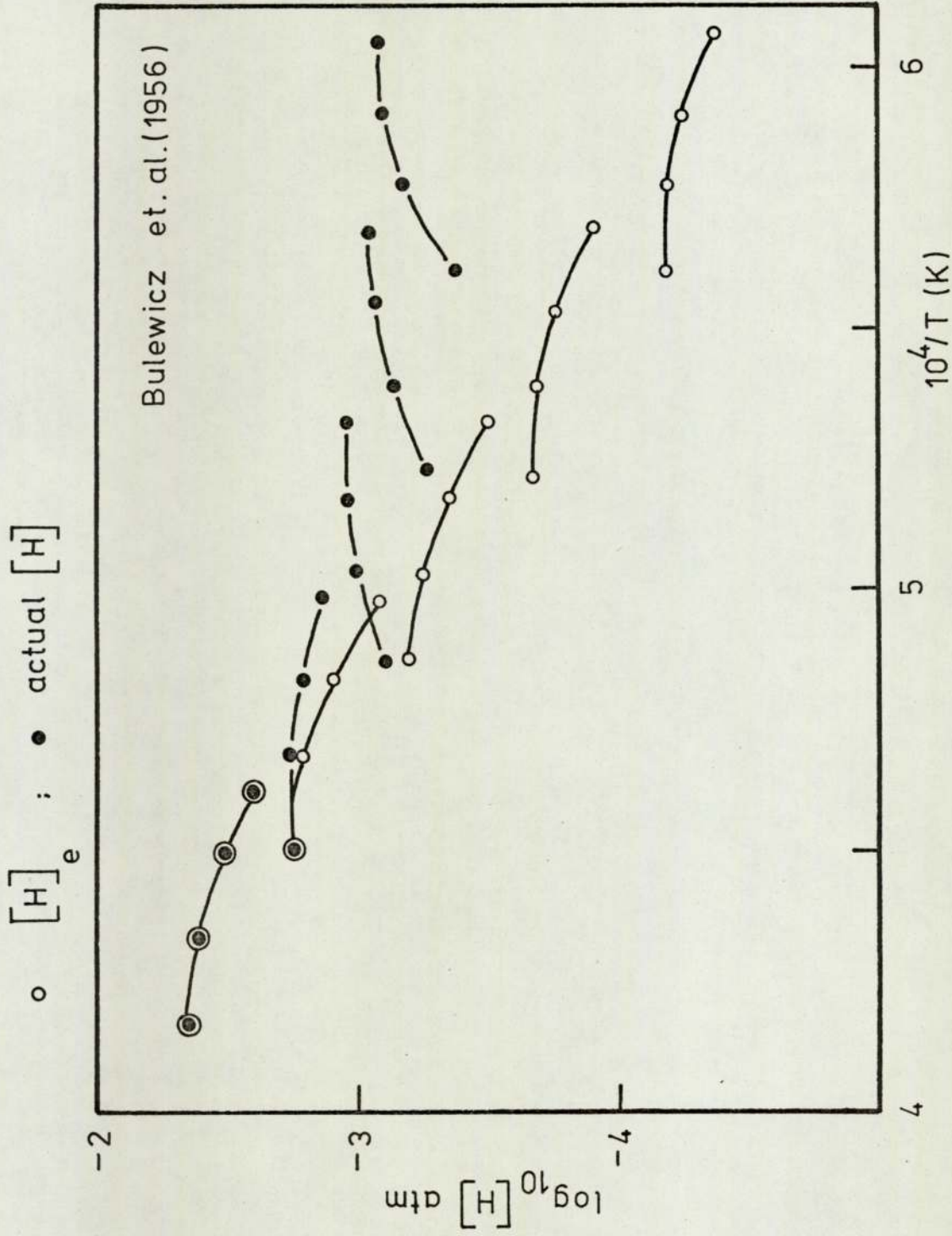
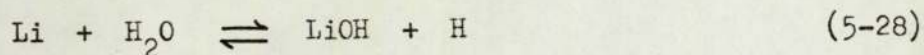


FIGURE V - 3 ATOMIC HYDROGEN CONCENTRATIONS IN HYDROGEN + OXYGEN + NITROGEN FLAMES

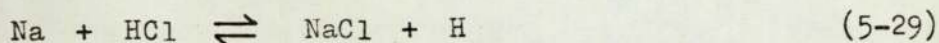


The values of the disequilibrium parameter derived from Bulewicz et al, is shown in Fig. (V-4). For an extensive discussion of flame kinetics see Page (1973).

In their studies on excess hydrogen atom concentrations in flames Bulewicz et al made two kinds of measurements. The comparison of Na D lines and Li resonance doublets intensities, for equal traces of these metals in the flame, where the free Li undergoes the balanced reaction expressed as



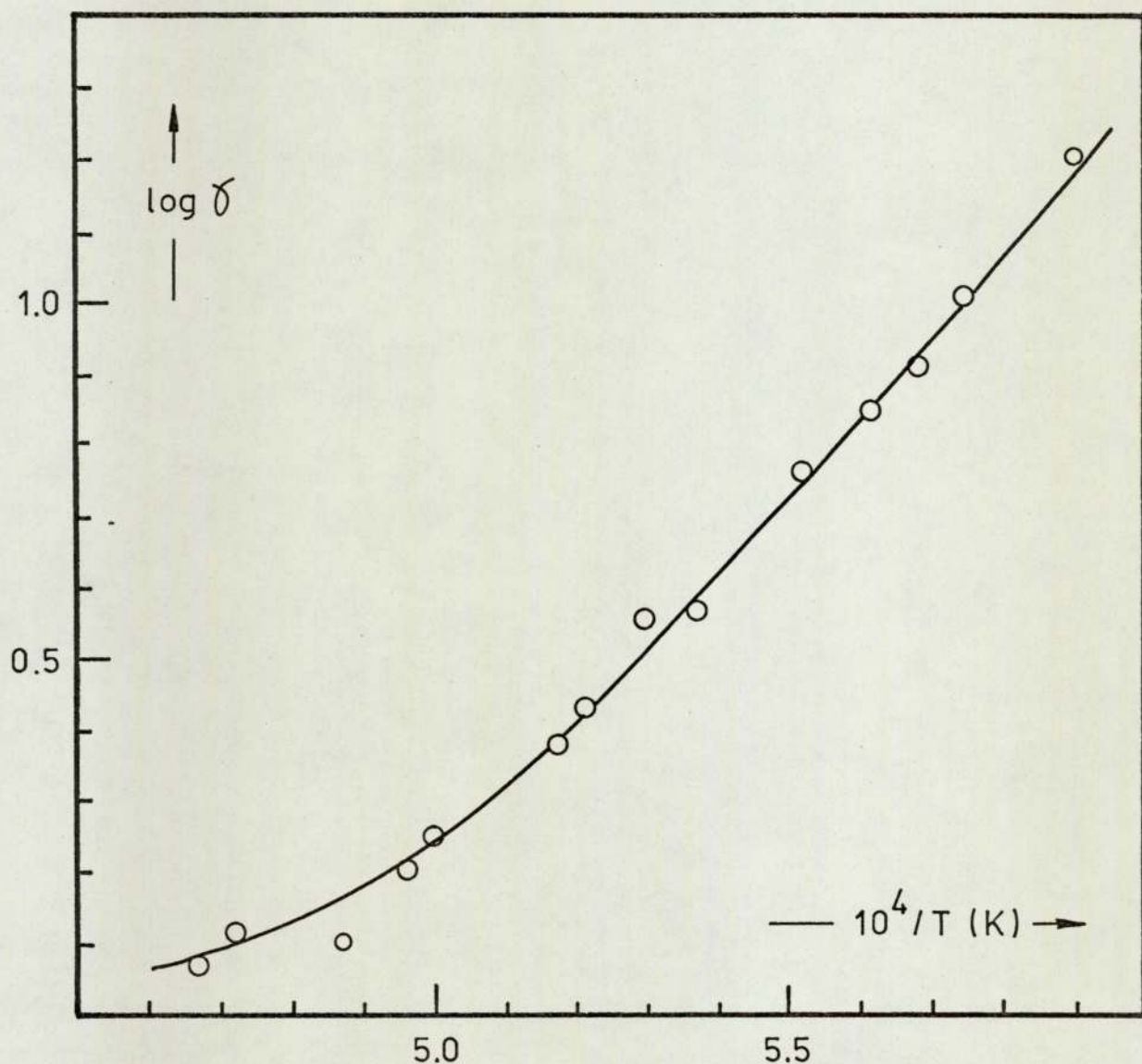
and measurements of the change of intensity of the D lines in the presence of chlorine considering the balanced reaction,



from the estimated equilibrium constants  $N_{\text{H}}$  could be obtained for the above two relations. Their results showed a good agreement in the two cases. Calculated  $N_{\text{OH}_e}$  concentrations combined with

$$\phi_{\text{Li}} = \frac{N_{\text{LiOH}}}{N_{\text{Li}}} \quad (5-30)$$

FIGURE V-4 DISEQUILIBRIUM PARAMETER

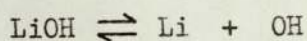




would give a relation as,

$$K'_{Li} \equiv \frac{N_{OH_e}}{\phi_{Li}} \quad (5-31)$$

The relation between  $K'_{Li}$  and the equilibrium constant  $K_{Li}$  for the reaction,



should be expected to hold over the temperature range. However, while the relationship was maintained well at high temperatures ( $>2100K$ ),  $K'_{Li}$  became progressively greater than  $K_{Li}$  as the temperature was decreased. The interpretation is that the equilibrium is still maintained but at lower temperatures,

$$N_H > (N_H)_e \quad (5-33)$$

therefore from measurements of  $N_{Li}$ ,  $N_H$  could be evaluated. The conclusion that should be drawn from the state of disequilibrium is that, while the radical concentrations in flames are close to their predicted thermodynamic equilibrium concentrations at high temperatures, they tend to deviate from these values at lower temperatures and are much in excess of the calculated values.

## CHAPTER 6

### 6. RESULTS AND DISCUSSIONS

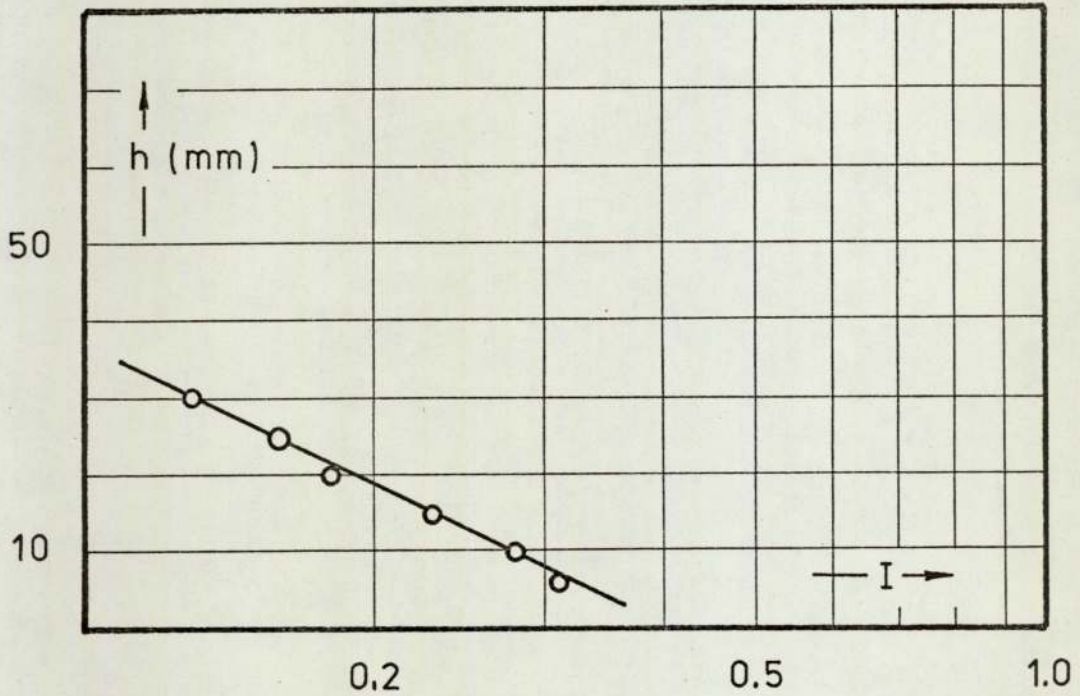
Within the experimental limits Fig.(V-1), as the flame conditions were changed, firstly by composition variations and secondly temperature variations, a distinct pattern has been observed. Such that, while at fuel rich mixtures the change in scattered intensity with flame height ( $\log I$  vs  $h$ ) graphs, show a bigger slope, as the mixture gets close to the stoichiometric  $H_2/O_2$  ratio, slopes decrease steadily. Even though the pattern is the same for all constant temperature cases, there is a difference in the range of this decrease, for different temperatures.

In Table (VI-1), the twenty different flames studied are listed, and given a flame number which they will be referred to from now on. Flame compositions are of the secondary burner inner flame, where the outer flame also has the same ratios. For all cases, primary burner composition was kept constant.

A typical variation of the scattered intensity, which is in arbitrary units of the PSD output, is shown in Fig. (VI-1). As seen from Fig. (V-1) this flame is close to the stoichiometric  $H_2 / O_2$  ratio, and therefore the graph has a relatively small slope. The change in the scattered intensity pattern at a



FIGURE VI-1 SCATTERED INTENSITY  
vs. FLAME HEIGHT



flame no. 4

TABLE (VI-1) THE FLAME CONDITIONS

FLAME NO.	PERCENTAGE COMPOSITION			MEASURED TEMPERATURE (K)
	H <sub>2</sub>	O <sub>2</sub>	N <sub>2</sub>	
1	37	5	58	1690
2	30	8	62	1700
3	36	9	55	1860
4	32	11	57	1900
5	61	2	37	1900
6	40	8	52	1970
7	43	7	50	1970
8	46	6	48	1970
9	43	10	47	1980
10	60	5	35	2020
11	50	8	42	2030
12	37	12	51	2040
13	65	7	28	2050
14	50	10	40	2060
15	70	4	26	2060
16	76	4	20	2060
17	43	12	45	2080
18	60	8	32	2100
19	60	10	30	2120
20	50	12	38	2170



constant temperature is expressed in Fig. (VI-2), where three different flames at 1970 K are shown, but at different compositions. The decrease in the slope as the stoichiometric  $H_2/O_2$  ratio is approached on the constant  $O_2$  scale is the important characteristic. When the composition is varied towards the fuel rich side, the slopes follow a sequence of higher values as the departure from the stoichiometric  $H_2/O_2$  ratio is increased.

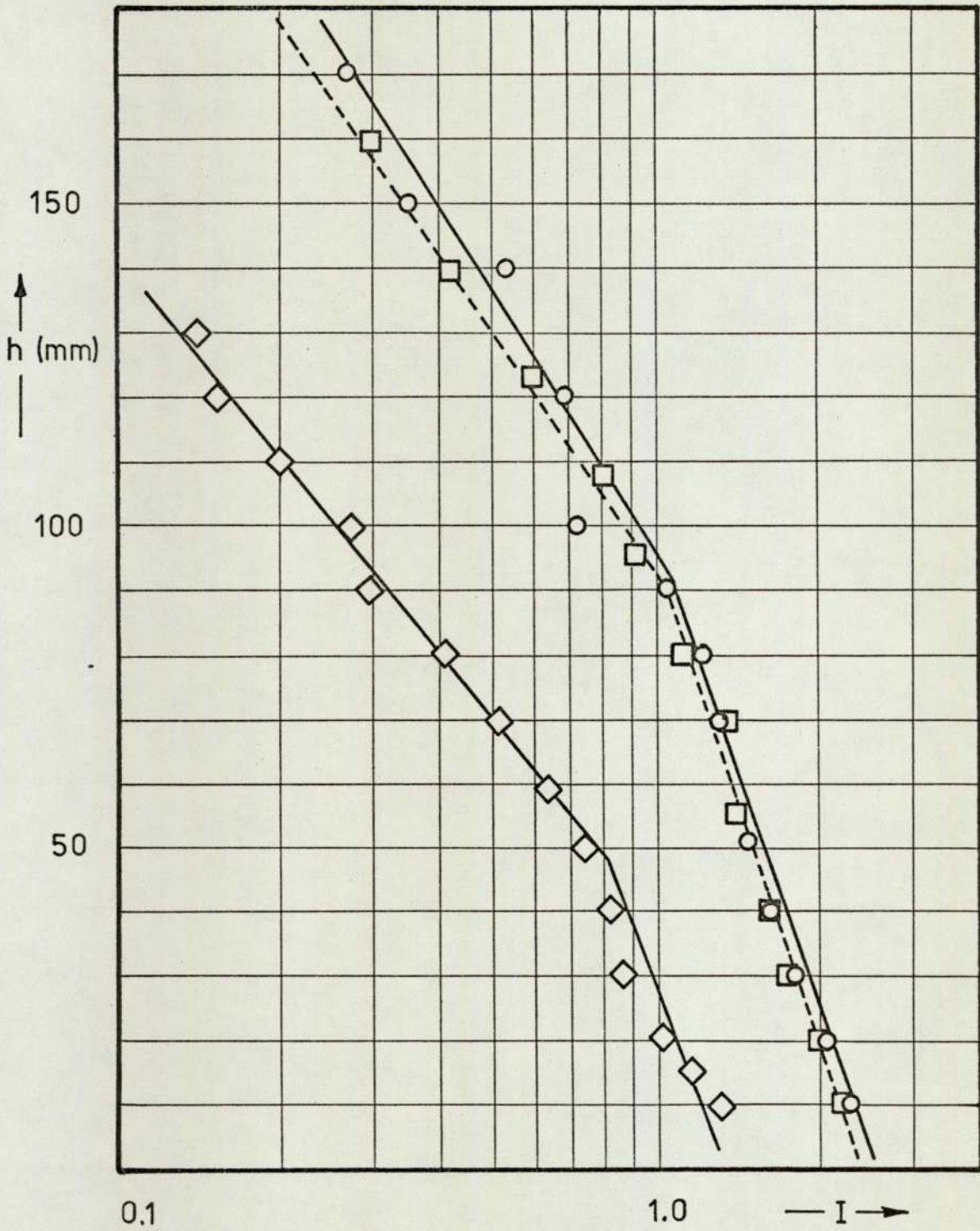
There is a similarity between the lower temperature close to the stoichiometric ratio case, and the high temperature cases, as far as the change of scattered intensity with flame height is concerned. A comparison for such conditions is given in Fig. (VI-3). This resemblance is valid not only for flame nos. 9 and 20, but for such other pairs too, while the higher limits, that is the furthestest point from the stoichiometric ratio for each constant temperature contour, show a big difference, in slope, and average scattered intensities.

The average scattered intensities in arbitrary units in terms of PSD output and  $d \log I/dh$  for each flame is listed in Table (VI-2),  $d \log I/dh$  is the reciprocal of the slopes mentioned earlier.

#### 6.1. ANALYSIS OF THE RESULTS

The intensity of the light scattered from an assembly of

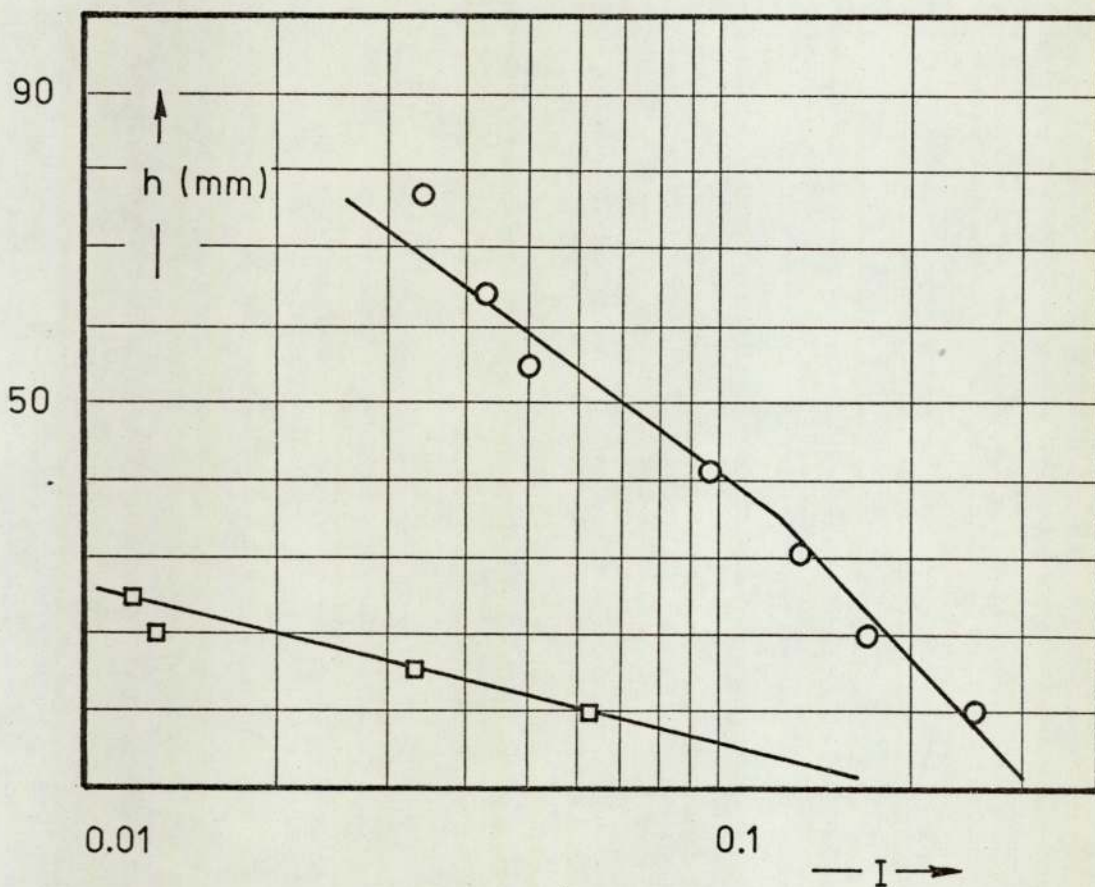
FIGURE VI-2 COMPOSITION RELATIONS



flame no :  $\diamond$  6  
                   $\square$  7    ---  
                   $\circ$  8    —



FIGURE VI-3 TEMPERATURE RELATIONS



flame no:  $\circ$  9

$\square$  20

TABLE ( VI-2) AVERAGE INTENSITIES &  $d\log I/dh$

FLAME NO.	$\bar{I}$ AVERAGE INTENSITY $( \bar{I} \times 100 )$	$d\log I/dh$ $(m^{-1})$
1	35	4.78
2	20	6.96
3	30	10.5
4	23	15.5
5	11	1.93
6	30	9.75
7	40	8.17
8	60	7.36
9	6	16.5
10	80	6.64
11	12	11.0
12	4	35.7
13	15	10.0
14	6	17.9
15	50	8.02
16	60	7.45
17	5	45.3
18	15	12.1
19	3	19.5
20	3	48.8



particles is a function of the particle properties, angle of scattering, number density and the diameter of the particle. From eq (2-3), it can be expressed in terms of the above factors, as,

$$I = \alpha \sum_i n_i a_i^6 \quad (6-1)$$

where the  $i^{\text{th}}$  group of particles has diameter  $a_i$  and number density  $n_i$ ,  $\alpha$  being the combination of other values in eq. (2-3).

When the carbon particles undergo an oxidation process in the flame, it is generally agreed that, the change is in the particle volume while the number density is only slightly effected.

In an oxidation process proceeding in the above way by an oxidising species attaching the particle surface, (Section 3.3.1.), which will now be referred to as X, the rate of loss of carbon can be expressed as,

$$-\frac{dC}{dt} = k_1 A [X] \quad (6-2)$$

The oxidising species in question were the hydroxyl radicals and the oxygen atoms. The equilibrium concentrations of such species are calculated from Gaydon & Wolfhard (1970) and Gurvich et al

(1962). They are listed in Table (VI-3)

The rate of loss of carbon is in fact the rate of decrease in the particle volume, hence can be expressed in terms of  $da/dt$ . When the intensity of the scattered light is taken from one diameter group, it will be,

$$I = \alpha n a^6 \quad (6-3)$$

and

$$\frac{d \ln I}{dt} = 6 \alpha n \frac{d \ln a}{dt} \quad (6-4)$$

which can also be interpreted as,

$$= 6 \alpha n k_1 \left[ X \right] / a \quad (6-5)$$

Defining

$$\beta = 6 k_1 (\alpha n)^{7/6} \quad (6-6)$$

the change in intensity becomes,

$$\frac{d \ln I}{dt} = \beta I^{-1/6} \left[ X \right] \quad (6-7)$$

From the experimental observations, the slowly varying function  $I^{-1/6}$  could be replaced by its average value, such that



TABLE (VI-3) CALCULATED RADICAL AND ATOM CONCENTRATIONS AT  
THERMODYNAMIC EQUILIBRIUM

FLAME NO.	$[OH]_e$ (atm x $10^{-5}$ )	$[H]_e$ (atm x $10^{-4}$ )	$[O]_e$ (atm x $10^{-8}$ )	$\delta$
1	0.14	0.71	0.03	16.60
2	0.34	0.57	0.09	15.50
3	1.91	2.51	1.78	4.22
4	4.98	2.63	8.48	3.20
5	0.35	6.05	0.26	3.20
6	4.00	6.58	7.51	2.11
7	3.23	7.18	5.56	2.11
8	2.60	7.74	4.15	2.11
9	5.82	7.0	11.7	1.99
10	2.62	13.2	4.74	1.58
11	5.70	11.9	13.3	1.50
12	16.0	8.1	62.4	1.41
13	4.98	16.6	10.9	1.33
14	10.3	13.8	32.0	1.25
15	2.67	19.3	5.91	1.25
16	2.55	20.2	5.41	1.25
17	17.8	12.6	74.3	1.26
18	9.13	21.4	28.8	1.00
19	14.0	23.3	51.2	1.00
20	30.4	25.6	188.0	1.00

$$\beta [X] = \bar{I}^{1/6} \quad d \ln I / dt \quad (6-8)$$

The value  $\beta [X]$  is determined experimentally and listed in Table (VI-4). Assuming thermodynamic equilibrium conditions, the correlation of the rate function  $\beta [X]$  with the oxidising species in question (OH and O) are also tabulated in the third and the fourth column of the same table. As described in Section 5.2.4., in the temperature range studied, hydrogen atoms are well above their thermodynamic equilibrium level. Introduction of the primary flame products will tend to reduce this disequilibrium, but not eliminate it. From Table (VI-4) even though the correlation is not exact in either case, there is strong evidence that the oxidising species X is the hydroxyl radical where  $\beta$  has of more constant value, rather than the oxygen atom.

The disequilibrium parameter ( $\delta$ ) for each flame condition is shown in Table (VI-3). They are calculated from Bulewicz et al (1956), Fig. (V-4). The fact that, their experiments were carried out in a different flame and at a fixed height of 4 cm above the surface of their Meker burner, makes it rather difficult to apply to the flames used in the present study. But, such an application would not be misleading. Introducing the disequilibrium parameters for each flame, Table (VI-5), the correlation is improved. The results again support the hypothesis of OH radicals being the oxidising species, by giving a more constant value for  $\beta$ .



TABLE (VI-4) RATE FUNCTIONS AND CORRELATIONS.

FLAME NO.	$\beta [X]$	$\frac{\beta[X]}{[OH]_e}$ $\times 10^{-3}$	$\frac{\beta[X]}{[O]_e}$ $\times 10^{-7}$
1	8.6	6178.0	3089.0
2	11.5	3380.0	1161.6
3	18.5	968.6	103.9
4	26.2	526.1	30.9
5	2.88	823.0	110.7
6	17.2	430.0	22.9
7	15.1	467.5	27.2
8	14.6	561.5	35.2
9	22.3	383.2	19.1
10	13.8	526.7	29.1
11	16.6	291.2	12.5
12	45.0	281.3	7.2
13	15.7	315.3	14.4
14	24.2	235.0	7.6
15	15.4	576.7	26.1
16	14.8	580.3	27.4
17	59.3	333.1	7.9
18	19.0	208.1	6.6
19	23.4	167.1	4.6
20	58.6	192.8	3.1

## 6.2. THEORETICAL APPROACH

Additional evidence for the nature of the oxidant can be found from kinetic theory, where the rate function  $\beta[X]$  can be estimated. At 2000 K and 1 atm total pressure the rms velocity for the collision frequency is calculated as  $7.06 \times 10^5 \times M^{-\frac{1}{2}}$  cm. sec<sup>-1</sup> where M is the molecular weight of the attacking species X. In terms of the partial pressure of X and the number of collisions, this can be expressed as,

$$6.47 \times 10^{23} \times P \times M^{-\frac{1}{2}} \text{ collisions. cm}^{-2} \cdot \text{sec}^{-1}$$

assuming that every X hitting the surface removes a carbon atom,

$$12.89 \times P \times M^{-\frac{1}{2}} \text{ (gr C removed) cm}^{-2} \cdot \text{sec}^{-1}$$

The initial intensity of the scattered light, could be used in conjunction with the particle radius, determined from electron micrographs Fig. (VI-4) as 25 nm, of the soot aggregates from the primary burner. The relation between the scattered intensity, and the particle radius could then be expressed as,  
 $I = 10^9 a^{\frac{1}{6}}$ . The rate function  $\beta$  is then given by,

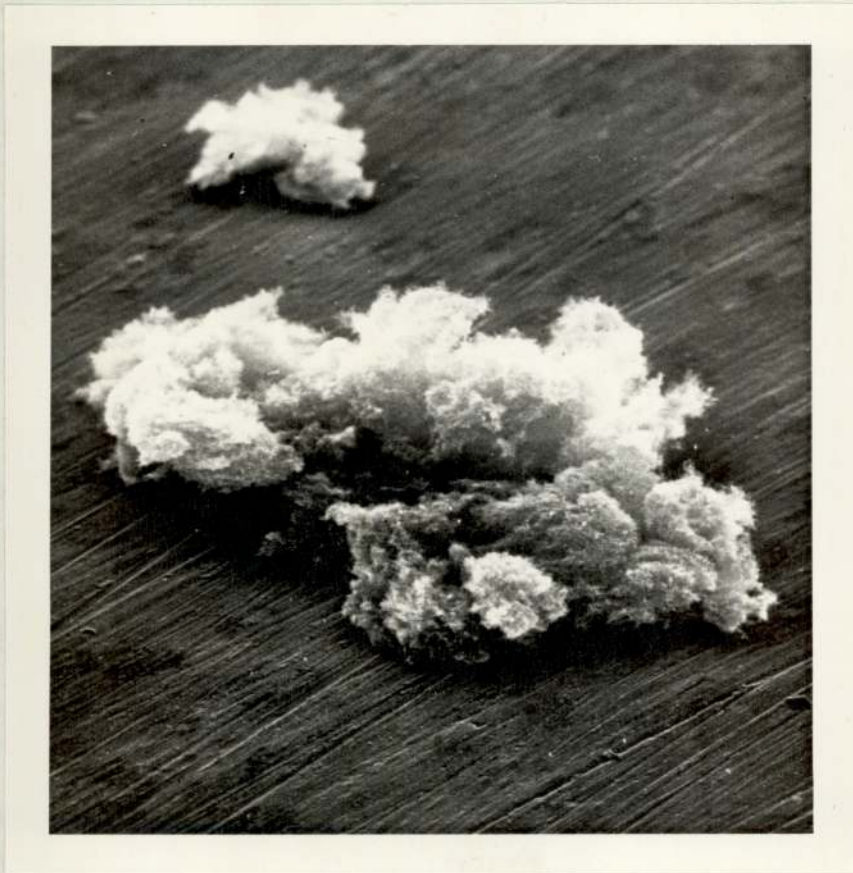
$$[X] \beta = 10^9 a \frac{2.6}{v(4\pi a^3)} \frac{dv}{dt}$$

substituting the rate of change in the particle volume (V) where v is the flame velocity,



FIGURE VI 4 ELECTRON MICROGRAPHS

(a)



magnification       $\times 100$

secondary    burner    off

(b)



magnification       $\times 2400$   
sample taken from secondary  
burner



TABLE (VI-5) CORRELATIONS REGARDING DISEQUILIBRIUM.

FLAME NO.	$\frac{\beta [X]}{[OH]_e \delta}$	$\frac{\beta [X]}{[O]_e \delta^2}$
1	372.2	11.2
2	218.0	4.83
3	229.5	3.59
4	165.4	3.05
5	254.0	10.5
6	203.8	5.14
7	221.5	6.11
8	266.1	7.91
9	192.6	4.82
10	334.4	11.65
11	194.1	5.55
12	199.5	3.62
13	237.1	8.14
14	188.0	4.86
15	461.4	16.70
16	464.2	17.53
17	264.3	4.97
18	208.1	6.60
19	167.1	4.60
20	192.8	3.10

$$[X]\beta = 1.39 \times 10^6 P$$

rate function is expressed in terms of the partial pressure of the oxidant. The average observed value of  $\beta[X]$  is  $25 \text{ m}^{-1}$ , which indicates a partial pressure of X to be  $1.79 \times 10^{-5} \text{ atm}$ . The comparison of the two species in question from Table (VI-3) shows that, this pressure while in agreement with the  $[\text{OH}]_e$  value, is quite large, as far as  $3 \times 10^{-7} \text{ atm}$  of  $[\text{O}]_e$  is concerned.

A collision efficiency of 1 in 10 is reasonable for hydroxyl radicals, and would allow for a disequilibrium parameter of 2.5. For the oxygen atoms to qualify as the oxidising species collision efficiency will have to be complete and even then a disequilibrium parameter of 8 would be required at temperatures as high as 2170 K, which is not the case. It is fair to say that oxygen atoms are  $\sim 250$  times less efficient within the experimental limits.

In the light of the experimental evidence and the theoretical considerations, the results support strongly an attack by hydroxyl radicals in the oxidation process of soot particles in fuel rich flames.



## CHAPTER 7.

### 7. CONCLUSIONS

The work was directed towards the nature of the oxidising species for soot particles in flames. Use of light scattering technique as a diagnostic tool, brought an interesting dimension in the kinetic study of such a system. The thesis is organised in a way that, previous work concerning the nature of soot particles follows a chapter on the general scattering theory, where the various experimental basis necessary in the final analysis are included in Chapter 4. A kinetic approach to the reactions in flames is discussed in Chapter 5.

When the light scattering from soot particles is mentioned, the absorption characteristics of these particles should also be included. It is well known that, soot particles in flames do absorb light as well as they scatter. In fact, two categories of previous reports can be found, where in the first, soot particles are assumed to absorb only and scattering is neglected, and the second accepts the opposite case. A combination of the two would be a more realistic approach since both scattering and absorption have a considerable contribution to the final extinction of the incident light beam. Such an attempt was made by the author. At 950 nm the absorption process is not obstructed by any other particle than soot (Page 1972) hence this wavelength was used in the experiments for absorption measurement. It

was found that the presence of the flame increased the absorption characteristic as if there is twice as much soot present in the system, no explanation could be offered for this at the present time. Further work concerning the absorption of light by soot particles in flames was prevented by a lack of available time. Hence the research was diverted to scattering measurements alone. The assumptions made include uniform particle characteristics throughout the entire flame and the experimental conditions. Since relative measurements were adopted, the absolute values of such characteristics were not involved. Particle orientation and the shape factors were not considered.

Even though an attack by the oxygen atom cannot totally be rejected, the results support strongly that the predominant oxidative attack on soot is by the hydroxyl radical. It must be stated that the exact description of the situation is very complex, due to incomplete knowledge of actual atom and radical concentrations, exact particle properties such as refractive indices and the shape of clusters. In any future study on this topic, one of the major works should be to implement better knowledge of the particle properties and attempt to figure the actual atom and radical concentrations in the flame conditions used. These investigations would be rather tedious and were not attempted firstly by unavailable amount of time, and secondly not to divert the work to other complex fields of flame studies.



The conclusion reached here is by considering the above assumptions, which further work could eliminate, and support strongly the argument put forward by Fenimore & Jones (1967), that the very active oxidant hydroxyl radical is the dominant oxidising species of soot in fuel rich flames within the previously stated experimental limits. Importance of the <sup>in</sup>situ measurements were emphasized within the text, employing such a technique makes a crucial contribution to the strong experimental evidence.

The author wishes to express his gratitude to Professor F. M. Page, without whose invaluable guidance during the three most enjoyable years at the University of Aston, this work would have been impossible.

APPENDIX



```
WASTE SARGAN  
DIMENSION AK2(15), AK3(15), AK4(15), AK5(15), AK6(15), HCH2O(15),  
CHCO2(15), HCH2(15), HCOH(15), HCO(15), HCH(15), HCH2(15), HCN(15)  
*****
```

```
CALCULATION OF FLAME TEMPERATURES  
PRIMARY BURDEN OFF, NO SOOT COMING INTO THE SECONDARY BURDEN
```

```
*****  
BASIS = 1 POUND  
YH2, YO2, YH2O ARE THE % H2, O2, H2O RESPECTIVELY IN THE REACTION  
AH = GR MOLE HYDROGEN / GR MOLE HYDROGEN IN THE REACTION  
AO = GR MOLE OXYGEN / GR MOLE HYDROGEN IN THE REACTION  
*****
```

```
TOTAL FLOW RATE = 1 GR  
TOTAL GR. MOLE OF INPUT GAS = 16.044  
DO TO 1-1, 15
```

```
READ(C, 1) AK2(C), AK3(C), AK4(C), AK5(C), AK6(C)  
1 FORTN(C, 10, 0)  
WRITE(C, 3) AK2(C), AK3(C), AK4(C), AK5(C), AK6(C)  
3 FORTN(C, 10, 1)
```

TO CONTINUE

The computer programme involved is included in the back cover.

```

DO 50 I=1,15
READ(1,21)PCB20(I),HCO2(I),HCH2(I),HCOH(I),HCO(I),HCH(I),
CHCN2(I),HCNO(I)
21 FORMAT(F10.4)
WRITE(2,23)PCB20(I),HCO2(I),HCH2(I),HCOH(I),HCO(I),HCH(I),
CHCN2(I),HCNO(I)
23 FORMAT(FF10.4)
50 CONTINUE
DO 301 IJ=25,45,5
DO 302 IK=5,45,5
Y02=I.J
Y02=I.K
Y02=100.0-(Y.I+Y02)
IF (Y02.LT.0.0.OR.Y02.LT.0.0)GO TO 301
TEP=20.0
GRMH2=(TEP*(Y02/100.0))/22.4
GRNO2=(TEP*(Y02/100.0))/22.4
GRMN2=(TEP*(Y02/100.0))/22.4
GMOLE=GRMH2+GRNO2+GRMN2
AI=GRNO2/GMOLE
AG=GRMH2/GMOLE
YCH=GRMH2*2.0
YCO=GRNO2*2.0
YCN=GRMN2*2.0
DO 13 H=1,15
DO 11 J=1,20
PO2=J/10000.0
AP=SQRT(PO2)
PO=AK5(N)*AP
DO 12 K=50,60
P2=K/100.0
PH2=AK2(O)+P2/AP
HP=SQRT(PH2)
POH=AK3(C)+P2/HP
PH=AK4(I)*HP
CMH=2.0*PH2+POH+POH+2.0*PO
FHM=CMH*AF
YAF=SQRT(CMH/2.0)
PMO1=AK6(N)*AP*YAF
X=PMO1/(2.0*FHM)
PMO=PMO1*(-Y+SQRT(1.0+X*X))
DN2=0.5*(FHM-PMO)
CMO=P2*2.0+PH2+POH+POH+PMO
CNM=2.0*P2+PMO

```

C  
C CHTR=CMH/CMO , CALCULATED FOR COMPARING WITH ( AF )  
C COXV6=CMN/CMO , CALCULATED FOR COMPARING WITH ( AG )  
C

```

CHTR=CMH/CMO
COXV6=CMN/CMO
P=P2+PO2+PH2+POH+PO+PH+202+PMO
IF (0.61.1.0500.00.0.LT.0.9500)GO TO 12
IF (((ABS(CM1-(CMH/CMH)))/AF).GT. 0.10).GO TO 12
IF (((ABS(CM1-(CMN/CMN)))/AO).GT. 0.10) GO TO 12
Y1=Y01/C01
Y2=Y02/C02
Y3=Y03/C03
IF ((ABS((Y1-Y2)/Y1)).GT. 0.05) GO TO 12
IF ((ABS((Y1-Y3)/Y1)).GT. 0.05) GO TO 12
IF ((ABS((Y2-Y3)/Y2)).GT. 0.05) GO TO 12

```



$V = (V1 + V2 + V3) / 3$

```

C
C   TOTAL HEAT CONTENT PER MOLE = THCPM
  THCPM = P2*HCH2O(C) + P02*HCO2(C) + P02*HCH2(C) + P01*HCO(C) + P0*HCO(C) +
C   P00*HCO(C) + P02*HCO2(C) + P00*HCO(C)
C   TOTAL HEAT CONTENT = THC
  THC = V*THCPM
C   HEAT OF FORMATION OF H2O IN KCAL/MOLE H2O = 57.75
  H2O = 57.75
C   HEAT LIBERATED HI
  HI = H2O*P2
C   TOTAL HEAT LIBERATED THL
  THL = HI*V
C   HEAT OF FORMATION OF THE FREE RADICALS IN KCAL/MOLE
C   HOP = 9.1   HEO = 59.56   HEH = 52.12   HEN = 21.64
  HOP = 9.1
  HEO = 59.56
  HEH = 52.12
  HEN = 21.64
C   HEAT USED TO FORM THE FREE RADICALS BUTFER
  BUTFER = HOP*P0 + P0*HIO + P0*HEH*P0 + HEO*P00
  THUTFER = BUTFER*V
C   NET HEAT PRODUCTION = HNP
  HNP = HI - THUTFER
  IF (ABS((THC - HNP)/THC) .GT. 0.1) GO TO 12
C   *****
C
  WRITE (2,160) V, H2, GPM02
  WRITE (2,161) V, O2, GPM02
  WRITE (2,162) V, H2, GPM02, TGM0LE
  WRITE (2,250)
250  FORMAT (5X, 'H2O', 10X, 'O2', 10X, 'H2', 10X, 'OH', 10X, 'H', 'O', 10X, 'H2O',
C   'H2', 10X, 'HO', 10X, 'H', 'O', 'H', 'O')
  WRITE (2,20) P2, P02, P02, P0H, P0, P0, P02, P00, P, M
  20  FORMAT (9I13.4, 12, /)
  WRITE (2,106) CNITP, DE, THCPM, BUTFER
  WRITE (2,107) COXYO, AO, THUTFER
  WRITE (2,108) CBY, Y1, THC, HNP
  WRITE (2,109) CMO, Y2
  WRITE (2,110) CMY, Y3, V
160  FORMAT (2H 2H2 = ,F4.2,15H          GPM02 = ,F5.5)
161  FORMAT (2H 2O2 = ,F4.2,15H          GPM02 = ,F5.5)
162  FORMAT (2H 2H2 = ,F4.2,15H          GPM02 = ,F5.5,
C   /15H          TGM0LE = ,F5.3, /)
106  FORMAT (1 CNITP = ,F7.4,10X, 'DE = ', F4.2,20X, 'THCPM = ', F7.4,
C   /10X, 'BUTFER = ', F7.4)
107  FORMAT (1 COXYO = ,F7.4,10X, 'AO = ', F4.2,44X, 'THUTFER = ', F7.4)
108  FORMAT (1 CBY = ,F7.4,10X, 'Y1 = ', F4.2,20X, 'THC = ', F7.4,
C   /10X, 'HNP = ', F7.4)
109  FORMAT (1 CMO = ,F7.4,10X, 'Y2 = ', F4.2)
110  FORMAT (1 CMY = ,F7.4,10X, 'Y3 = ', F4.2,10X, 'V = ', F4.2, / / /)
  12  CONTINUE
  11  CONTINUE
  13  CONTINUE
  102  CONTINUE
  101  CONTINUE
  100  STOP
  END

```

REFERENCES

- Aden A. L. (1951), J. Appl. Phys., 22, 601
- Arthur J. R. (1949), Nature, 164, 537
- Arthur J. R. (1950), Nature, 165, 557
- Ates H. F., Page F. M. (1975) in press
- Atlas D., Kerker M., Hirschfeld W. (1953), J. Atmos. Terr. Phys.,  
3, 108
- Behrens H. (1952), Z. Phys. Chem., 199, 1
- Bird R. B., Stewart W.E., Lightfoot E. N. (1960), Transport  
Phenomena, J. Wiley, Tokyo
- Brabbs T.A., Belles F.E. Brokaw R.S. (1971), Thirteenth Symposium  
(Intl.) on Combustion p.129
- Browne W.G., White D.R., Smookler G.R. (1969), Twelfth Symposium  
(Intl.) on Combustion p.557
- Bulewicz G.H., James C.G., Sugden T.M. (1956), Proc., Roy.Soc. A.,  
235, 89
- Clarke A.E., Hunter T.G., Garner F.H. (1946), J. Inst. Petrol 32,  
627
- Clyne M.A.A., Thrush B.A. (1963), Proc. Roy. Soc. A, 275, 544
- Dalzell W.H., Williams G.C., Hottel H.C. (1970), Comb. and Flame,  
14, 161
- Datschefski G. (1962) Dissertation, Univ. of Sheffield, England
- Davey H. (1927) in Bone W.A. and Townend D.T.A., Flame and  
Combustion in gases, Longmans,  
London



- Erickson W.D., Williams G.C., Hottel H.C. (1964), Comb. and Flame, 8, 127
- Espenscheid W.F., Kerker M., Matijevic E. (1964), J. Phys. Chem., 68, 3093
- Fairbarn A.R., Gaydon A.G. (1955), Fifth Symposium (Intl.) on Combustion p. 324
- Faitani J.J. (1968), S.A.E. Transactions, 77, 1080
- Fenimore C.P., Jones G.W., Moore G.E. (1957), Sixth Symposium (Intl.) on Combustion p. 242
- Fenimore C.P., Jones G.W. (1958) J. Phys. Chem., 62, 693
- Fenimore C.P., Jones G.W. (1959) J. Phys. Chem., 63, 1154
- Fenimore C.P. (1964), Chemistry in Premixed Flames, Pergamon, N.Y.
- Fenimore C.P., Jones G.W. (1967), J. Phys. Chem., 71, 593
- Fenimore C.P., Jones G.W. (1969), Comb. and Flame, 13, 303
- Field M.A., Gill D.W., Morgan B.B., Hawksley P.G.W. (1967) Combustion of Pulverised Coal, Leatherhead
- Finaev Yu A. (1965), Non-stationary Heat and Mass Transfer, (ed. by Gurvich et al) Ac. of Sc. Belorussian SSR Inst. of Heat and Mass Transfer p.112
- Fristrom R.H., Westenberg A.A. (1965), Flame Structure, Mc-Graw Hill, N.Y.
- Gans R. (1912) Ann. Physik., 37, 881
- Gaydon A.G., Wolfhard H.G. (1970), Flames, Their Structure, Radiation and Temperature, Chapman and Hall, London, 3e.
- Getzinger R.W., Blair L.S. (1969), Comb. and Flame, 13, 271

- Gill D.W. (1958), BCURA Monthly Bulletin, 22, 487
- Graham J.A., Brown A.R.G., Hall A.R., Watt W. (1957), Soc. Chem. Ind. (London) Conf. on Industrial Carbon and Graphite p.309
- Griffiths E., Awbery J.H. (1929) Proc. Roy. Soc. A., 123, 401
- Grune W.N. (1962) Ind. Water Wastes, 7 (2), 29; (3) 72
- Gurvich L.V. et al (1962), Thermodynamic Properties of Industrial Substances, Akad- Nauk, USSR
- Hald A. (1962), Statistical Theory with Engineering Applications, J. Wiley, N.Y.
- Hammarstrand K. (1974), Varian Inst. Appl., 8, 8
- Hoyermann K., Wagner H. Gg., Wolfrum J. (1967), Ber. Bunsenges Physik. Chem., 71, 599
- Homann K.H., Wagner H. Gg. (1968), Proc. Roy. Soc. A., 307, 141
- Jensen D.E., Padley P.J. (1966), Trans. Faraday Soc., 62, 2137 & 2140
- Jensen D.E., Padley P.J. (1967), Eleventh Symposium (Intl.) on Combustion, p 357
- Jensen D.E., Kurzius S.C. (1967) Aero Chem. Research Inc. Report, TP 149
- Jensen D.E. (1973) European Symp. Comb. Inst., Academic Press, London p. 382
- Jones A.R. (1972), J. Phys. D: Appl. Phys., 5, L1
- Jones D.S. (1955), Phil. Mag., 46, 957
- Kaskan W.E. (1958) Comb. and Flame, 2, 229
- Kaskan W.E., Schott G.L. (1962), Comb. and Flame, 6, 73



- Kelly R., Padley P.J. (1969), Trans. Faraday Soc., 65, 355
- Kerker M. (1969), The Scattering of Light and other Electromagnetic Radiation, Academic Press, N.Y.
- Kunugi M., Jinno H. (1967), Eleventh Symposium (Intl.) on Combustion, p. 257
- Lee K.B., Thring M.W., Beer J.M. (1962), Comb. and Flame, 6, 137
- Lewis B., von Elbe G. (1963), Combustion, Flames and Explosion of Gases, Ac.Press Inc., N.Y., 2e
- Lowan A.N. (1948), Tables of Scattering Functions for Spherical Particles, Natl. Bureau of Std., Appl. Math. Ser. 4, U.S. Government Printing Office, Washington D.C.
- Macfarlane J.J., Holderness F.H., Witcher F.S.E. (1964), Comb. and Flame 8, 215
- Magnussen B.F. (1971), Thirteenth Symposium (Intl.) on Combustion p. 869
- Mavrodineau R. (1965), Flame Spectroscopy, J. Wiley, N.Y.
- Miller W.J. (1967), Eleventh Symposium (Intl.) on Combustion, p. 245
- Miller E.R. (1969), Ph.D. Thesis, University of Aston
- Millikan R.C. (1962) J. Phys. Chem., 66, 794
- Millikan R.C. (1962 a), Temperature, Its Measurements and Control in Science and Ind., Am. Inst. Phys., Vol. 3, part 2., p. 497, Reinhold, N.Y.
- Minkoff G.J., Tipper C.F.H. (1962), Chemistry of Combustion reactions, Butterworths, London
- Mie G. (1908), Ann. Physik., 25, 377

- Mulcahy M.F.R., Smith I.W. (1969), *Rev. Pure and Appl. Chem.*,  
19, 81
- Nagle J., Strickland-Constable R.F. (1962), *Proc. 5th Carbon  
Conf.*, 1, 154
- Narasimhan K.S., Foster P.J. (1965), *Tenth Symposium (Intl.)  
on Combustion* p.473
- Olaf J., Robock K. (1961), *Staub*, 21, 495
- Padley P.J., Sugden T.M. (1958), *Proc. Roy. Soc. A.*, 248, 248
- Padley P.J., Sugden T.M. (1959), *Seventh Symposium (Intl.) on  
Combustion*, p.235
- Padley P.J. (1960), *Trans. Faraday Soc.*, 56, 449
- Page F.M. (1955), *Disc. Faraday Soc.*, 19, 87
- Page F.M., Sugden T.M. (1957), *Trans. Faraday Soc.*, 53, 1092
- Page F.M. (1972), *Private Communication*
- Page F.M. (1973), *Chemical Reaction and Ionisation in Flames,  
Phy. Chem. of Fast Reactions,  
Ch. 3.*, Plenum Press, London
- Palmer H.B., Cullis C.F. (1965) *Chemistry and Physics of Carbon*,  
ed. Walker P.L. Jr., Ch. 5, E.  
Arnold Ltd., London
- Park C., Appleton J.P. (1973), *Comb. and Flame*, 20, 369
- Parker W.G., Wolfhard H.G. (1950), *J. Chem. Soc.* p.2038
- Payne K.G., Weinberg F.J. (1959), *Proc. Roy. Soc. A.*, 250, 316
- Place E.G., Weinberg F.J. (1967), *Eleventh Symposium (Intl.) on  
Combustion*, p. 245
- Ratcliffe S.W., Appleton J.P. (1971), *Comb.Sci. & Tech.*, 4, 171



- Rayleigh Lord (1881), *Phil. Mag.*, 12, 81
- Rosner D.E., Allendorf H.D. (1968), *AIAA J*, 6, 650
- Rosner D.E., Allendorf H.D. (1970), *Heterogeneous Kinetics at Elevated Temperatures*, ed. G.R. Belton, Plenum, N.Y., p. 231
- Sabra A.I. (1967), *Theories of Light*, Oldbourne, London
- Sawyer R.F. (1970), *Astronautics and Aeronautics*, 8, 62
- Schott G.L., Kinsey J.L. (1958), *J. Chem. Phys.*, 29, 1177
- Schott G.L. (1960), *J. Chem. Phys.*, 32, 710
- Schott G.L., Bird P.F. (1964), *J. Chem. Phys.*, 41, 2869
- Sentfleben H., Benedict E. (1917), *Ann. Physik (IV)*, 54, 65
- Sinclair D. (1947), *J. Opt. Soc. Am.*, 37, 475
- Smith E.C.W. (1940), *Proc. Roy. Soc. A*, 174, 110
- Stratton J.A. (1941), *Electromagnetic Theory*, Mc-Graw Hill Book Co. Ltd., London
- Street J.C., Thomas A. (1955), *Fuel*, 34, 4
- Strehlov R.A., Cohen A. (1962), *Phys. Fluids*, 5, 97
- Stull V.R., Plass G.N. (1960) *J. Opt. Soc. Am.*, 50, 121
- Tesner P.A. (1959), *Seventh Symposium (Intl.) on Combustion*, p. 546
- Tesner P.A., Snegiriova T.D., Knorre V.G. (1971), *Comb. Flame*, 17, 253
- Tu C.M., Davis H., Hottel H.C. (1934) *Ind. Eng. Chem.*, 26, 749
- Van de Hulst H.C. (1949) *Physica*, 15, 740
- Van de Hulst H.C. (1957) *Light Scattering by Small Particles*, Wiley, N.Y.

Warren D.R. (1952), Proc. Roy. Soc. A, 211, 96

Weinberg F.J. (1968), Proc. Roy. Soc. A, 307, 195

Whittaker E.T., Watson G.N. (1947), A Course of Modern Analysis,  
Cambridge Univ. Press, London

Wolfhard H.G., Parker W.G. (1950), Fuel, 29, 325

Yagi S., Kunii D. (1955), Fifth Symposium (Intl.) on Combustion  
p. 231



```

0 PROGRAM (FXXX)
1 INPUT 1=GR0
2 OUTPUT 2=LPO
3 COMPRESS INTEGER AND LOGICAL
4 EXTENDED
5 TRACE 4
6 END
7 MASTER SARWAN
8 DIMENSION AK2(15),AK3(15),AK4(15),AK5(15),AK6(15),HCH2O(15),
9 HCH2(15),HCH2(15),HCOH(15),HCO(15),HCN(15),HCN2(15),HCNO(15)
10 *****
11 C
12 C CALCULATION OF FLAME TEMPERATURES
13 C PRIMARY BURNER OFF ,NO SOOT COMING INTO THE SECONDARY BURNER
14 C
15 C *****
16 C BASIS = 1 MINUTE
17 C YH2,YO2,YN2 ARE THE % H2,O2,N2 RESPECTIVELY IN THE REACTION
18 C AF= GR MOLE NITROGEN / GR MOLE HYDROGEN IN THE REACTION
19 C AU= GR MOLE OXYGEN / GR MOLE HYDROGEN IN THE REACTION
20 C *****
21 C
22 C TOTAL FLOW RATE = TFR
23 C TOTAL GR. MOLE OF INPUT GAS = TGMOLE
24 C DO 10 I=1,15
25 READ(1,1)AK2(I),AK3(I),AK4(I),AK5(I),AK6(I)
26 1 FORMAT(5F0,0)
27 WRITE(2,5)AK2(I),AK3(I),AK4(I),AK5(I),AK6(I)
28 3 FORMAT(5E10,7)
29 10 CONTINUE
30 C DO 30 I=1,15
31 READ(1,21)HCH2O(I),HCO2(I),HCH2(I),HCOH(I),HCO(I),HCN(I),
32 HCN2(I),HCNO(I)
33 41 FORMAT(8F0,0)
34 WRITE(2,25)HCH2O(I),HCO2(I),HCH2(I),HCOH(I),HCO(I),HCN(I),
35 HCN2(I),HCNO(I)
36 43 FORMAT(8E10,4)
37 30 CONTINUE
38 C DO 301 IJ=40,10,5

```

```

39 C DO 302 IK=3,40,5
40 YN2=IJ
41 YO2=IK
42 YH2=100,0-(YN2*YO2)
43 IF(YH2,EO,0,0,UP,YH2,LT,0,0)GO TO 301
44 TFR=20,0
45 GRMH2=(TFR*(YH2/100,0))/22,4
46 GRMO2=(TFR*(YO2/100,0))/22,4
47 GRMN2=(TFR*(YN2/100,0))/22,4
48 TGMOLE=GRMH2+GRMO2+GRMN2
49 AF=GRMH2/TGMOLE
50 AU=GRMO2/TGMOLE
51 YNH=GRMH2*2,0
52 YNO=GRMO2*2,0
53 YNN=GRMN2*2,0
54 DO 15 M=1,15
55 DO 11 J=1,40
56 P02=J/10000,0
57 AP=SQR(P02)
58 PH=AK5(M)*AP
59 DO 12 K=30,60
60 PZ=K/100,0
61 PHZ=AK4(M)*PZ/AP
62 BP=SQR(PHZ)
63 PHH=AK3(M)*PZ/BP
64 PHN=AK6(M)*BP
65 GNN=2,0*PHZ+PHH*P02*2,0*PZ
66 ENN=GNN*AF
67 YAF=SQR(ENN/2,0)
68 PNU=AK6(M)*AP*YAF
69 X=PNU/(2,0*ENN)
70 PNO=PNU*(1-X*SQR(1,0*X*X))
71 PHZ=0,5*(ENN-PNO)
72 CNU=PZ*2,0*P02*PHH*P0*PNO
73 GNN=2,0*PHZ+PNU
74 C
75 C CNTR=GNN/CNH ; CALCULATED FOR COMPARING WITH ( AF )
76 C CUXYG=CNO/CNH ; CALCULATED FOR COMPARING WITH ( AU )
77 C
78 CNTR=GNN/CNH
79 CUXYG=CNO/CNH
80 P=PZ+P02+PHZ+PHH*P0+PH*P02*PNO
81 IF(P,GT,1,0500,OR,P,LT,0,9000)GO TO 12
82 IF((ABS(AF-(GNN/CNH)))/AF,GT,0,10) GO TO 12
83 IF((ABS(AU-(CNO/CNH)))/AU,GT,0,10) GO TO 12
84 Y1=YNH/CNH
85 Y2=YNO/CNO
86 Y3=YNN/CNH
87 IF((ABS((Y1-Y2)/Y1)),GT,0,05) GO TO 12
88 IF((ABS((Y1-Y3)/Y1)),GT,0,05) GO TO 12
89 IF((ABS((Y2-Y3)/Y2)),GT,0,05) GO TO 12
90 Y=(Y1+Y2+Y3)/3
91 C
92 C TOTAL HEAT CONTENT PER MOLE = THCPM
93 THCPM=P2*HCH2O(M)+P02*HCO2(M)+PH2*HCH2(M)+PHH*HCN(M)+P0*HCO(M)+
94 CPH*HCN(M)+PN2*HCN2(M)+PNO*HCNO(M)
95 C TOTAL HEAT CONTENT = THC
96 THCPY*THCPM
97 C HEAT OF FORMATION OF H2O IN KCAL/MOLE HFH2O = 57,75
98 HFH2O=57,75
99 C HEAT LIBERATED HL

```

```

100 HL=HFH2O*PZ
101 C TOTAL HEAT LIBERATED THL
102 THL=HL*Y
103 C HEAT OF FORMATION OF THE FREE RADICALS IN KCAL/MOLE
104 C HFUN = 9,7 HFV = 30,30 HFM = 52,12 HFNO = 21,64
105 HFVN=9,1
106 HFV=59,56
107 HFM=52,12
108 HFNO=21,64
109 C HEAT USED TO FORM THE FREE RADICALS HUTFER
110 HUTFER=HFUN*PHH+HFV*P0+HFM*PH+HFNO*PNO
111 THUTFER=HUTFER*Y
112 C NET HEAT PRODUCTION = HNP
113 HNP=THL-THUTFER
114 IF(ABS((THC-HNP)/THC),GT,0,10)GO TO 12
115 C *****
116 C
117 WRITE(2,100)YH2,GRMH2
118 WRITE(2,101)YO2,GRMO2
119 WRITE(2,102)YH2,GRMH2,TGMOLE
120 WRITE(2,250)
121 250 FORMAT(5X,'PHZ01',10X,'P021',10X,'PHZ1',10X,'PHH1',11X,'P01',11X,'PH1',
122 C10X,'PN21',10X,'PNO1',11X,'P1',7X,'M1')
123 WRITE(2,20)PZ,P02,PHZ,PHH,PH,P0,PHN,PN2,PNO,P,M
124 20 FORMAT(9E10,4,13,1)
125 WRITE(2,100)CNTR,AF,THCPM,HUTFER
126 WRITE(2,107)CUXYG,AO,THUTFER
127 WRITE(2,106)GNN,Y1,THC,HNP
128 WRITE(2,109)CNU,Y2
129 WRITE(2,110)GNN,Y3,Y
130 100 FORMAT(7H XH2 = ,F4,2,15H GRMH2 = ,F5,3)
131 101 FORMAT(7H XO2 = ,F4,2,15H GRMO2 = ,F5,3)
132 102 FORMAT(7H XH2 = ,F4,2,15H GRMN2 = ,F5,3)
133 C10H TGMOLE = ,F5,3,1)
134 106 FORMAT(1 CNTR = ,F7,4,10X,AF = ,F4,2,20X,THCPM = ,F7,4)
135 C10X,HUTFER = ,F7,4)
136 107 FORMAT(1 CUXYG = ,F7,4,10X,AO = ,F4,2,44X,HUTFER = ,F7,4)
137 108 FORMAT(1 GNN = ,F7,4,10X,Y1 = ,F4,2,20X,THC = ,F7,4)
138 C10X,HNP = ,F7,4)
139 109 FORMAT(1 CNO = ,F7,4,10X,Y2 = ,F4,2)
140 110 FORMAT(1 GNN = ,F7,4,10X,Y3 = ,F4,2,10X,Y = ,F4,2,11)
141 12 CONTINUE
142 11 CONTINUE
143 13 CONTINUE
144 302 CONTINUE
145 301 CONTINUE
146 500 STOP
147 END
148 FINISH
149 EJ
150 *****

```